Fluvial Facies Architecture and Provenance History of the Abrahamskraal-Teekloof Formation Transition (Lower Beaufort Group) in the Main Karoo Basin

by

Francisco Paiva

PVXFRA001

Supervisor: Dr Emese M. Bordy

A thesis presented for the degree of Master of Science in Geology

In the Department of Geological Sciences at

November 2015

DECLARATION

1. I know that plagiarism is wrong. Plagiarism is to use another's work and pretend that it is one's own.

2. I have used the South African Journal of Geology convention for citation and referencing. Each contribution to, and quotation in, this project from the work(s) of other people has been attributed, and has been cited and referenced.

3. This project is my own work.

4. I have not allowed, and will not allow, anyone to copy my work with the intention of passing it off as his or her own work.

Signed by candidate

Signature Removed

Signature _____

Francisco Paiva

Date:

Acknowledgements

First of all, I would like to thank my supervisor Dr Emese Bordy for the enormous support and dedication to this project. Without her commitment this work wouldn't have been possible. I also wish to thank all my family members who even from far away managed to always give me comfort, strength and motivation to continue.

My special thanks goes to all people that indirectly or directly contributed to this project. Among those I thank the technical staff in the Department of Geological Sciences at UCT, who are always ready to help. You are the heart of the Department.

I would like thank my colleagues Mhairi Reid, Sanda Spelman and Kenneth Chukwuma for their priceless help during my fieldwork. One can search for them, just like for "*Easter eggs*", in the different photo-panels in this work. I acknowledge the warm reception, guidance and support in the field by the researchers of the Evolutionary Studies Institute at Wits University, and in particular, I would like to thank Dr Michael Day and Prof Bruce Rubidge.

Last but not least, I acknowledge the following for financial support:

- BP Angola for giving me an opportunity and putting their trust into me to sponsor my studies for the past 7 years; and for fully covering the operational costs of this research.

- Palaeontological Scientific Trust (PAST) for conference grant to my supervisor, Dr Bordy, to attend the 18th Biennial Conference of the Palaeontological Society of Southern Africa, July 11 -14, 2014 in Johannesburg, South Africa.

Muito Obrigado!

Abstract

The Middle Permian lower Beaufort Group in the southern main Karoo Basin comprises of the fluvio-lacustrine Abrahamskraal and the overlying Teekloof and correlative Middleton Formations. These units are mainly made up of mudrocks with subordinate fine-grained sandstone-rich intervals. The objective of this mainly qualitative facies analysis study is the evaluation of the vertical and lateral abundances of the facies associations in order to decouple the preserved tectonic and climatic signals in the formations. The results on the stratigraphic trends should aid paleo-environmental, paleontological, and basin analysis studies, and improve our understanding of reservoir dynamics (e.g., permeability, connectivity) when used as outcrop analogues for subsurface fluvial reservoirs.

High resolution facies mapping showed that flat-topped, laterally continuous (for 10s of Kms) channel-belt complexes are the most common external architecture of the channel sandstones in all formations. This is confirmed by the width and thickness measurements which show that the sandstones are mainly narrow sheets with W/T ratios between 10 and 100. However, very thick, vertically stacked amalgamated sequences are also encountered at the base of the Teekloof and Middleton Formations. Furthermore, the facies mapping also demonstrated contrasting architectural patterns across the boundary of the Abrahamskraal and overlying formations, with downstream accretion elements (~25%) dominating in the former, and lateral accretions (~30%) prevailing in the latter. This, together with the stratigraphic distribution of the seven architecture types defined for the formations, suggests that the upper Abrahamskraal Formation formed in a high energy, braided fluvial system, whereas the lower Teekloof and Middleton Formation most likely formed in a meandering fluvial system.

Palaeo-slope reconstructions based on the palaeocurrent measurements point to the same sediment transport direction for all formations, however the transport direction is from the southwest and the south in the south-western south-eastern parts of the basin respectively. Mineral modal analyses based on petrographic point counting of sandstones indicate that the sediments were sourced from rocks typical of orogens in all provenance areas during the depositional period. Similarly, geochemical data remain consistent across the formations and indicate that deposition occurred in a semi-arid climate with constrained chemical weathering. Sedimentological analyses also show that calcareous soils and seasonal flash-floods were common. Given the consistency in climate and provenance throughout the depositional period, it is proposed that tectonics was the main driving force behind the contrasting architectural patterns observed across the boundary of the Abrahamskraal and overlying formations.

Contents

1. Introduction

Geological processes that govern sedimentation such as climate, discharge rate, vegetation, tectonics, base level changes, have a direct and/or indirect impact on the sedimentological and stratigraphic patterns that develop in both continental and marine sedimentary successions. Such processes can be broadly placed into two distinct groups: allogenic and autogenic processes. While some of processes are independent of others (e.g., tectonics from climate), many are interconnected, affecting one another. In addition, they often operate simultaneously, leaving behind a composite and highly complex geological record (Catuneanu, 2006).

Tectonics and climate, the two main allogenic forcing mechanisms of continental deposition (Catuneanu, 2006), are intrinsically associated with the history and evolution of the main Karoo Basin of South Africa, the target of this study. The overall tectonic and climatic settings of the basin are well-studied and thought to be fairly well-understood. A purely retro-arc foreland basin model (Catuneanu et al., 1998; Catuneanu, 2006; Johnson et al., 2006) is the most accepted hypothesis for the main Karoo Basin. However, some divergent models do exist (Turner, 1999; Tankard et al., 2009, 2012; Lindeque et al., 2012). Climatic setting interpretations are less ambiguous over large time spans. Geological and geochemical evidence found in the Karoo Basin, indicates a climatic evolution from glacial at the base of the succession (~300 Ma, Late Carboniferous) to semi-arid desert conditions at the top (~185 Ma, Early Jurassic; Catuneanu et al., 1998; Johnson et al., 2006; Rubidge, 2005). However, the variability and relative impact of climate and tectonics on the sedimentary patterns is often difficult to determine, specifically at small time scales that are $<10^6$ yrs.

The variability of sedimentary processes associated with changes in climate and tectonics, both vertically (i.e. over time) and laterally across the basin, has made detailed lithostratigraphic subdivision (mostly at member, but occasionally even at formation level) of the Permian Lower Beaufort Group problematic. Over the last 40 years the literature has seen a proliferation of informal and often discordant nomenclatures (for summaries see Cole and Wipplinger, 2001; Day and Rubidge, 2014). This is because the stratigraphic boundaries that define the delimitations of formations and members, are often gradual and spatially irregular (Cole and Wipplinger, 2001; Day and Rubidge, 2014). This issue constitutes an ongoing debate, and is being addressed by the South African Committee for Stratigraphy (SACS) on an ongoing basis (Cole and Wipplinger, 2001; Day and Rubidge, 2014).

1.1. Research Description and Aims

This research is a multi-proxy sedimentological and stratigraphic study, aiming at establishing the palaeo-environmental conditions, particularly the climate and tectonics of the upper Abrahamskraal and lower Teekloof formations; the oldest two Permian formations in the Beaufort Group, respectively (Figure 1). Two

different study areas were investigated for this project. They are located in stratigraphically equivalent regions of the main Karoo Basin, one in the southwest and the other in the southeast of the basin, in the provinces of the Western and Eastern Cape, respectively (Figure 1B). Note that, the correlative of the Teekloof Formation east of 24°E longitude is known as the Middleton Formation (Figures 1B and 3). For ease of reference the nomenclature "Teekloof Formation" is the general term adopted here for both formations, and a distinction is made between the two study areas, which are referred to as the western (W) and eastern (E) facies areas.

Understanding and untangling the complex tectonic and climatic signals left behind in the deposits of the Permian Lower Beaufort Group in the main Karoo Basin are the main motivations of this study. In addition, it is hoped that this study can provide a methodology that quantitatively refines the stratigraphic subdivisions of the area. Furthermore, the results are to be used as independent assessment for regional correlations and relative quantification of the processes that govern sedimentation, which is information needed in fields like palaeontology and water or hydrocarbon reservoir characterization.

Assuming that the imprint of the major palaeo-environmental changes can be found in the sedimentary patterns and palaeontological record of the two formations, this fieldwork-based research relies on the systematic assessment of the main sedimentary facies across the contact of the two formations. The sedimentological characterisation method used in this project is similar to the fluvial facies analysis approach of Miall (1985) and its further developments (Miall, 1988; Reading, 2001; Colombera et al., 2013; Gulliford et al., 2014; Wilson et al., 2014). Establishing the major differences between the formations at facies association level, and evaluating the reason of the facies transition between the two are the major methodological steps. Quantitative facies analysis focused on the aspects of quantification of both the internal geometry of deposits, i.e. fluvial architectural elements, and the external geometry and proportions of deposits.

Apart from the field-based methodology, which consisted of descriptions, measurements, identification and logging of the facies, sample collection, measurement of palaeocurrent indicators, indoor analytical (see Methodology, Ch. 3) techniques ranged from X-ray spectroscopy (XRF, XRD) and reflected light microscopy for quantification of the types and shapes of the sediment particles (i.e., quantitative provenance analysis).

In summary, the aim of this research is to improve the understanding of the Lower Beaufort Group regarding its (a) sedimentological heterogeneities, (b) the provenance history and (c) the parameters governing the major sedimentological and stratigraphic trends. More specifically, the objectives are to:

- Describe, categorize and interpreting of the regional sedimentary lithofacies;
- Identify and quantify the facies associations and their vertical and lateral variability;

- Evaluate the provenance of the sediments by palaeocurrent studies as well as mineralogical and chemical investigations;
- Analyse the micro-scale properties of the formations using transmitted light microscopy, XRF and XRD of bulk rock and clay fractions in selected samples.

The results, aimed at determining the relative contributions of allogenic controls on the depositional processes, are expected to:

1. Provide insights into the mechanisms driving sedimentation, namely the interplay between rates of sediment supply and accommodation space creation which are intrinsically dependent on tectonics and climate. Thus, the reconstructing of the likely scenarios that resulted in the observed facies patterns can help untangle and understand both tectonic and climatic signals.
2. Aid a) remote viewing techniques that are used for water management and hydrocarbon exploration by providing outcrop analogues, and, b) palaeontological research by providing semi-quantitative lithostratigraphic framework for regional correlations, and suggesting environmental reasons for the stratigraphic changes.

2. Geological Background

The Karoo Supergroup contains a rich geological history that reflects events for ~120 Ma, from the formation of Late Carboniferous glacial deposits to the extrusion and intrusion of Early Jurassic igneous complexes (Figure 1 and 2)(Johnson et al., 1996; Catuneanu et al., 2005). The Permian fluvio-lacustrine Abrahamskraal and Teekloof formations are the oldest formations of the Beaufort Group in the main Karoo Basin, and, represent the first fluvial deposits within the Karoo Supergroup. The formations are underlined by a transitional succession that captures the deeper marine/lacustrine deposits (Lower Ecca Group) as well as the shallower shelf, beach and deltaic deposits (Upper Ecca Group)(Johnson et al., 1996; Catuneanu et al., 2005). The stratigraphy of the Karoo Supergroup in the southern main Karoo Basin in presented in Figure 3.

2.1. General Geographic Setting of main Karoo Basin and Study area

Karoo basins, which is a name given to similar aged basins to main Karoo Basin of South Africa (Catuneanu et al., 2005), are spread all over southern Africa. These basins comprise of Late Palaeozoic to Early Mesozoic deposits that formed during the time of Gondwana (Johnson et al., 1996; Catuneanu et al., 1998, 2005). In southern Africa, this succession is called the Karoo Supergroup and is mainly found in the extensive main Karoo Basin of South Africa, in the Kalahari Karoo Basin and in many subsidiary basin in South Africa, Namibia, Botswana, Zimbabwe and Mozambique (Johnson et al., 1996)(Figures 1 and 3). Furthermore, Karoo-like deposits are found not only in sub-Saharan Africa (as far north as Angola and DRC), but also in South America, Australia and Antarctica (Catuneanu et al., 1998).

In the main Karoo Basin, even the similar aged rock formations show different facies in the different parts of the basin due to the sheer size of the depositional area. For this research, two study areas exposing the transition of the Permian Abrahamskraal and Teekloof formations (both part of the Lower Beaufort Group) were chosen, because they were reported to expose different facies along the E-W strike of the main Karoo Basin. The western study area has an extent of ~100 km and is located about 400km northeast of Cape Town, between the towns of Sutherland, Fraserburg, Beaufort West and Leeu-Gamka in the Western Cape Province (Figure 1B). The eastern study area is ~60 km in extent and is located east of the Jansenville in the Eastern Cape Province (Figure 1B). The study areas present good exposures of the target formations in form of road cuts, hillsides and incised valleys (detailed outcrop locations can be found in the appendices, Ch. 6.3, Table 13).

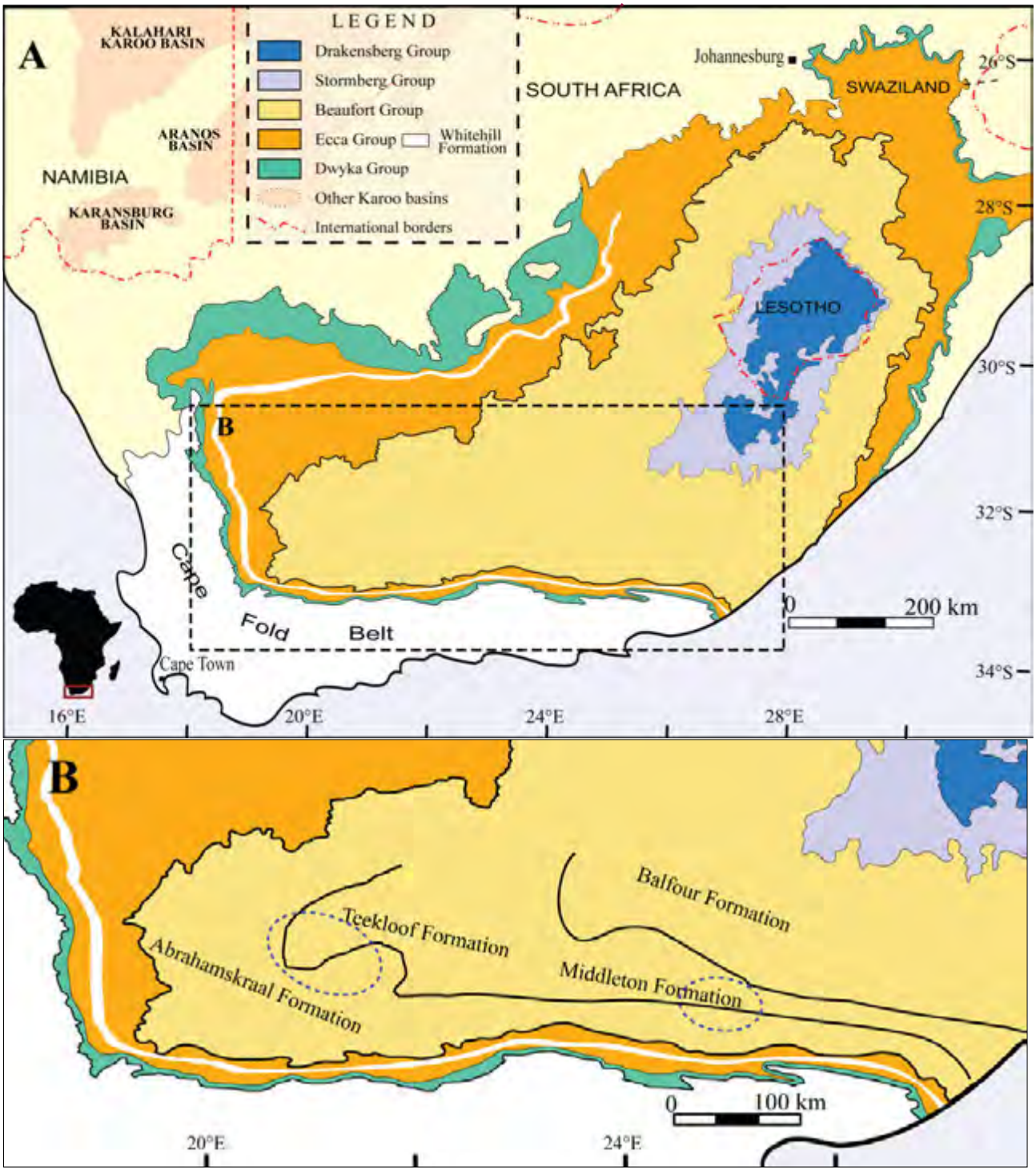

Figure 1: Geological map of the main Karoo Basin in South Africa (**A**), the study areas (blue dashed circles) and the formations forming the Lower Beaufort Group (**B**).**A**- The Karoo Supergroup covers 2/3 of the South Africa, and its sedimentary sequence starts with the glacial deposits of the Dwyka Group (Late Carboniferous), and ends with the mainly aeolian deposits of the Clarens Formation (Stormberg Group). The sedimentation in basin was terminated by the emplacement of the extrusive volcanic and sub-volcanic complex of the Drakensberg Group some ~183 Ma. **B** shows the spatial distribution of the formations in the Lower Beaufort Group (Adelaide Subgroup) highlighting the two study areas, confined to the transition of the Permian Abrahamskraal and Teekloof formations, found in the southwest and southeast parts of the basin. Note that east of longitude 24°E, the Teekloof Formation transitions into the Middleton Formation. The need for these regional formation names is currently being reviewed by the Karoo Task Group of the South African Stratigraphic Committee.

2.2. Tectonic setting of the Karoo Supergroup

The main Karoo Basin of South Africa is generally accepted to have been a retro-arc foreland basin (Johnson et al., 1996; Catuneanu et al., 1998) as shown in Figure 2. Nevertheless, some workers consider that a purely retro-arc foreland basin model does not adequately explain the evolution of the basin (e.g., Turner, 1999; Tankard et al., 2009, 2012; Lindeque et al., 2012). With regards to the subsidiary Karoo Basins, there is a general consensus, and, almost all of them are reported to be intra-cratonic thermal sag basins or rift basins with northern or north-western faults systems (Johnson et al., 1996; Catuneanu et al., 2005; Tankard et al., 2009).

Catuneanu et al.(1998) argues for a purely retro-arc foreland basin model for the generation of the main Karoo Basin. The model explains the observed stratigraphic relationships in the basin as the result of the flexural behaviour of the Gondwanan lithospheric plate (Figure 2) which reacted to the compressional tectonic setting that was generated because of the subduction of the Palaeo-Pacific Plate under the supercontinent and the pene-contemporaneous formation of the Cape Fold Belt. The different periods of supracrustal loading and unloading events during the Cape Orogeny strongly influenced the evolution (rates and spatial movement direction of the depocentre) of the major flexural tectonic provinces in the basin, namely, the foredeep, forebulge, backbulge, foreslope and foresag from the Late Carboniferous until the Early Jurassic. A disputing hypothesis by Tankard et al.(2012) suggests that the Cape Orogeny only started playing a role in the evolution of the main Karoo Basin much later, from the Early Triassic (~240Ma) onwards. In addition, Tankard et al.(2012) proposes a model where the main Karoo Basin was initiated by rigid basement block movement associated with crustal faults and lithospheric deflection due to subduction-driven mantle flow.

Turner (1999) on the other hand, indicates that a purely foreland basin model does not properly explain the deposits of the Upper Karoo Supergroup. This model speculates that a mantle-plume induced thermal anomaly created crustal deformation, volcanism and extensional regimes from the mid-Triassic (~230Ma) onwards, affecting the stacking patterns of the Upper Karoo succession.

According to the retro-arc foreland basin model (Catuneanu et al., 1998), the main Karoo Basin was characterised by two first-order tectonic events of (1) orogenic loading and (2) unloading, respectively (Figure 2). During the Permian, the southern main Karoo Basin accommodated what are called the proximal stratigraphic facies. Those developed in the proximal foredeep depression formed due to a continuous large-scale subsidence (thus base-level rise) driven by the orogenic loading of the Cape Fold Belt (Figure 2B).

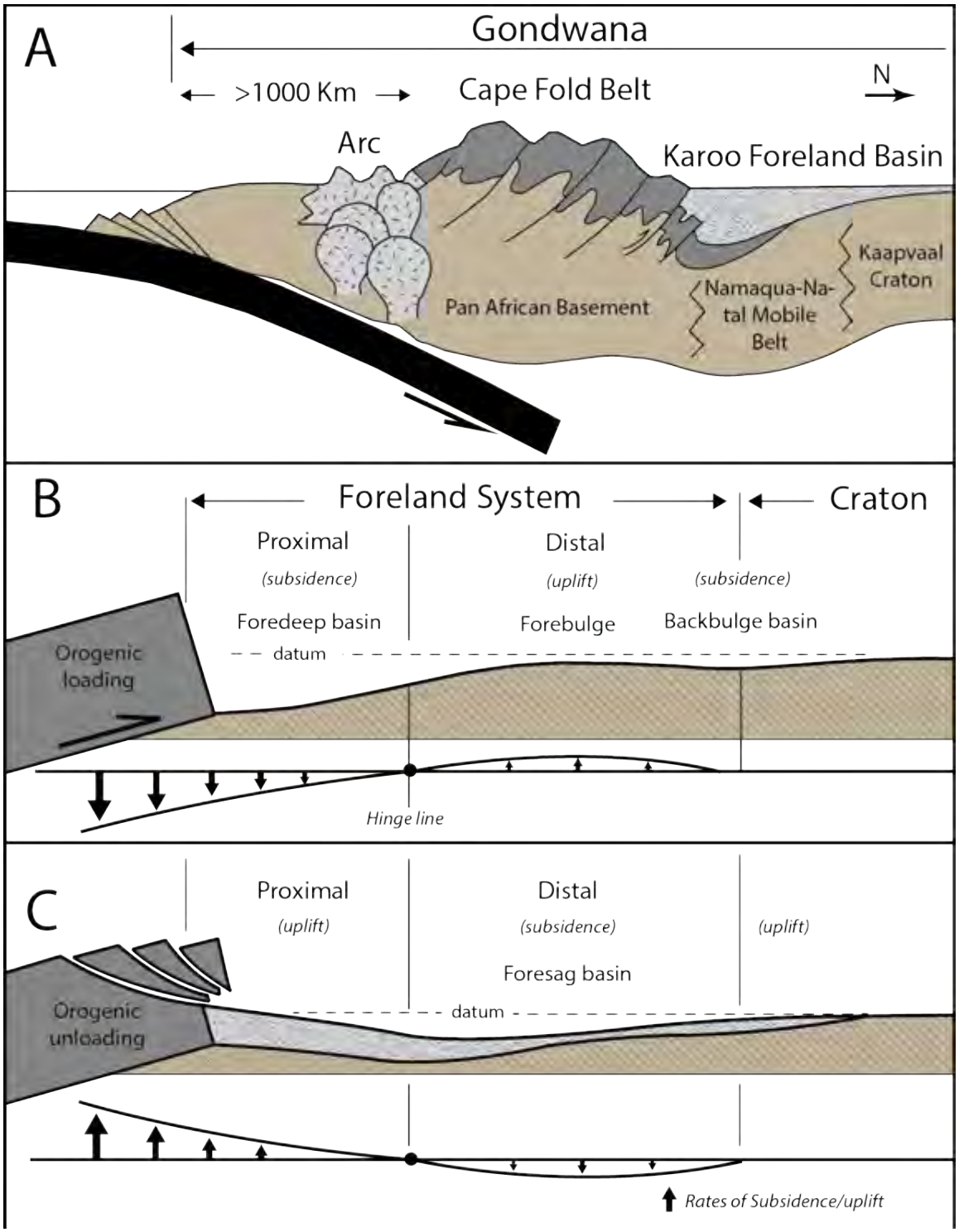

Figure 2: Geotectonic setting (A) and the different flexural provinces (B, C) developed across the southern margin of Gondwana during the evolution of the Karoo retro-arc foreland basin. This model suggests that the formation of the main Karoo Basin was a result of the subduction of the Palaeo-Pacific Plate underneath the southern margin of Gondwana. The simultaneous rise to the Cape Fold Belt as an orogenic load resulted in flexural down-sagging of the overriding plate. The different flexural provinces within the basin (i.e., foredeep, forebulge, back-bulge, foreslope and foresag) were created by episodes of loading and unloading of the Cape Fold Belt, and explain the spatial facies distribution and vertical stacking patterns observed in the Karoo Supergroup. Figure adapted from Catuneanu et al. (1998).

2.3. Stratigraphy of the Karoo Supergroup

The succession of the Karoo Supergroup is of extreme importance to South Africa's economy as well as its scientific community, because it contains large deposits of different ore minerals, fossil fuels (De Wit, 2011), and offers a window into the deep past of continent's geological evolution. Furthermore, the Karoo strata also encloses a world renowned fossil heritage, which is the backbone of its biostratigraphic subdivision (Cole and Wipplinger, 2001; Hancox and Rubidge, 2001).

Lithologically, the Karoo Supergroup is subdivided into five groups, which in ascending order are: the Dwyka, Ecca, Beaufort, Stormberg and the Drakensberg Groups (Figures 1 and 3)(Johnson et al., 1996). The thicknesses of the different Karoo strata vary from the south to the north, and most units become thinner towards the north (Catuneanu et al., 1998; Bordy et al., 2005).

The Karoo sedimentation started with the glaciogenic deposits of the Dwyka Group in the Late Carboniferous (Figure 3). This unit comprises mainly tillites and diamictites, and is subdivided into a southern (proximal), laterally continuous marine facies (Elandsvlei Formation), and, a northern (distal), irregular terrestrial and subaqueous facies (Mbizane Formation)(Visser, 1986; Johnson et al., 1996; Catuneanu et al., 1998). The Dwyka Group has a paraconformable lower contact with the Witteberg Group of the Cape Supergroup(Johnson et al., 1996). The upper boundary is diachronous and conformable with the Prince Albert Formation of the Ecca Group. The Group has a maximum thickness of ~800m (Visser et al., 1990) in the south.

The Early Permian-Middle Permian Ecca Group contains siltstones, sandstones, greywackes and gas- and coal-bearing shales that show different facies across time and space (Figures 1 and 3). This is partly because in the south the Ecca Group consists of deep marine, laterally extensive deposits (e.g., Prince Albert and Whitehill formations), that grade into shelf turbidites (e.g., Laingsburg and Ripon formations) followed by shallow marine and shore deposits (e.g., Waterford and Volksrust formations). In the north, the Ecca Group is known for its large coal deposits (Vryheid Formation) (Cadle et al., 1993; Johnson et al., 1996) and for its well-documented, *Glossopteris*-dominated flora, invertebrates and vertebrates as well as trace fossils. The Ecca Group attains a maximum thickness of 3000 m (Catuneanu et al., 2005), and both its upper and lower boundaries are conformable and diachronous.

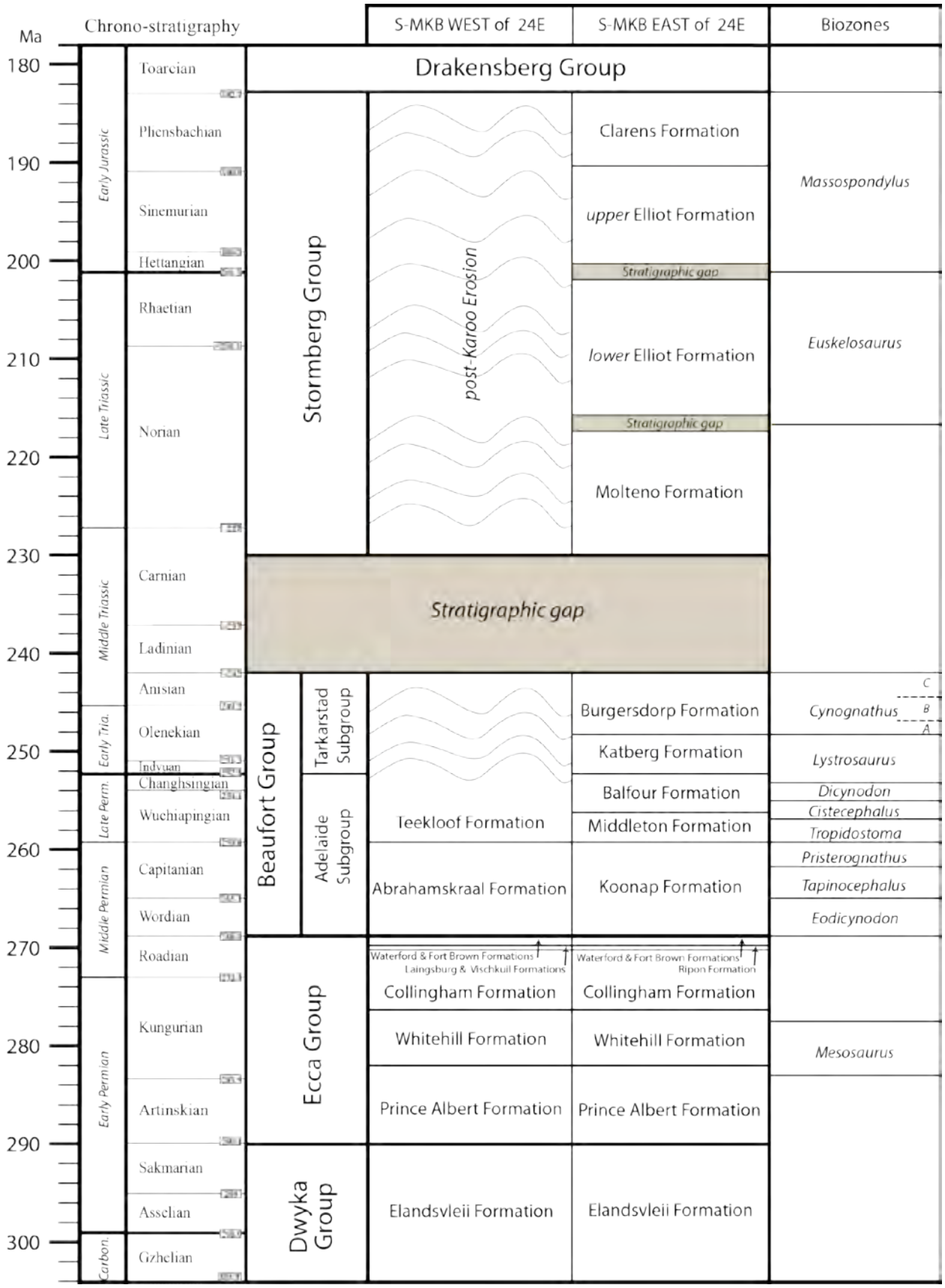

Figure 3: The litho- and bio-stratigraphy of the Karoo Supergroup in the southern main Karoo Basin (S-MKB). The Karoo Supergroup succession started some 304 Ma ago with the glaciogenic deposits of the Dwyka Group and it was terminated by the extrusion of basaltic lavas of the Drakensberg Group in the Early Jurassic (~183 Ma). This stratigraphic table shows the nomenclature of the Karoo Supergroup in the proximal (southern) facies only. Modified after Rubidge(2005) and Rubidge et al.(2013).

The Middle Permian to Middle Triassic Beaufort Group, consists of continental (i.e., alluvial and lacustrine) clastic sedimentary rocks, that are mainly mudstones and sandstones with a cumulative thickness of ~5000 m (Rubidge, 2005)(Figures 1 and 3). In contrast to the diachronous and conformable lower contact with the Ecca Group, the Beaufort Group is separated from the overlying Stormberg Group by the largest stratigraphic gap within the Karoo Supergroup (~12 Ma) (Johnson et al., 1996; Catuneanu et al., 1998; Rubidge, 2005), also known as the "Ladinian Gap" (Veevers et al., 1994) or the "Mid-Triassic Lacuna" (Figure 3)(Cole, 1992).

The Beaufort Group preserves outstandingly rich and fairly diverse vertebrate fossil assemblages that are dominated by pre-mammalian land-dwelling tetrapods (Keyser and Smith, 1978; Hancox and Rubidge, 2001; Rubidge, 2005). The succession is considered a global biostratigraphic standard for the Middle Permian to Early Triassic vertebrates (Rubidge, 2005). The abundant therapsid fossil fauna of the Beaufort Group allowed the stratigraphic subdivision of the Beaufort Group into eight assemblage zones: *Eodicynodon, Tapinocephalus, Pristerognathus, Tropidostoma, Cistecephalus, Dicynodon, Lystrosaurus and Cynognathus*(Figure 3) (Rubidge, 2005).

The Late Triassic to the Early Jurassic Stormberg Group is made up of a basal fluvio-lacustrine succession (Molteno and Elliot Formations) and an upper, mainly aeolian unit of the Clarens Formation (Figures 1 and 3) (Bordy and Catuneanu, 2001). The Stormberg succession is over 1000 m thick (Catuneanu et al., 2005) and contains several stratigraphic gaps within and between the formations (Bordy et al., 2005). The Group conformably grades into Drakensberg Group.

The Karoo sedimentation was terminated by the extrusion of the lavas and emplacement of the subvolcanic complex of the Drakensberg Group some ~183±1 Ma ago (Figures 1 and 3)(Duncan et al., 1997). The extrusive and intrusive igneous rocks of the Group are mainly basaltic, and locally andesitic in composition; they attain a preserved thickness of~1400m (Johnson et al., 1996). The Drakensberg Group, though only sedimentary in nature in its lowermost part, is still part of the Karoo Supergroup as it marks the end the tectonic cycle that predates the break-up of Gondwana (Catuneanu et al., 1998; Turner, 1999).

2.3.1. SW AND SE MAIN KAROO BASIN

In the southern part of the main Karoo Basin, where the key study areas are situated (Figure 1B), the Karoo Supergroup is made up of the Dwyka, Ecca and Beaufort groups. This region of the main Karoo Basin represents the so-called proximal facies of the different tectono-stratigraphic depositional settings of the foreland basin model (Catuneanu et al., 1998)(Figure 2). To date, no major stratigraphic gaps have been documented in the south main Karoo Basin. In the SW (west of longitude 24°) this conformable succession abruptly terminates in the Lower Beaufort Group (Teekloof Formation, see Figure 3), due to post-Karoo uplift and erosion events, and is

uncomfortably overlain by recent Cenozoic sediments (Keyser and Smith, 1978; Johnson et al., 1996). East of longitude 24°, the succession is more complete, and includes the Upper Beaufort Group, the "Ladinian Gap" and the Lower Stormberg Group (Figures 1 and 3).

In the study area (Figure 3), the Elandsvlei Formation of the glaciogenic Dwyka Group was deposited during the 1st-order cycle of supra-continental loading of the basin, which resulted in the proximal foredeep environment (Figure 2B), the so called Karoo Sea or Karoo Trough (Visser, 1986; Johnson et al., 1996; Catuneanu et al., 1998). The diamictites of the Elandsvlei Formation were deposited in open waters from suspension settling (from floating and melting ice-sheets) and debris-flow (from semi-grounded melting ice sheets), which explain the large lateral extent of the Dwyka Group.

The Ecca Group is composed of sixteen formations, which reflect the increased lateral facies variations in the basin during the Permian (Figure 3)(Johnson et al., 2006). In the south, the main formations in ascending order are: Prince Albert, Whitehill, Collingham, Ripon, Fort Brown and Waterford formations. Climatically, the end of the Dwyka glaciation event in the Early Permian is the main factor that allows the differentiation of the Ecca Group lithologies from the underlying Dwyka Group. The southern Ecca Group was deposited in the foredeep during the first order loading phase of the Karoo foreland basin (Figure 2).The Lower Ecca Group units (up to the Collingham Formation)are dominated by deep water deposits, while the post-Collingham formations (e.g., Laingsburg, Rippon, Waterford formations) comprise sub-aqueous fan, clastic shelf, nearshore and deltaic sediments (Figure 3).

The Beaufort Group is subdivided into the Permian Adelaide and the overlying Triassic Tarkastad Subgroups (Figure 3). The Adelaide Subgroup occupies the south of the basin, and is made up of the Abrahamskraal, and the overlying Teekloof (western facies) and Middleton (eastern facies) formations (Johnson et al., 1996, 2006; Day and Rubidge, 2014). The Permian fluvio-lacustrine Lower Beaufort Group was deposited during the several second order tectonic unloading and loading events of the Cape Fold Belt, which resulted in the uplift and subsequent subsidence events in the southern main Karoo Basin (Catuneanu et al., 1998)(Figure 2C).

3. Methodology

AN OVERVIEW

The methodology applied in this research relies on both qualitative and quantitative approaches as well as their integration. Qualitative and semi-quantitative studies, such as facies analysis, aid the identification and interpretation of the sedimentary units especially in the field. However, emphasis is also put on the different quantitative methods (e.g., X-ray diffraction and fluorescence: QXRD and XRF), point counting for sandstone provenance, because these improve the reliability of interpretations and allow better comparisons with other studies. Illustrated summaries on the principles behind the applied methodology are presented in Figures 4, 5, 6, 7 and 8. More specifically, the different methods applied in this study are:

- Sedimentary facies analyses, mainly based on the fluvial lithofacies analysis work of Miall (1996, 1985, 1987) (Table 1, Figures 4, 5 and 6);
- Quantitative facies analyses, mainly based on the work of Gibling (2006) and Colombera et al. (2013), and which entails the quantification of: (a) the architectural elements making up the internal geometry of outcrops (Figure 9, Tables 2 and 3); as well as (b) the external geometry, i.e. dimensions (Figure 10, Table 4) and general architecture;
- Palaeocurrent analyses, mainly based on the orientation measurements of ancient flow indicators and their assessment via rose diagrams;
- Petrographic analyses, which include microscopic description of textural properties and point counting of the compositional phases in sandstones (i.e., modal analysis of mineral and rock fragments)(Ingersoll et al., 1984; Dickinson, 1985);
- Sedimentary geochemical analyses, which uses X-ray spectroscopy of samples with X-Ray Fluorescence (XRF) and X-Ray Diffraction (XRD).

In this outcrop-based study, data on internal and external architecture of the strata was gathered in two distinct study areas in the southern main Karoo Basin (Figure 1B). All visited sites are listed in Table 15 (in the appendices). They are natural exposures on hillsides, incised valleys and artificial road-cuttings. Outcrop documentation followed the modus operandi of facies analysis (Figure 6), in other words the following observations were made in the field: main rock types, grain sizes, sedimentary structures, colours, bounding surfaces and the shape and dimensions of the sedimentary units. To digitally capture the field data for detailed facies studies, photographs taken perpendicular to outcrops were photo-merged and traced (Wizevich, 1992; Miall, 1996).

3.1. Sedimentary Facies Analysis

Facies analysis method constitutes the backbone for the interpretation of ancient sedimentary processes and depositional settings that are preserved in the sedimentary rock record. This method relies on the observation and identification of the physical and/or biological properties of the sedimentary rocks (i.e., the sedimentary facies). In addition, through their comparison to the "building blocks" (i.e. bio- or lithofacies) of idealised facies models, interpretations about the origin of the sedimentary facies can also be made. The use of facies models (Figure 4) began in the 1960s when a variety of models had been created that were specific to certain depositional environments (Miall, 1985; Walker, 1984).

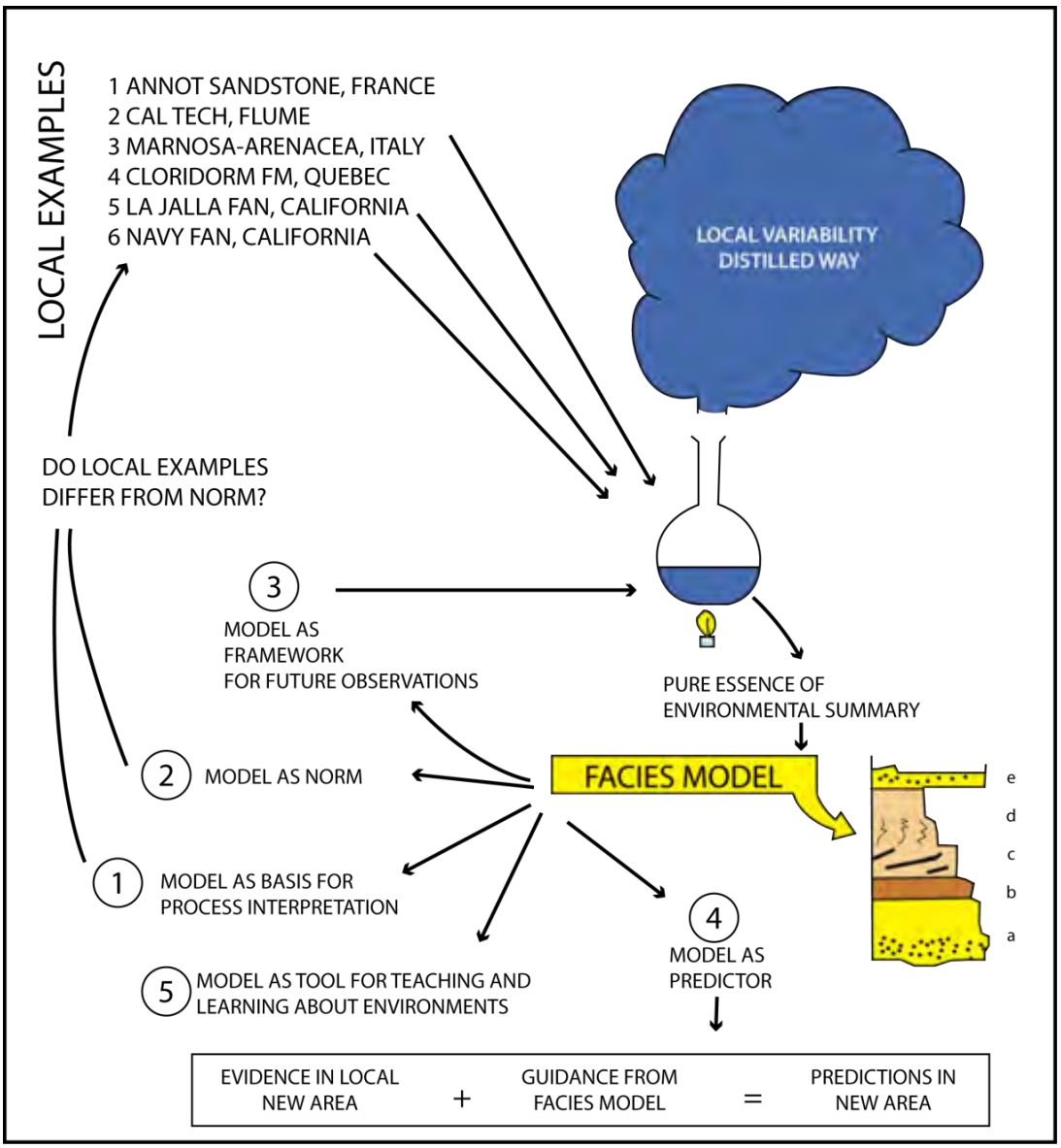

Figure 4: The five main uses of facies models and the process involved in generating and improving facies models. Modified after Walker (1984).

Fluvial lithofacies models are among the more studied and most complete sedimentary facies models (Bordy, 2000). They are based on ideas of Allen (1983) and Miall (1985, 1996) who were instrumental in developing the currently used schemes for the description and classification of ancient fluvial systems. Central to the concept of fluvial facies models is the idea that fluvial systems are made up of units that are repeated, hierarchical and predictable, and therefore, their systematic and hierarchical study will likely result in an effective understanding of the genesis of these complex, heterogeneous systems (Figure 5).

The basic building blocks of fluvial facies models are the lithofacies types, which are termed **facies elements**. The lithofacies classification scheme adopted here, based on the work of Miall (1985, 1988, 1996), is a descriptive approach of the strata that assesses key sedimentary properties, namely: the grain-size and textural features of the rocks. Lithofacies are codified primarily according to the main grain size, as well as the sedimentary features of the facies (e.g., “G” for “gravel” or “m” for “massive"). In this study, 22 basic lithofacies units were identified, and are shown in Table 1.

Facies associations are groups of a number of facies elements that form together under specific depositional circumstances. A lithofacies association with a distinctive 3-D geometry, is called an **architectural element** (AE)(Miall, 1985; Colombera et al., 2013; Wilson et al., 2014). AEs are defined as components of a fluvial depositional system with characteristic facies association that are interpretable as sub-environments. They are genetic units, therefore, interpretations are inheritably associated with their descriptions (Colombera et al., 2013; Wilson et al., 2014).

In the process of facies analysis, the identification of architectural elements, i.e., facies associations, is the next step in the hierarchical chain of the modus operandi (Figure 6). Originally, 9 main architectural elements were proposed by Miall (1985; 1996), however, in recent years, modification to this scheme was undertaken by different authors (Gibling, 2006; Reading, 2009; Colombera et al., 2013). The nomenclature of architectural elements used in this study is adapted from Colombera et al. (2013) (Table 3) who in essence modified Miall’s scheme (Miall, 1985, 1996). The same nomenclature is used in the FAKTS (Fluvial Architecture Knowledge Transfer System) database by the Fluvial and Eolian Research Group at Leeds University, and it is hoped that the results of this study would be integrated into that dataset with time.

The classification and identification of the architectural elements builds upon the criteria proposed by Miall (1985, 1996), and it is based on the nature of their **bounding surfaces**, geometry, scale and internal organization of the sedimentary facies found within them (Gibling, 2006; Colombera et al., 2013). Because architectural elements are 3D depositional units, they are laterally variable and bounded by various types and scales of surfaces (Table 2); (Miall, 1985; Colombera et al., 2013).

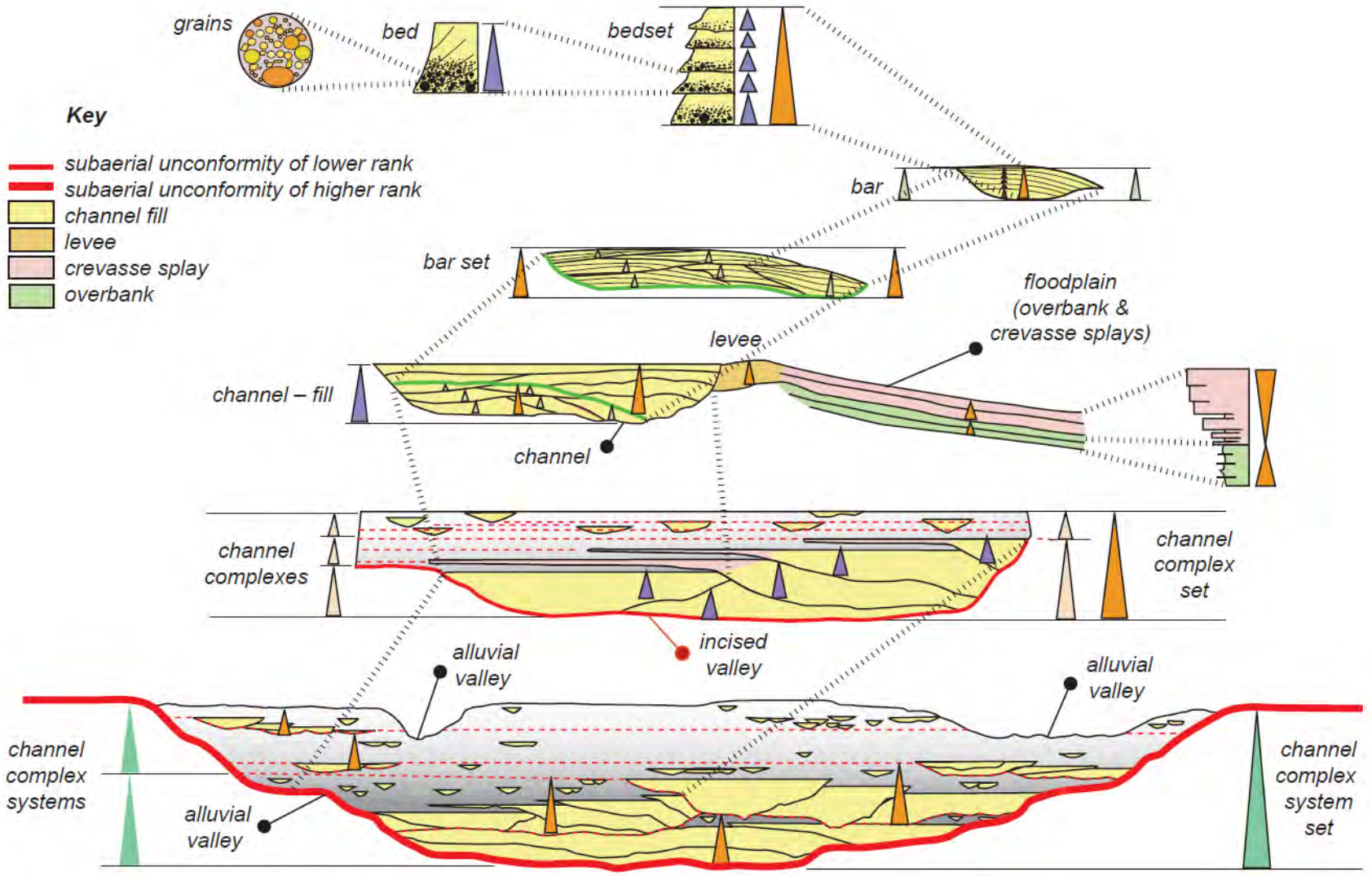

Figure 5: Illustrations of the hierarchical nature of fluvial lithofacies and assemblages that they build. Note that the geometries and internal characteristics are not only hierarchical, but also repeated (e.g., smaller channels in larger, higher order channels) in fluvial systems, adding further elements of complexity to these systems. Adapted from Miall (2013).

Table 1: Fluvial Lithofacies encountered in this study, their codes, descriptions and interpretations (modified after Miall, 1985). W1, W2 - subareas 1 and 2, in the western field area. E - Eastern field area.

Facies Code	Facies description	Interpretation	Abrahamskraal Formation			Teekloof Formation		
			W1	W2	E	W1	W2	E
Gmm1	Gravel, matrix-supported, massive breccias. Clasts (av. 5 cm) are sandstones granule/pebbles, mudstones, concretions. Weak grading.	Mostly found at the base of new channel deposit sequences (i.e. basal gravel). Form from plastic debris flow during bank collapse, due to renewed channel flow strength. Lack of structures means rapid flow speed reduction and/or rapid decrease in sediment overload.	√	√	√		√	√
Gmm2	Gravel, matrix-supported, massive breccias. Clasts (av. 9 cm) are mostly rip-up mudstones chips. Concretions and sandstone pebbles are common. Described as clast rich sandstones. Weak to normal grading.	Mostly found in the middle of channel sequences. Termed as intra-formational gravels. Form from plastic debris flow, due to sudden renewed channel flow strength. Grading may indicate a consist waning of channel flow strength.	√	√	√		√	√
Gcm	Gravel, clast-supported, massive conglomerates. Clasts (av. 10cm) are mainly sandstones granules/pebbles and concretions. Mudstones and fossilised wood are found. Weak Grading.	As in Gmm1. Roundness of sediment may indicate long travel distances or high energy grinding action.		√	√		√	√
Gch	Gravel, clast-supported, horizontal bedded conglomerates. Clasts (av. 5cm) are sandstones granules/pebbles, mudstones, concretions and fossilised wood. Weak grading.	Basal gravels. Form by longitudinal bedforms in open channels. Possibly produced during lower frequency, high magnitude discharge events. Horizontal bedding indicates sustained flows.	√		√			√
Sm	Sand, mostly fine, occasionally medium and rarely coarse grained, massive.	Sediment-gravity flow deposits, very high deposition rates. Alternatively internal structures destroyed by bioturbation, dewatering or weathering.	√	√	√	√	√	√
Sh	Sand, mostly fine, occasionally medium and rarely coarse grained. Horizontal laminations.	Upper flow regime in shallow water depths, plane-bed flow conditions destroying dunes and ripples.	√	√	√	√	√	√
Sl	Sand, mostly fine, occasionally medium. Low angle (<10°) cross-beds.	Large scale dunes and barforms. Scour fills, humpback or washed-out dunes, antidunes. Sl may also form from lateral migration the channel.	√	√	√	√	√	√
St	Sand, mostly fine, occasionally medium and rarely coarse grained. Trough cross-beds.	Common at the base of channel storey elements. Forms from the migration of 3D sinuous-crested and linguoid dunes. Higher flow regime than Sp.	√	√	√	√	√	√
Sp	Sand, mostly fine, occasionally medium and rarely coarse grained planar cross-beds (~ 30°).	Commonly found at the base of channel belts. Forms from migration of dunes (transverse bedforms). May also form in lateral migration channel.	√	√	√	√	√	√

Sr1	Sand, very fine to fine, climbing ripple cross laminations.	Represents low flow regime. Sr can form on levees, crevasse channels and point bars during waning phases of flow.	√	√	√	√	√	√
Sr2	Sand, very fine to fine, wavy or trough ripples (flasers).	Migration of ripples in a lower flow regime. Mud drapes define the troughs and they occur when currents periodically stop allowing mud to settle.			√			
Ss	Sand, fine to very coarse, may be pebbly, broad shallow scours. Normal grading.	High energy flow scour-structures filled by sediments during the waning phase of floods. Grades into fines facies.	√	√	√	√	√	√
Sb	Sand, very fine, often fine and occasionally medium grained. Ball-and-pillow structures and convolute laminations.	Soft sediment deformation caused by water escaping the sediments. Due to fast rates of sedimentation disrupting previously settled deposits.	√	√	√	√	√	√
Fl1	Fines, mud size, laminated, purple-red colour.	Waning flood deposits in overbank or abandoned channels. Purple-red colour may indicate subaerial and oxidizing conditions shortly after deposition.	√	√	√	√	√	√
Fl2	Fines, silt size, laminated, olive green grey colour.	Waning flood deposits in overbank or abandoned channels. Green-grey colour may indicate subaqueous and reducing conditions shortly after deposition.	√	√	√	√	√	√
Fsm1	Fines, mud size, weakly laminated to massive, purple-red colour, blocky weathering.	As in Fl1. Absence of laminations may indicate either quick deposition (e.g. mass-movement), or bioturbation.	√	√	√	√	√	√
Fsm2	Fines, silt size, massive, olive green grey colour, blocky weathering.	As in Fl2. Absence of laminations may indicate either quick deposition (e.g. mass-movement), or bioturbation.	√	√	√	√	√	√
Fb	Fines, silt/mud size, ball-and-pillow structures and convolute bedding.	As in Sb.	√	√	√	√	√	√
Fm	Fines, silt/mud, massive, desiccation cracks	Overbank and abandoned channel deposits. Prolonged subaerial exposition causing mud-drapes to crack, indicating settings with low deposition rates.	√	√	√	√	√	√
Fr	Fines, silt/mud, massive, roots, bioturbation, mottling texture of colours (green grey and purple red).	Overbank, abandoned channel deposits, with strong indications of bioturbation (dendrites), rootlets. Mottling texture likely originates due to the imperfections in the matrix caused by the bioturbation, affecting the reducing/oxidizing reaction environments responsible for the colourations.		√	√		√	√
T	Very fine grained, often cherty layers	Volcaniclastic deposit consolidated subaerial volcanic ash fall.			√			
P	Paleosol with pedogenic concretion nodules, etc.	Ancient soil with chemical precipitation.	√	√	√	√	√	√

Table 1 continued

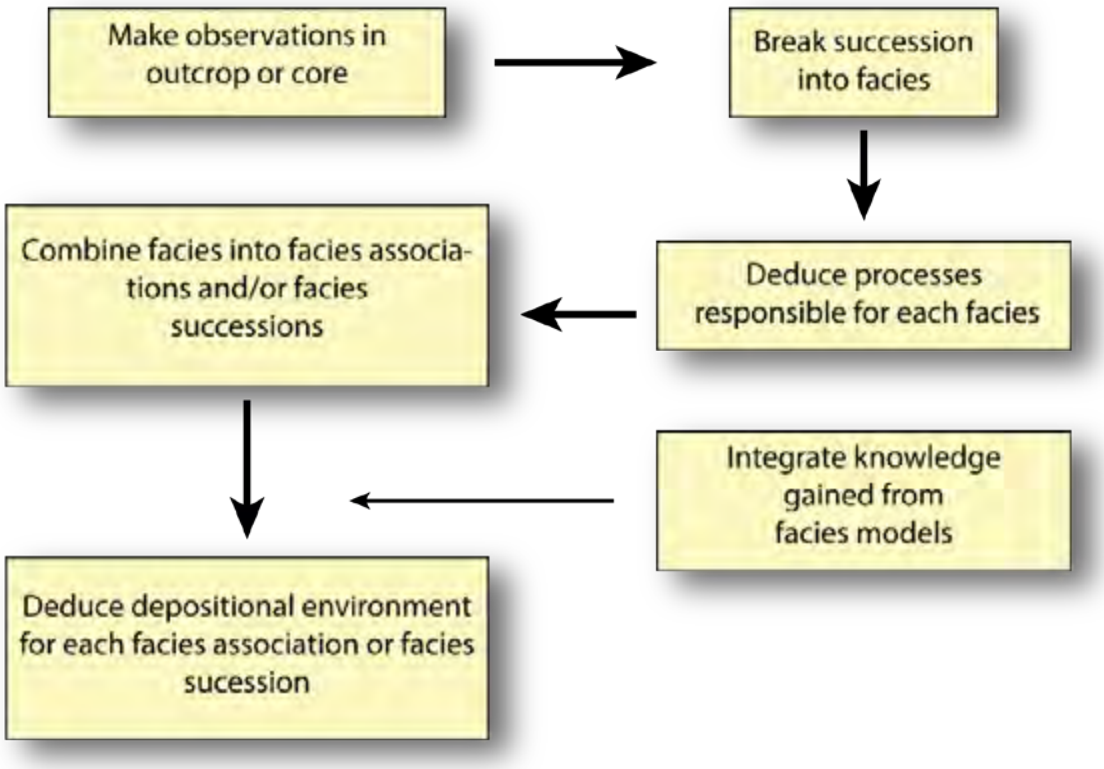

Figure 6: Flowchart illustrating the modus operandi in facies analysis. Note the hierarchical approach and the need to systematically describing sedimentary systems and organizing observations and measurements. Multiple working hypotheses are also recommended (modified after Walker, 1984) .

Bounding surfaces are subdivided into orders (rankings), based on observable characters such as lateral extension, erosional or accretionary features Table 2. Therefore, the recognition of the nature and rank of the bounding surfaces is an important element in facies analysis, however, in practice the attribution of order (rank) to these 3D objects is difficult, as bounding surfaces are interpretative in nature and are not always well-exposed (Bridge and Mackey, 1993).

Through the recognition, classification and numbering of hierarchically ordered sets of bounding surfaces, fluvial deposits are divided into two major groups (genetic packages) of larger scale **depositional elements**, namely: **Channel Complexes** (deposits formed within active fluvial channels) and **Floodplain with splay Complexes**, which includes all deposits formed adjacent the main channel, mainly through aggradational processes (Colombera et al., 2013). Figure 7 shows a schematic representation of the nomenclature and hierarchy of the elements, starting from AEs. Note that the full hierarchy for floodplain-related elements is often very difficult to decipher, because without good exposures it is very difficult to establish main boundaries and geomorphic relations between different splay complexes (Gulliford et al., 2014; Wilson et al., 2014). Thus the schematic hierarchy presented in Figure 7is not entirely applicable to floodplain elements, and that is the main reason why more emphasis is usually placed on Channel Complexes.

Table 2: Bounding surfaces. After Miall(1988) and Collinson(1996).

Order	Nature of the Surface	Significance and Process
1st	Separates individual cross-bedded sets	Migration of dune bedform under steady flow conditions.
2nd	Separates cossets of contrasting set type	Change in hydrodynamic conditions through time, related to short-term unsteady flow or local non-uniformity.
3rd	Inclined erosion surfaces within coset or group of cosets	Medium-term change in hydrodynamic conditions related to stage fluctuation or major shifting of flow across/around a bar form.
4th	Separates units with discrete accretionary integrity	Shift of bar/sub-channel pattern related to inherent channel flow stability or to reorganization during a major flood.
5th	Surfaces with a marked shift in grain size, bedform scale, etc. Laterally extensive with relief	Shifting and erosion of a channel floor. Isolated channels with relief reflect channel switching. Extensive surfaces within larger sandbodies record channel migration.
6th	Separates major channel sand bodies from contrasting facies (i.e. from fine-grained sediment or from different channel facies	Major change in fluvial regime. May record shifts or base level or climatic or tectonic changes

Sandstone bodies in channel complexes can often be qualitatively classified as the product of a certain fluvial style. The classification scheme used in this work is summarized in Figure 8 (Gibling, 2006). A simplified flowchart for classification can be found in the appendices (Figure 34). The classification is based on the dimensions, geomorphic setting and architecture of the deposits. Note that the system used here is an end-member classification system, where mobile channel belts are either braided or meandering rivers. In reality, that is not an accurate way of classifying all fluvial systems, which exist as a spectrum of styles between braided/low sinuosity and high sinuosity rivers. This simplistic system is used because it allows easier comparisons with data provided in Gibling (2006).

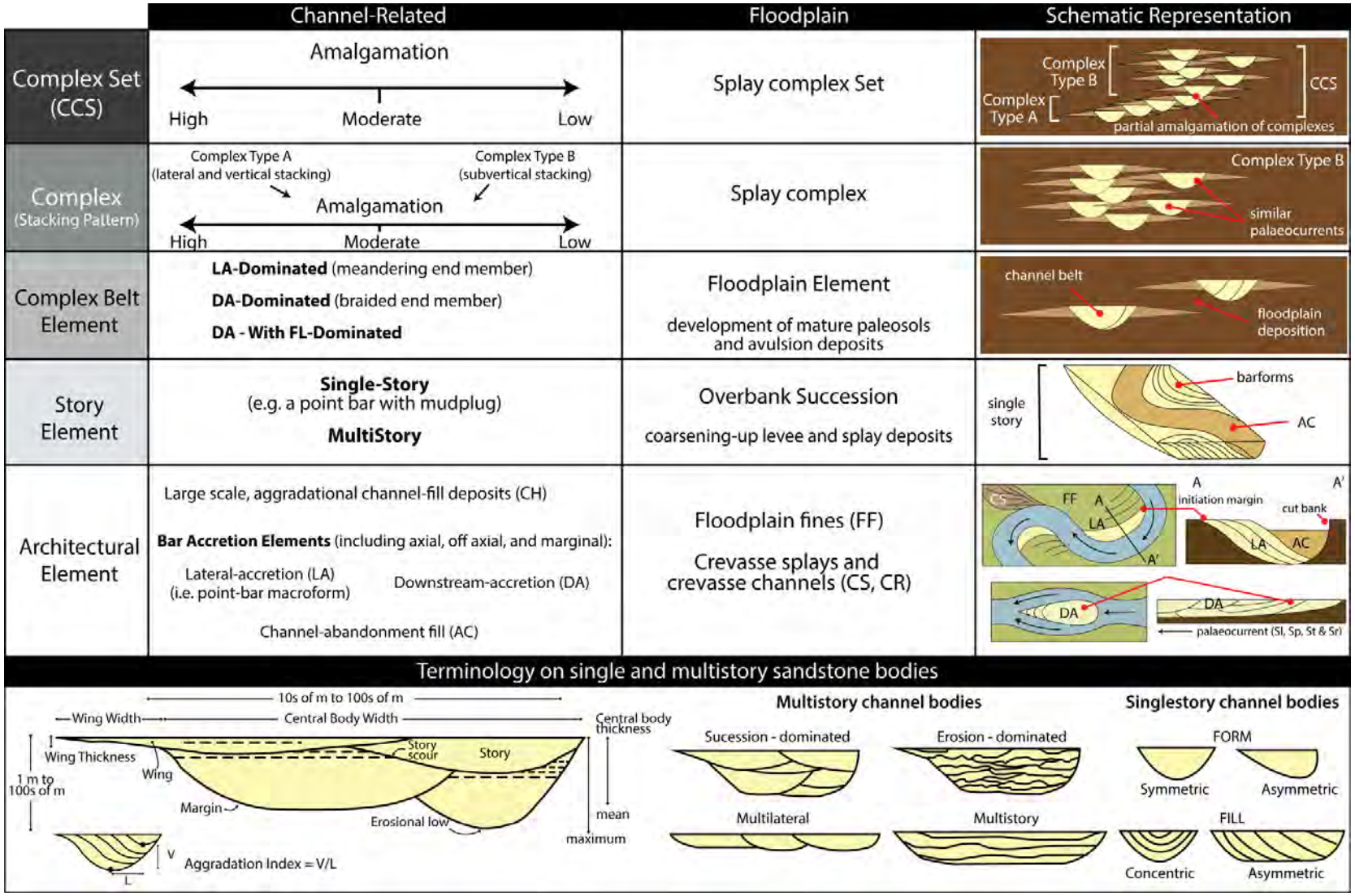

Figure 7: Schematic representation and terminology of the hierarchy of large scale fluvial building blocks from Architectural Elements (AEs) up to Complex Sets (CCS) and internal architecture of sandstone bodies. Note that for floodplain elements, the full hierarchy is less applicable, as it is very difficult to identify, correlate and separate floodplain element in the field. Facies and architectural elements descriptions used in this work are found in Table 1 and Table 3respectively. Concepts of hierarchical subdivision are derived from the works of Miall (1996), Payenberg et al. (2011) and Colombera et al. (2013). Figure adapted from Gibling (2006) and Gulliford et al. (2014).

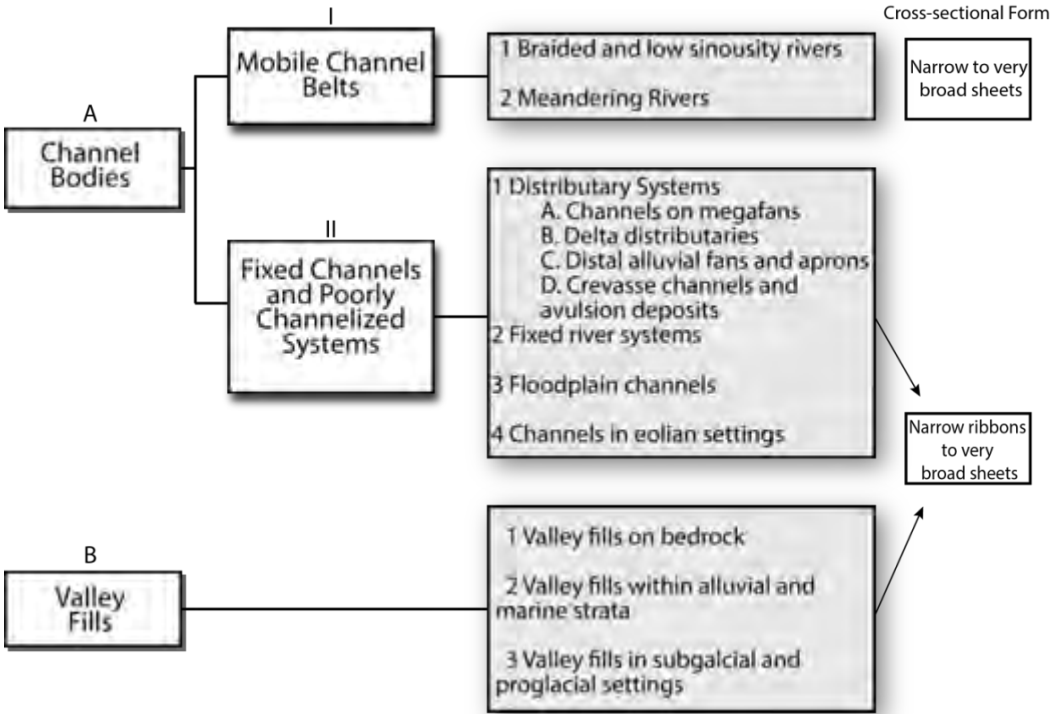

Figure 8: Qualitative classification of sandstone bodies based on their dimensions, geomorphic setting and architecture. Braided and meandering rivers are the end members of a spectrum of fluvial styles that include up to 16 fluvial styles. A more detailed qualitative subdivision is provided in Miall (1996). Figure adapted after Gibling (2006).

3.2. Quantitative facies analysis

Quantitative facies analysis uses the framework of traditional facies analysis methods which are qualitative in nature, and, implements them on quantification exercises over statistically representative number of outcrops (Colombera et al., 2013). This method assures a greater deal of confidence when interpretations are made or conclusions are drawn. Moreover, it provides a more robust basis for comparisons as well as proxies for numerical, graphical modelling of facies models and petroleum system simulation models at basinal scale.

Quantitative facies methods have become more prominent and relevant recently, mainly due to affordability and improvements in computing power and a shared interest in facies models by both academia and industry-based geoscientists (e.g., hydrocarbon exploration industry). Worth noting the research done by the Fluvial and Aeolian Research Group at Leeds University (FARG) and notably Drs L. Colombera and M. Gibling (Dalhousie University, Canada) whose work generated sophisticated databases has greatly advanced this method.

The quantitative approaches used in this work are:

(1) Evaluation of the Architectural Elements' (AEs) proportions in a given formation (Table 3). Three different methods of averaging the AEs results are used, because each method presents different degrees of implementation and errors (Colombera et al., 2013). **Method 1** averages out all genetic elements in the stratigraphic section of a given formation. Averaging Method 1 is easy to implement.

However, areas or stratigraphic portions with bigger sample sizes will be over-represented in the results. **Method 2** subdivides the stratigraphic section into subsets. This method presents a moderate difficulty of implementation, where final results are compiled as the average of all subsets. The drawback is that areas with low sampling size are over-estimated, since each subset will have the same weight in the final average. **Method 3** requires the quantification of the AEs within their respective depositional complex element (e.g. DA, LA, HO proportions within the Channel Complex; LV, CR within Floodplain Complex). Results for each stratigraphic section in question are then re-scaled according to the ratio of depositional elements in that section (i.e. the ratio of Channel Complex vs. Floodplain Complex). The different methods are illustrated in Figure 9.

(2) Quantitative and qualitative assessments of the external architecture of the dimensions of the sandstone bodies as detailed in Gibling (2006); and the assessment of the different overall Architecture Types (Wilson et al., 2014). The quantitative study relies on the use of the width-thickness ratio (W/T) of channel sandstone bodies for classification. Width vs. thickness plots are performed in a log-log scale. The procedure for obtaining the sandbody dimensions is illustrated in Figure 10; trigonometry (Equation 1) is used to derive the actual from the apparent dimension of the sandbodies. The classification scheme of the sandstone bodies according to their size is presented in Table 4. The qualitative classification scheme of channel sandstone deposits is a nomenclature-based system for palaeo-environmental interpretation (Figures 8 and 34). Further qualitative terminology, both descriptive and genetic, is shown in Figure 7.

Table 3: Architectural Elements identified in this study. Based on Miall(1985) and Colombera et al.(2013.)

Architectural Element	Geometry	Characteristics and interpreted Sub-environment
CH - Aggradational Channel Fill	Finger, lens or sheet	Vertically stacked depositional increments dominated by horizontal $2^{nd}/3^{rd}$-order bounding surfaces. Deposits are added onto downstream elongated incisional concave-upward bases. CH represents the overall aggradational infill of active channels.
LA - Lateral-Accretion Barform	Wedge, sheet, lobe	Laterally stacked depositional increments, onto sharp, 3^{rd}-order sub-horizontal to slightly concave-upward and often erosional bases. LAs represent the infill of channel belts by laterally migrating bars (e.g., meander point bars).
DA - Downstream-Accretion Barform	Lens, resting on a flat or channelled base	Downstream stacked depositional increments at low angle to the palaeo-flow onto sub-horizontal to slightly concave-upward and often erosional bases. Downstream-dipping low angle (<10°) $2^{n}d/3^{rd}$-order bounding surfaces. DAs represent the infill of channel belts by downstream-migrating bars.
DLA - Downstream and Lateral-Accretion Barform	Wedge, lens	DLAs differ from LAs and DAs in that bedding geometries are dominantly oblique accretions, with a combination of downstream accretions (downstream ends) and crossbar accretion (along flanks). Upstream and vertical-accretions are often observed but are volumetrically minor. DLAs represent the infill of channel-belts by the migration of bars that accrete both downstream and laterally in comparable proportions.

HO - Scour-Hollow Fill	Scoop-shaped hollow with asymmetric fill	Major scour-hollow fills with incisional concave-upward scoop-shaped bases, with inclined or horizontal surfaces or both. HOs represent the infill of deeply incised trough shaped scours within channel belts.
GB - Gravel Barform	Lens, ribbon	Coarse-grained (> granule) elements that commonly form in irregular erosional bases. Formation linked to migrating dunes/foresets; often fine upwards and downwards. Represent deposition during peak flow or high energy events.
SG - Sediment Gravity-Flow	Lobe, ribbon, sheet; interbedded with GB	Irregular, sharp but often non-erosional bases representing gravity-flow sheets/lobes. Genetically related to levees, or possibly a complex association of them.
AC - Abandoned Channel-Fill	Lens, Ribbon	Channelized, heterolithic unit dominated by vertical accretion of low deposition energy facies assemblages. Upper portion form in the ponded waters of abandoned channels from suspension settling and organic accumulation.
LV - Levee	Tapering wedges thin away from channel-belt margin	Heterolithic unit separating channels from the floodplain, with poorly defined base and internal surfaces that may off-lap and/or down-lap. Palaeo-flow is usually at high angles to the channel border. LVs represent the sedimentary and geomorphic expression of the most proximal overbank deposition next to channel-belt margins.
CR - Crevasses Channel	Lens, ribbon	Channelized, sandy unit with concave-upward base. The close association with other floodplain deposits (i.e. LV, CS, and FF) is a key feature for their identification. CRs represent the infill of channels emanating from the river into the adjacent floodplain and active during floods.
CS - Crevasse Splay or Lacustrine Deltas	Fan, tongue shaped. Flat and sharp lobes with slightly erosive bases	Sandy unit that borders channel-belt margins and thin away from them as they interfinger or grade laterally into other elements. Tabular bedding is common, but down-lapping internal accretion surfaces, dipping at low-angle are also possible as CSs record the progradation of the splay onto the floodplain or into standing bodies of water. No amalgamation of thin coalescing splays; differs CSs from LVs. Crevasse splays and lacustrine deltas are difficult to distinguish. CSs represent the sedimentary and geomorphic product of splay progradation and aggradation through the periodic unconfined flow from crevasse channels tapping channel-belts during floods.
SF - Sandy Sheetflood-Dominated aggradational floodplain	Tabular, Lenticular and usually vertically stacked bodies	Sandy unit with sharp, planar to irregular lower bounding surfaces that range from non-erosive to slightly erosive. Deposits are vertically stacked in an overall aggradational character. Since LV and CS are also sandy deposits produced by unconfined flows on the floodplain, the geomorphic expression and internal geometrical organization of the SF are fundamental to distinguish them from LV and CS elements. SFs are differentiated from FFs based on grain size, because the proportion of sandy deposits demonstrates that traction-current deposition is dominant over suspension settling.
FF - Overbank Fines	Thin to thick tabular blankets. Abandoned channel	Fine-grained, mudstone-dominated bodies with laterally persistent depositional increments that are vertically stacked and bounded by planar surfaces, demonstrating an overall aggradational character. Pedogenesis is common. FFs are the sedimentary expression of vertically aggrading flood basins, in which suspension settling from subaerial unconfined flows is the dominant process.

3.3. Palaeocurrent analysis

Palaeocurrent data provides essential information for palaeo-drainage and provenance reconstruction for the studied sedimentary succession. The palaeocurrent orientation data were obtained from various sedimentary structures e.g., parting lineation, trough and planar cross-bedding. Among the measured features in this study, trough and planar cross-beddings (St and Sp) are the most commonly measured palaeocurrent indicators in the lower Beaufort Group. The formation, accuracy and reliability of these palaeocurrent indicators have been theoretically modelled and empirically studied over the last decades (Reineck and Wunderlich, 1968; Duke et al., 1991; Bridge, 1997; Leclair, 2002).

A total of 117 palaeocurrent readings were gathered and the data were plotted using the rose diagram software Rose.Net (Table 6, Figure 28). General palaeocurrent direction, vector magnitude (or flow strength) and consistency ratio (or deviation from main direction) were among the results obtained.

3.4. Petrographic Studies

Petrographic analysis was performed using transmitted light microscopy on 30-µm-thick sandstone thin sections. This method provided insight into the mineralogical composition and textural properties of the sandstone such as grain size, sorting, roundness, matrix-content, etc. General textural descriptions and point counting of coarse-grained (>0.0625 mm) mineral phases were undertaken. The observed mineral proportions and textural features were the basis for comparisons (within and between formations) and also for better understating of the sedimentary processes that generated them.

Point counting is a modal analyses process that allows a relatively quick, semi-quantitative evaluation of the mineral phases in the rock, and the results can be used for provenance identification. During point counting, a total population size of 300 counts was obtained on coarse-grained mineral phases. Provenance studies were based on the *Gazzi-Dickinson methodology* and its further developments (Dickinson, 1970; Ingersoll et al., 1984; Cox and Lowe, 1995). Quartz-Feldspar-Lithics (QFL) ternary diagrams were utilized to plot the results of the modal analysis, and interpretations were drawn based on the representative provenance fields that subdivide the QFL diagram. The provenance fields considered are: Continental Block, Recycled Orogen and Magmatic Arc. Mineral phases counted are monocrystalline quartz (Qm), polycrystalline quartz (Qp), alkali feldspar (Kf), plagioclase feldspar (Pf), volcanic lithics (Lv), plutonic lithics (Lp), metamorphic lithics (Lm), sedimentary lithics (Ls) and accessory minerals (Accs) which included micas, opaque minerals, pyroxenes and amphiboles.

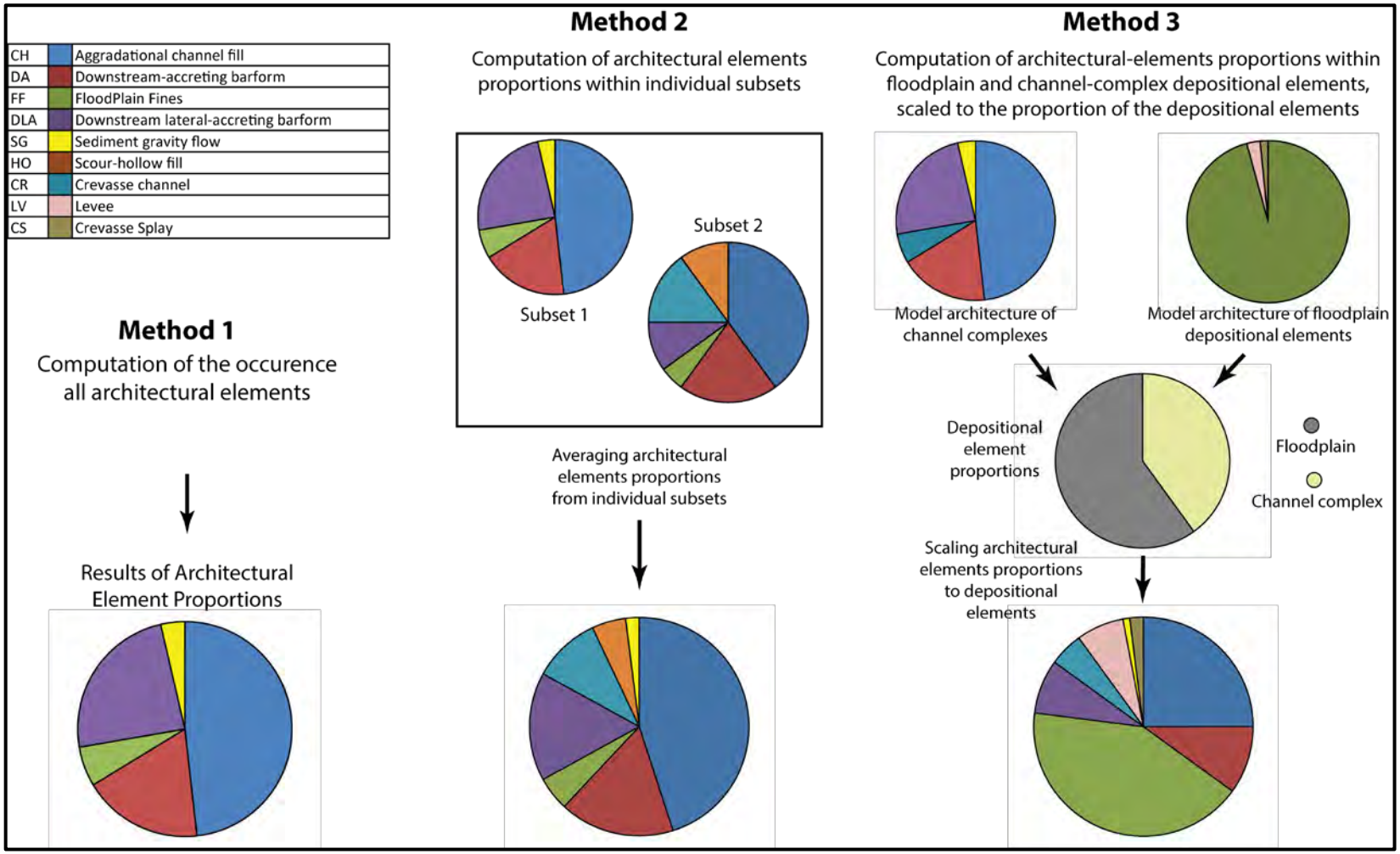

Figure 9: Representation of the different averaging methods used in the quantification of the architectural elements (AE). Different methods are used due to different degrees of difficulty of implementation, bias and confidence levels. **Method 1**, averages out all elements in a given formation or stratigraphic section. **Method 2** subdivides the target stratigraphic section into subsets, and the genetic elements (AE) are first averaged within each subset. Subset results are then averaged to a final result. **Method 3** requires the quantification of architectural elements within each depositional element, and then the results for the formation or stratigraphic section are re-scaled according to the proportions of depositional elements in the formation. Note pie charts are not to scale, merely used for visual representation. Adapted from Colombera et al. (2013).

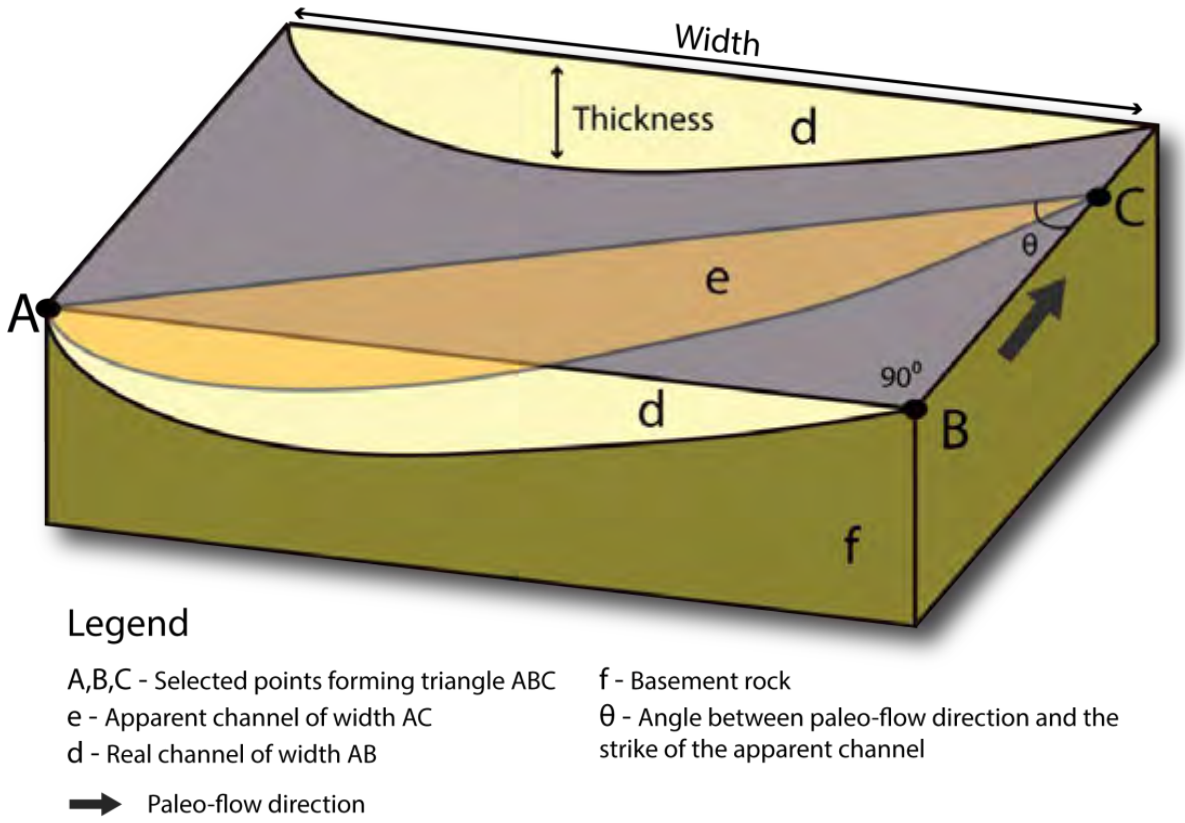

Figure 10: Schematic reconstruction of the true and apparent cross-sectional views of a channel body in an outcrop. Apparent cross-section of the channel body arises when the channel is exposed along cuts that are not perpendicular to the channel's longitudinal axis. The true dimensions of the channel can be estimated using the main palaeocurrent direction (a proxy for the channels longitudinal axis) and the apparent orientation and dimensions of the channel body. Adapted from Bordy (2000).

$$\frac{AB}{\sin\theta} = \frac{AC}{\sin 90°}$$

$$AB = AC.\sin\theta$$

Equation 1: Equation to estimate real width (AB) of a palaeo-channel deposit. Expression derived using the sin relation on triangle ABC of Figure 8. Note that the Legend is the same as in Figure 10.

Table 4: Classification scheme of fluvial channel bodies according to dimensions. Adapted from Gibling (2006)

Width (m)		Thickness (m)		Width/Thickness	
Very Wide	$> 10\,000$	Very Thick	> 50	Very Broad Sheets	$> 1\,000$
Wide	$> 1\,000$	Thick	> 15	Broad Sheets	> 100
Medium	> 100	Medium	> 5	Narrow Sheets	> 15
Narrow	> 10	Thin	> 1	Broad Ribbons	< 15
Very Narrow	< 10	Very Thin	< 1	Narrow Ribbons	< 5

3.5. X-Ray Spectroscopy

3.5.1. XRD

X-ray diffraction (XRD) is one of most commonly used technique for the studying of crystalline substances. The popularity of this method is due to the ease of sample preparation, the availability and affordability of the equipment (Singer, 1984; Hillier, 2003). This methodology makes use of electromagnetic radiation that is fired onto planar surfaces of prepared rock samples. Identification of mineral phases is achieved by recording the angle (2θ) and the intensity of reflected X-ray beams. In this project, XRD was implemented to identify and quantify the rock mineralogy, including clay minerals, which play essential role in the study of palaeo-environmental conditions of sedimentary rocks(Singer, 1984). XRD analyses were performed on two different sample formats: (1) bulk rock powder and (2) clay fraction. Both methods have advantages and disadvantages (further discussed Appendices), and the two methods were used to complement each other.

Bulk rock XRD scans were submitted for phase quantification (Table 8). To prepare the samples for QXRD, two stages of milling (starting from rock crushes) were employed to ensure homogeneous particle size distribution. Dry milling was first, using a disk-and-cylinder mill apparatus. It was followed by wet milling, using ethanol in a McCrone micronizer. In the XRD machine in the Department of Chemical Engineering (UCT), the samples were loaded as randomly oriented powders, and the spectra were obtained using a Bruker D8 Advance powder diffractometer with Vantec detector and fixed divergence and receiving slits with Co-Ka radiation (2θ range from 2 to 75°). The phases were identified using Bruker Topas 4.1 software (Coelho, 2007) and the relative phase amounts (weight %)were estimated using the Rietveld method. In the samples XRD spectra it is possible to detect the presence (low intensity peaks at $2\theta < 12°$; Figure 30) of clay minerals. However, identification and quantification of the clays were not possible, as it would require further processing methods beyond the scope of this project. More details on sample preparation can be found in the appendices (Ch. 6.2.2, Page 90). XRD scan results are presented in Figures 30 and 41 in the appendices.

For the clay fraction XRD scans, clay-sized particles were physically separated through wet sieving, and then suspended onto glass slides (the "glass slide method" of Moore and Reynolds, 1989). The main advantage of the clay fraction method is that it increases the resolution clay phases XRD spectra by having a high concentration of clays, and possibly a preferred orientation too, which enhances the intensity of diffraction from the basal planes of platy clay minerals (Singer, 1984; Moore and Reynolds, 1989; Hillier, 2003). Clay XRD scans were performed on a Philips PW 1390 XRD machine in the Department of Geological Sciences(UCT), which uses a Cu K-α X-Ray tube (wavelength of 1.542 A), accelerating voltage= 40 kV and current=25mA. Bragg's 2θ angles between

2.5 and 60° were used for analysis at a rate of 2.875°/min. The resultant XRD pattern of 2θ vs. intensity was used to calculate the d-spacing of the most intense peaks by solving for the Bragg equation. Further details on sample preparation can be found in the appendices.

3.5.2. XRF

X-ray Fluorescence (XRF) is a standard and mature analytical technique, routinely used in geochemical laboratories (Loubser and Verryn, 2008). The principles of XRF, X-ray radiation and ionization of samples, are well-understood and used to determine bulk chemical composition (major and trace elements) of samples (Loubser and Verryn, 2008). For this project, XRF was performed on powdered rock samples and only major elements were analysed.

Over the years, in the study of sedimentary rocks geochemical data, many geochemical trends and proxies have been proposed and developed (Peterson, 2009). Trends and proxies used in this project are: the chemical index of alteration (CIA) (Nesbitt and Young, 1982; Fedo et al., 1995; Goldberg and Humayun, 2010); A-CN-K (Al - Ca + Na - K) ternary diagram (Nesbitt and Young, 1984); and, the index of compositional variability (ICV)(Cox et al., 1995). The plots aid the evaluation of mineral composition, tectonic setting, palaeo-climatic and weathering conditions during the deposition of the lower Beaufort Group sediments.

CIA is one of the most accepted weathering proxies applied to siliciclastic rocks (Bahlburg and Dobrzinski, 2011) and was introduced by Nesbitt and Young (1982) (here referred to as CIA standard or CIA_{st}) to assess the degree of chemical and physical weathering experienced sediments at the time of deposition. In addition to being used as a proxy for climate during deposition, the method allows interpretations of the sediment provenance terranes (Nesbitt and Young, 1982, 1984; Fedo et al., 1995; Bahlburg and Dobrzinski, 2011). CIA standard (CIA_{st}) is shown in Equation 2, which is gives a ratio between the immobile element Al and the labile elements Na, Ca and K, with respect to the easy-weathering feldspars. The assumptions are that with increased chemical weathering, especially under humid, tropical climates, the labile elements would be washed out from the sediments through hydrolysis, leading to the formation of kaolinite clay mineral (Fedo et al., 1995; Bahlburg and Dobrzinski, 2011). However, if physical weathering is prevalent, the sediment would more likely maintain its original bulk composition, and the dominant mineralogy would be illitic clays.

$$CIA_{st} = \frac{Al_2O_3}{Al_2O_3 + CaO^* + Na_2O + K_2O} \times 100$$

Equation 2: Standard Chemical Index of Alteration (CIA_{st}) as in Fedo et al. (1995) and Nesbitt and Young (1982). Molar proportions are calculated for each major oxide by dividing the XRF output weight% by each oxide's molar masses. CaO* refers to the amount of Ca in silicates only, which means that Ca in carbonates and apatite need to be subtracted or removed in the sample preparations.

CIA molar (CIA_{mo}), presented in Equation 3, was introduced by Goldberg and Humayun (2010), for a more sensitive measure of the degree of chemical alteration, and to remove uncertainties from Ca in carbonates, and possible K from illitization or metasomatism(Goldberg and Humayun, 2010).Unlike CIA_{st}, CIA_{mo} is not constrained to 100% (compare Equations 2 and Equation 3). Therefore, it relies on the relative stoichiometric abundances of the elements, which in turn, can be linked to specific minerals. E.g., CIA_{mo} for fresh feldspar is 1, and comes from the fact that the ratio of Al to K/Na in feldspars is 1:1. Similarly, in illites, which mainly result from weathering of feldspar, the ratio of Al to K is 4:1; therefore, CIA_{mo} for fresh illite should be equal to 4. CIA_{mo} rises toward infinite as chemical weathering increases. Values smaller than 1, usually indicate the presence of carbonates in the samples (Goldberg and Humayun, 2010).

$$CIA_{mo} = \frac{Al_2O_3}{CaO^* + Na_2O + K_2O}$$

Equation 3: Molar Chemical Index of Alteration (CIA_{mo}). Molar proportions are calculated for each oxide, by dividing the XRF output weight% by each oxide's molar masses. CaO* refers to the amount of Ca in silicates only, which means that Ca in carbonates and apatite need to be subtracted or removed in the sample preparations.

The A-CN-K ternary diagram is a graphical representation of the degree of chemical weathering and can be used to evaluate the variation in climate and/or source rock types through time (Nesbitt and Young, 1984; Fedo et al., 1995; Goldberg and Humayun, 2010).

The index of compositional variation (ICV), introduced by Cox et al.(1995), is a ratio that analyses the proportion of different oxides (except silica, see Equation 4)with respect to alumina (Al_2O_3). Silica is not included to avoid dilution, because it is a very abundant oxide in the sediments (Cox et al., 1995). ICV decreases with increased degree of chemical weathering, and takes into account all the sources of Ca.

$$ICV = \frac{Fe_2O_3 + K_2O + Na_2O + CaO + MgO + MnO + TiO_2}{Al_2O_3}$$

Equation 4: Index of Compositional Variation (ICV) is derived from the weight percentages of the major oxides and measures the degree of chemical weathering in clastic sediments.

4. Results

4.1. Description of the Western Sedimentary Units

In the western part of the main Karoo Basin, two adjacent study areas of about ~100 km in extent, marked W1 and W2, were investigated in detail. Stratigraphically, the areas cover ~600 m thick succession, which includes the upper Abrahamskraal Formation; namely the arenaceous Moodenaars Member and mudstone-rich Karelskraal Member; as well as the overlying Poortjie Member of the lower Teekloof Formation.

Architecture of the deposits and contained bounding surfaces ('boundaries') facies elements as are presented in the Facies Plates (Figures 11, 12, 13 and 14 respectively).

4.1.1. ABRAHAMSKRAAL FORMATION

The average dimensions of the outcrops in the Abrahamskraal Formation are 5 m in thickness and 100 m width. Occasionally, the widths extend for more than 300 m, and a few outcrop horizons can be tracked for 10s of km. whilst most outcrops are dominated by mudstones, sandstone-dominated outcrops are also common. Well-developed fluvial sedimentary features are preserved, showing the full range of elements, from erosive gravel beds, trough-cross bedded sandstones to vertically stacked mudstones. Weakly developed paleosols, mudcracks and soft sediment deformation are the most common post-depositional features.

The study area is also considerably affected by dolerite intrusions, which often significantly alter and destroy not only the paleontological, but also sedimentological information such as the architecture and internal geometry of the sandstone beds.

4.1.1.1. GRAVEL FACIES

Gravel beds (GB architectural element) are a common feature in the Abrahamskraal Formation, forming up to 10% of the channel belt deposits (Figure 11). They commonly appear as small to elongated lenticular ribbon-like deposits (from 1 m to ~15 m in width; 0.4 to 1 m thick) mainly at the base channel belt elements. They rest on irregular lower scour surfaces (4^{th} and 5^{th} order boundaries - see Figure 11) and are made up mainly of pebble sized clasts.

Together with the overlying sandstones, the gravels form upward fining successions (UFS). The gravel facies, in particular Gmm2, grade into the above sandstones; although occasionally, they may have erosive upper contacts. The sandstones associated with the gravels also tend to be clast rich (clasts up to 10 cm, Gmm2 facies Figure 11; see Table 1 for more descriptions).

Conglomerates and breccias with various internal features are found throughout the area (Facies Gmm1 and Gmm2; Gch - Table 1, and Facies Plate 1 in Figure 11 for descriptions). The dominant

facies are poorly sorted, massive and matrix-supported breccias (Gmm1 and Gmm2). Horizontal bedding is also observed in some facies that tend to be clast-supported (Gch facies, see Figure 11).

Compositionally, the poorly sorted clasts are mudstones, sandstones, and fossilised wood, small bones and carbonate concretion nodules. Clasts sizes, range from 2 to 20 cm (av. ~5 cm). The matrix is mainly made up of fine sand and very fine dark grey, clayey sediment.

4.1.1.2. SANDSTONE FACIES

Sandstone bodies of various sizes comprising a variety of sandstone facies are found in the study area. The term "sandstone bodies" is used here as general and descriptive term for sandstone dominated deposits of various sizes in both channel and floodplain complexes (e.g., a storey or even a full channel belt element). Sandstones in the channel and floodplain complexes are differentiated here primarily based on their dimensions, facies and other geologically relevant features. Channel-related sandstones bodies tend to be thicker, have gravel facies as well as a wider range of sandstone facies elements, whereas floodplain sandstones are often fully engulfed in thick successions of mudstones and form tabular sheets that are up to 1 m thick, 50 to 100 m wide (i.e. narrow sheets) and have straight, non-erosive 4^{th}-order lower boundaries. However, often the boundaries are also wavy and erosive; with up to 20 cm deep scours (see Figures 13A and 14A).

When part of a channel complex element, sandstone facies make up the vast majority of this element (Figure 11). Sandstone bodies are narrow sheets with up to 7 meters in thickness and ~220 m in width (Table 5). The whole channel belt element usually rests on 4^{th}/ or $5t^{h}$-order erosive boundaries, with scouring reliefs of up to 1.5 m. Individual sandstone beds/stories, i.e. architectural elements making up the channel element deposit, are up to 1 m thick and 6-15 m wide (ribbons) and have lenticular or wedge shapes (Figure 11).

Downward accretion bars (DAs) are vertically stacked multi-storey, ribbon-sized lenses (see Table 5) that are the most common internal architecture of the channel complex elements in the upper Abrahamskraal Formation (Figures 11A and 15). Laterally accreted wedges are the other common internal architecture for the upper Abrahamskraal Formation(Figure 20). Channel-shaped deposits are also found in the study area.

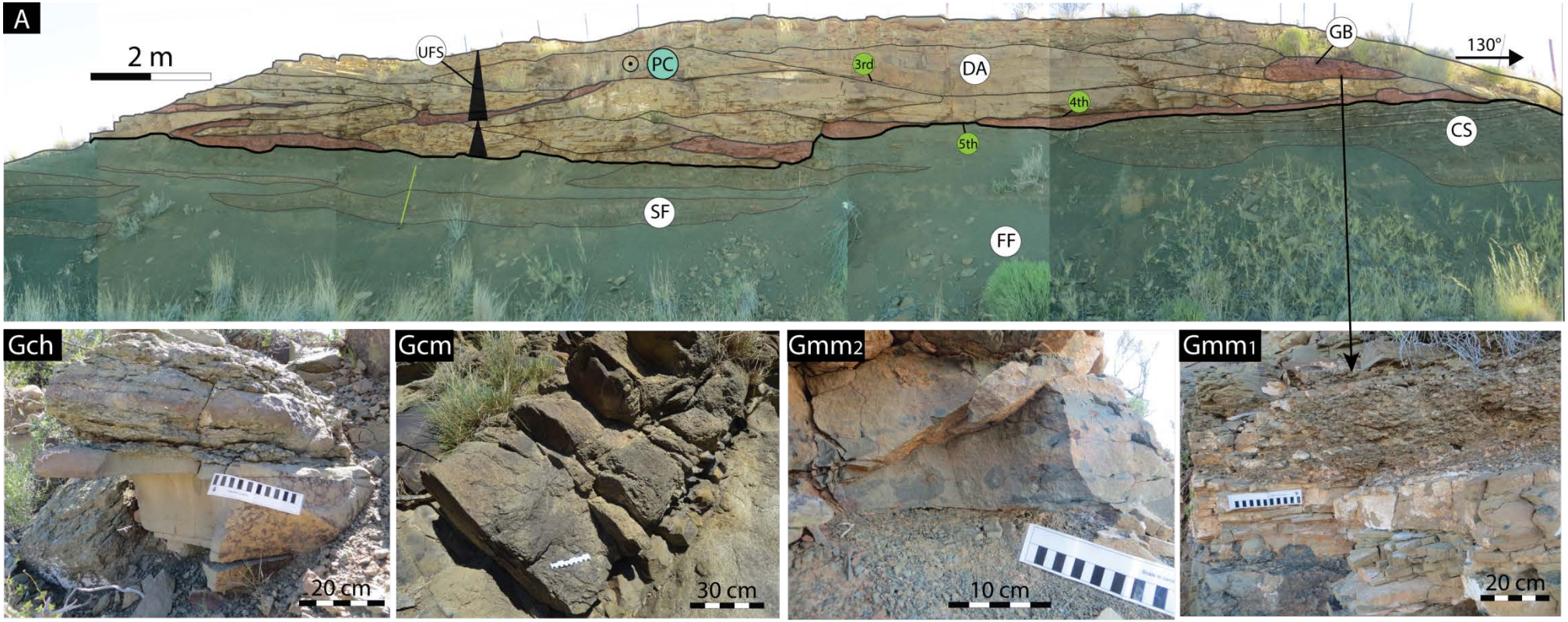

Figure 11: Facies Plate 1. Facies mapping of the architectural elements (AEs; white circles) and facies elements in a typical Abrahamskraal Formation outcrop (A1 site). A - False coloured image of the outcrop (yellow and orange = channel deposits, green = floodplain deposits) with marked surface boundaries (green circles). Palaeocurrent (PC) is into the outcrop. Main internal architecture are vertically stacked downward accretion bars (DAs), resting on 3rd-order downward accretion surfaces. The entire channel belt rests on an erosive 5th-order boundary (~1 m relief); often occupied gravel bars (GB) lenses. Two upward fining sequences (UFSs) have been identified. Floodplain elements are crevasses splay sandstone strings (CS), sandy and normal aggradational floodplain fines (SF and FF). Facies elements in display: **Gch** - Gravel clast-supported and horizontal imbrications; **Gcm** - Gravel clast-supported and massive; **Gmm1** - massive, matrix-supported breccias with pebble-sized clasts of sandstones, nodules and mudstones chips; **Gmm2** - Intra-formational, massive, clast-rich sandstone/matrix-supported breccias with pebble-sized rip-up mudstones; **P** - Proto-palaeosol layer with pedogenic nodules

The laterally accreted wedges (channel-related deposits) and sheet-like (floodplain related) sandstone bodies increase in abundance up the stratigraphy in the upper Abrahamskraal Formation. The stacked architectural elements usually rest on irregular, erosional (occasionally, sharp and non-erosive) 3rd-order boundaries; laminated fines are often found on the contacts.

In the floodplain related sandstone bodies, the most common facies are massive, horizontally and ripple cross-laminated sandstones (Sm, Sh and Sr). In channel-related deposits a much larger variety of facies are encountered and range from trough cross-bedded sandstones (St), which are the most common internal sedimentary structures, to horizontally and ripple cross-laminated sandstones (Sh and Sr1 respectively), as well as massive (Sm) and low-angle cross bedded (Sl) sandstones (Table 1). The sedimentary structures are often found in a vertical sequence that starts with Sl/St at the base, followed by Sp and then Sr at the top. The sequence is also coupled with an observable grain-size decrease (Figures 12 and 14).

Field descriptions and petrographic studies indicate that the Abrahamskraal Formation is dominated by fine-grained sandstones, but overall the grain sizes range from very fine- to coarse-grained. In terms of trends, channel sandstone bodies exhibit the vertical grain size decrease, whereas, the most prominent trend in floodplain sandstones is a lateral grain size change: elongated sandstone sheets commonly grade into siltstones/mudstones laterally in the outcrop (see Figure 13A).

4.1.1.3. MUDSTONE FACIES

Mudstone facies are part of the floodplain complex elements and constitute most of the upper Abrahamskraal Formation. The average outcrop dimensions are 8-20 m in thickness and 150 m in width (Figure 13).

Internal architecture of the mudstone units as well as their coarser grained interbeds (siltstones and very fine sandstones) are generally laterally continuous narrow sheet, along the outcrops and hillsides. In addition, some deposits are found filling up concave-up, channel-shaped structure (AC architectural elements) usually 1 m thick, 3 m wide (Figure 13A) .

The fine-grained rocks vary in colour between the more abundant olive green grey and the less profuse purple-red mudstones/siltstones. In fact, variations in colour together with grain size and sedimentary structures are the basis for the subdivisions of the fines facies (F).

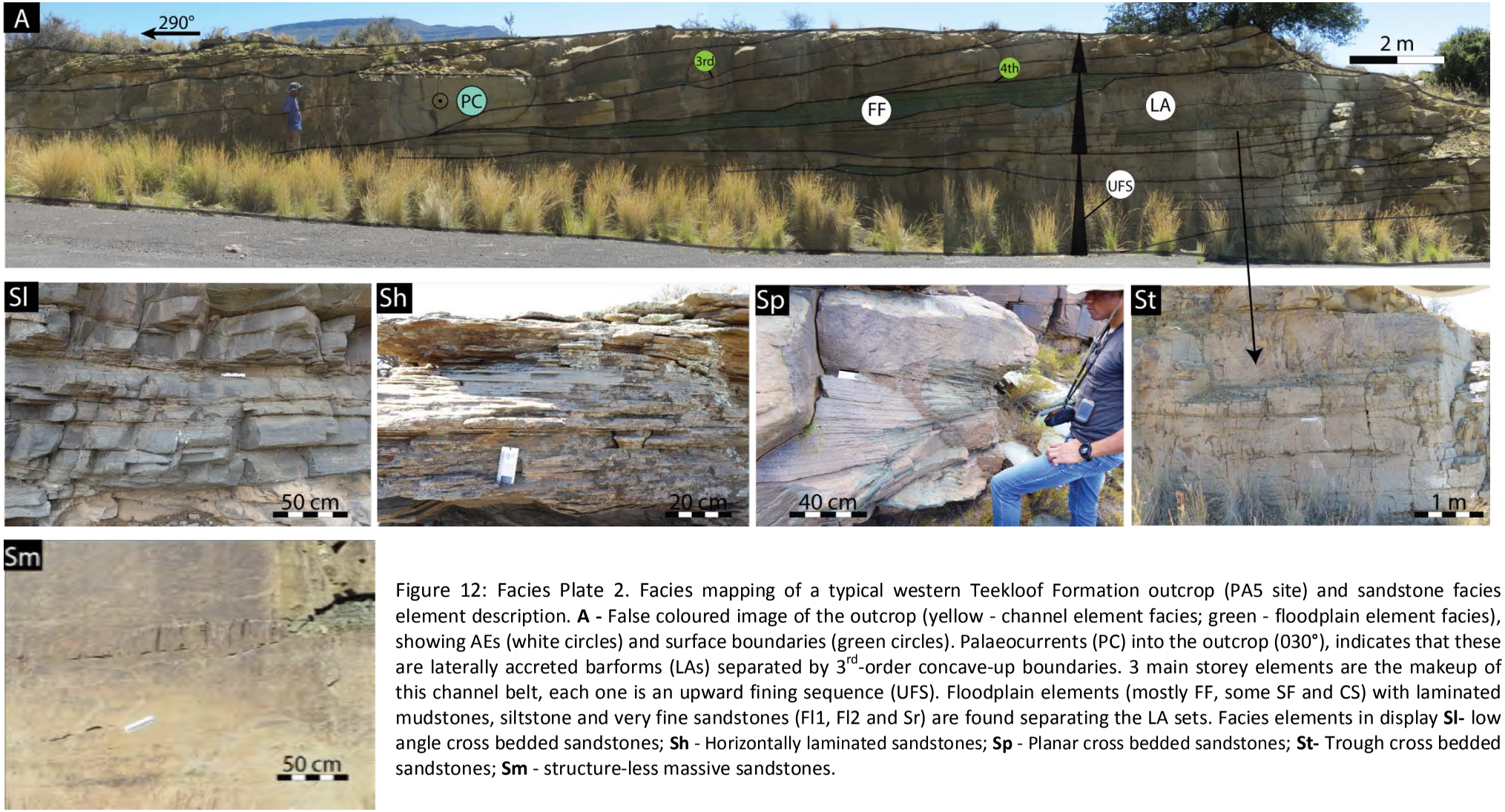

Figure 12: Facies Plate 2. Facies mapping of a typical western Teekloof Formation outcrop (PA5 site) and sandstone facies element description. **A -** False coloured image of the outcrop (yellow - channel element facies; green - floodplain element facies), showing AEs (white circles) and surface boundaries (green circles). Palaeocurrents (PC) into the outcrop (030°), indicates that these are laterally accreted barforms (LAs) separated by 3rd-order concave-up boundaries. 3 main storey elements are the makeup of this channel belt, each one is an upward fining sequence (UFS). Floodplain elements (mostly FF, some SF and CS) with laminated mudstones, siltstone and very fine sandstones (Fl1, Fl2 and Sr) are found separating the LA sets. Facies elements in display **Sl-** low angle cross bedded sandstones; **Sh** - Horizontally laminated sandstones; **Sp** - Planar cross bedded sandstones; **St-** Trough cross bedded sandstones; **Sm** - structure-less massive sandstones.

The main lithofacies facies in the Abrahamskraal Formation are the massive and horizontally laminated mudstones of red purple colours (Fl1; Fsm2) and the massive (occasionally laminated) olive green grey siltstones (Fl2; Fsm2)(Figure 13). Massive, horizontally laminated siltstones and ripple-cross laminated very fine grained sandstones (Sr) of olive-green grey colour are also common (Facies Plate 3 - Figure 13 and Table 1).

In the mudstones, carbonate concretions are locally abundant (Figure 13). Occurring as dark grey or dark brown concentric nodules, they range in size from 2 cm up to 60 cm in diameter. Occasionally, the carbonate nodules are found concentrated forming palaeosol layers (P). Other common features in the mudstones are desiccation cracks (Fm) and variety of vertebrate fossils. Fossilised wood and trace fossils are also present.

4.1.2. THE LOWER TEEKLOOF FORMATION (POORTJIE MEMBER)

The lower Teekloof Formation predominantly comprises floodplain complex deposits, which are well-exposed in the hill sides, valley gorges and road cuts in the area. On average, the exposed sandstone complexes are 6 m thick and 60-100 m wide, and form broad ribbons and narrow sheets. Although dolerite intrusions are more common in this part of the stratigraphy, fortunately areas with low dolerite concentration allowed good preservation of the architectural features in the sandstones and fossil remains.

4.1.2.1. GRAVEL FACIES

Gravel beds are not common features in the Teekloof Formation. Gravel beds are narrow to broad ribbons (~50 cm thick, 5-8 m wide) at the base of the channel element deposits and form fining up successions with the overlying sandstones facies. The gravels tend to be mainly matrix-supported breccias (Facies Gmm2) that compromise very angular mudstone clasts, sub-rounded/sub-angular sandstone pebbles and the common carbonate nodules fragments set in a sandy matrix (Figure 11 and Table 1).

4.1.2.2. SANDSTONE FACIES

Similar to the upper Abrahamskraal Formation, floodplain-related sandstones in the lower Teekloof Formation show a tabular, sheet-like architecture (Figure 13A); with narrow sheet like bodies (Table 4). Surface boundaries of mainly 3rd-order are mostly straight and non-erosive. Erosive, irregular with down-scouring (~15 cm relief) boundaries are also common for these sandstones.

As for the channel complex deposits, five regularly spaced sandstone bodies were identified; these are 10-15 m apart and are traceable laterally for several tens of kilometres in the study area. This arenaceous interval in the lower Teekloof Formation, identified as the Poortjie Member of in the

literature (Cole and Wipplinger, 2001; Day and Rubidge, 2014), is classified here as channel complex set (CS; see Figure 7 for the terminology; Figure 21 for field description). Surface boundaries of individual channel belts, when possible to assess, do not indicate much down-scouring (i.e., primarily non-erosive lower boundaries).

Individual channel belt deposits tend to be narrow and broad sheets. Internally, the main architecture of the lower Teekloof Formation is laterally accreted wedges (Figures 12 and 23). The wedges rest on smooth, straight, often concave-up lateral accretion surfaces (3rd order). Separating the wedges, laminated siltstones are common (Fl2 facies; see Figures 12 and 23). Floodplain sandstones display mostly Sm and Sr facies, and occasionally Sh. For channel related sandstones, St and Sl are very common facies elements in the lower Teekloof Formation. Massive, horizontal and ripple cross-laminated sandstones (Sm, Sh and Sr) are the other common sedimentary structures. Ripple marks and parting lineations are also present (see Figures 12 and 14).

4.1.2.3. MUDSTONE FACIES

Floodplain complex elements (fines) are more abundant in the lower Teekloof Formation compared to the upper Abrahamskraal Formation. Floodplain elements form large, 5 m thick, 100 m wide units at the different sites. Individual bed geometry resembles laterally continuous sheets. Less commonly, concave-up mudstone channel fills (AC) are also found (Figure 13). Mudstone deposits are also found on the 3rd-4thorder surface boundaries of the lateral accreted sandstones. Mudstone deposits alternate between the massive and/or laminated red-maroon claystones (Fl1; Fsm1) and the often massive olive green grey claystones/siltstones (Fsm2). Carbonate nodules are very common in the mudstones (P).

4.2. Description of the Sedimentary Units in the Eastern Facies Area

The eastern facies area of the main Karoo Basin enabled the coverage of a 400 m thick stratigraphic section over an area of about 60 km in diameter. When compared to their western counterparts, the exposed outcrops in the eastern facies area are fewer, mainly due to the high vegetation cover in this area. Nevertheless, good exposures are found in incised valleys and hillside sections. Structurally, large folds are observed in the study area, which in the south expose older formations of the Ecca Group as well. Tilted strata are common throughout the study area, and the base of the mapped Middleton Formation (Teekloof Formation equivalent) is consistently folded across the study area.

4.2.1. ABRAHAMSKRAAL FORMATION (FORMERLY KNOWN AS KOONAP FORMATION)

The best exposures of the 'Koonap' Formation are found in small incised valleys that are about 15-20 m high and a couple of 100s m wide.

Gravel facies in the eastern facies area vary from massive, pebbly conglomerates and breccia beds that are clast-supported (Gcm, Gch) to pebble-size, matrix-supported intra-formational rip-up clasts breccias (Gmm2 - Figure 11 and Table 1). Well-sorted, clast-supported and massive conglomerates (Gcm) are more common than horizontally bedded gravels (Gch). The gravel beds are broad ribbons and narrow sheets that are on average 0.5 m thick and 10 m wide. Resting on erosive and irregular lower contacts, they are found at the base of channel deposits and grade into the overlying sandstones. Intra-formational gravels are also common in the eastern facies area, especially within sandstone beds where they either form small, 1 m thick and 4m wide lenses or single clast stingers that are <10 cm thick.

Sandstones bodies vary from single storey to multi-storey deposits (Table 1, Figures 12 and 14). On average, they are ~4 m thick and 120 m wide. Individual beds tend to form vertically stacked lenses, and occasionally laterally accreted sheets. Grain sizes range from fine to coarse grained; medium-grained sandstones dominate the outcrops. Horizontal lamination (Sh) and planar cross-bedding (Sp) are common; however ripple cross-laminations (Sr) are the dominant sedimentary structure in the 'Koonap' Formation. Well-defined by mud drapes, Sr facies vary from climbing ripples (Sr1) to trough-shaped flaser ripples (Sr2) (Facies Plate 4, Figure 14).

The mudstone facies consists of lateral extensive sheet-like deposits that are up to 20 m thick and extend for 100s of metres. The facies is characterized by an alternating sequence of laminated, purple-red mudrocks (Fl1) and olive green-grey, massive siltstones (Fsm2 - Table 1, Figures13 and 14). A mottling texture in all mudrocks is very common in the field (Fr). In floodplain complexes, up to a metre thick, very-fine and fine-grained sandstone beds are sheet and ribbon shaped (CS, CR elements) and less-commonly channel-shaped. Furthermore, the aggradational, laterally continuous, very fine and fine-grained sandstones are recognized as sandy sheet-flood architectural element (SF - Figure 14A). Pedogenic nodules horizons (P), denoting palaeosols are very common in the area, and so are laminated tuffs (T).

4.2.2. MIDDLETON FORMATION (TEEKLOOF FORMATION EQUIVALENT)

Best exposures of the lower Middleton Formation are found in hillsides 20-30 m high and a couple of 100s m wide. The characteristics of the gravel, sandstone and floodplain facies in the lower Middleton Formation are identical to the 'Koonap' Formation, with the exception of the Sr2 facies that is rare in the lower Middleton Formation (see previous section). The main differences are found in the dimensions of the channel complexes with thicker and wider channel complexes dominating the base of the Middleton Formation (see Table 5 and Figure 23).

Figure 13: Facies Plate 3. Facies mapping of a floodplain complex deposit (A4N site, western Abrahamskraal Formation) and fines facies elements. **A** - Shows boundaries tracing of the outcrop, and it is made of an alternating succession of the green-grey siltstones and red-maroon mudstones (Fl1, Fsm1, Fsm2 facies), plus the thicker and coarser sandstone interbeds (Sm, Sr, Sh). The outcrop represents multiple splay generations, where each is terminated by the sandstones. Lower and upper bounding surfaces vary from straight, non-erosive to wavy and erosive (50cm relief); indicating aggradational sheet-flood deposition or the scouring action of short-lived higher energy flows. Tabular laterally continuous sheets are the characteristic internal geometry of the floodplain complexes. Lateral grain size variation (LGV) with sandy or silty beds laterally grading into silty or muddy beds is also a common feature. These beds are thought to represent LV or CS elements, because they tend to fine in a direction perpendicular to the main channel flow. Fines facies are: **Fl1** - Laminated red-maroon mudstones; **Fl2** - Laminated green-grey siltstone; **Fsm1** - Massive red-maroon mudstone; **Fsm2** - Massive green-grey siltstone; **Sb** - Soft sediment deformation in sandstones; **Fb** - Soft sediment deformation at the mudstone-sandstone interface; **Fm** - Sand-filled desiccation cracks in mudstone; **P** - Well-developed palaeosol layer with calcareous concretion nodules.

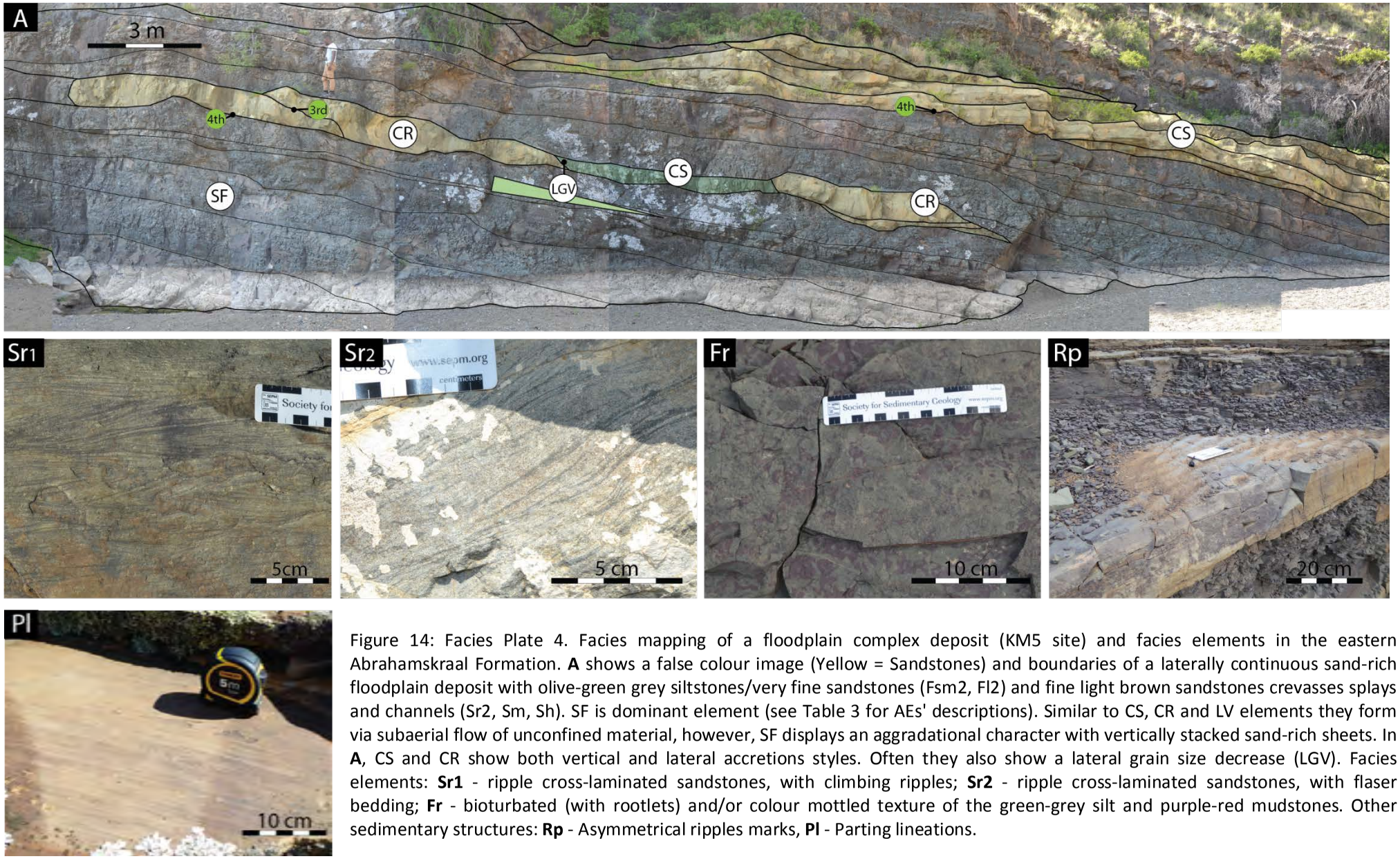

Figure 14: Facies Plate 4. Facies mapping of a floodplain complex deposit (KM5 site) and facies elements in the eastern Abrahamskraal Formation. **A** shows a false colour image (Yellow = Sandstones) and boundaries of a laterally continuous sand-rich floodplain deposit with olive-green grey siltstones/very fine sandstones (Fsm2, Fl2) and fine light brown sandstones crevasses splays and channels (Sr2, Sm, Sh). SF is dominant element (see Table 3 for AEs' descriptions). Similar to CS, CR and LV elements they form via subaerial flow of unconfined material, however, SF displays an aggradational character with vertically stacked sand-rich sheets. In **A**, CS and CR show both vertical and lateral accretions styles. Often they also show a lateral grain size decrease (LGV). Facies elements: **Sr1** - ripple cross-laminated sandstones, with climbing ripples; **Sr2** - ripple cross-laminated sandstones, with flaser bedding; **Fr** - bioturbated (with rootlets) and/or colour mottled texture of the green-grey silt and purple-red mudstones. Other sedimentary structures: **Rp** - Asymmetrical ripples marks, **Pl** - Parting lineations.

4.3. Quantitative Lithofacies Facies Analysis

Quantitative facies analysis was performed at facies association level of architectural elements (e.g. Lateral accretion bars-LA). Facies elements (e.g., lithofacies types Fm, Sm, St) were only analysed qualitatively, their descriptions, interpretations and distribution over the study areas and in the various formations can be found in Table 1 and in the Facies Plates (Figures 11, 12, 13 and14).The results of the facies quantification exercise are displayed in the form of pie-charts in Figure 16 and 17. External architecture was analysed in terms width-versus-thickness (W/T) plots, and their summary is presented in Table 5. The rest of W/T plots are presented in Figures 18 and19.

4.3.1. FACIES ASSOCIATIONS PERCENTAGES (INTERNAL ARCHITECTURE)

The quantification process of the facies associations is presented through the example shown in Figure 15 that illustrates a representative outcrop exposing the typical internal architecture of the Abrahamskraal Formation in the western study area. Bounding surfaces are outlined to produce a false colour facies map (AEs) so that elements can be quantified. The channel belt element (yellow in Figure 15A and B) is almost entirely made of lenticular downward accretion bars, which rest on 3rd-order down-current bounding surfaces (Figure 15B). The channel belt element rests on an erosive 5th-order bounding surface with up to 2m down-cutting. Numerous ribbons of GB facies (on average55 cm thick and10-15 m wide) are found at the base of the channel belt.

The entire channel belt overlies a floodplain complex element (green in Figure 15A and Figure 15B)that contains laminated purple-red mudstones (Fl1 facies), the dominant olive green-grey massive siltstones (Fsm2) as well as several crevasses splay elements (CS and CR) and occasionally sandy-sheet flood deposits (SF).

Centimetre-scale sedimentary logs of the outcrops are used to assess the relative proportions of the floodplain complex elements (CS, CR and SF), as well as the channel-related GB element (Figure 15).

The results show that the Abrahamskraal Formation has a channel complex vs. floodplain complex elements ratio of roughly 6:4 in the west (W1), and 3:7 in the east. Within channel-related elements, the Abrahamskraal Formation in the west is dominated by downstream accretion bars (DA ~30%). Other main constituents are hybrid downstream-lateral accretion (DLA ~ 23%), and laterally accretion (LA ~ 15%) elements. In the east, DAs are present throughout the Formation, but their proportions are significantly less (<10%). In contrast, the channel complex elements are dominated by LAs (~20%) (Figure 16). It is worth noting however that in the eastern area fewer outcrops were used for quantification than in the western study area.

Gravel bars (GB) are also a common architectural element in the channel-related elements of the Abrahamskraal Formation. Although volumetrically low, the presence of the GB element is

ubiquitous at the base of the channel complexes, and significant for reconstructing paleo-channel conditions as they represent the highest energy stages of the palaeo-flow.

Aggradational overbank fines (FF) element is the most dominant element of the floodplain-related elements, constituting in occasions up to 50% of the Abrahamskraal and 60% of the Teekloof formations, respectively. The exception is found at W1 site in the Abrahamskraal Formation, where FF elements are ~ 15% (for method 1 and 2), and, this could be due to lower proportions of floodplain complexes at W1 area; or in contrast, there could be a sampling bias towards channel complex related outcrops. Other common floodplain-related elements are levees (LV), sandy sheet-floods (SF); crevasses channels (CR) and sites splays (CS). The abundance of SF elements increases from ~ 5% in the west to ~20% in the east for both formations (Figures 16 and 17).

The Teekloof Formation is dominated by LA elements (~20%), contains some DA elements (8% and 15% only at sites W2 and E1 respectively) and lacks element GB (Figures 17 and 19).

All in all, the main difference in the internal architecture between the Abrahamskraal and the Teekloof formations is that GB and DA elements more predominant in the former, whereas, LA elements dominate the latter formation.

Discrepancies between the averaging methods 1, 2 and 3 are at their greatest inW1 area, where the proportions of the floodplain complex elements change from ~35% in Method 1 to ~65% in Method 3 (Figure 16W1). This is probably due to the fact more data (quantitatively and qualitatively) was collected from this study area (W1), due to easier accessibility to the outcrops for closer and more detailed inspection.

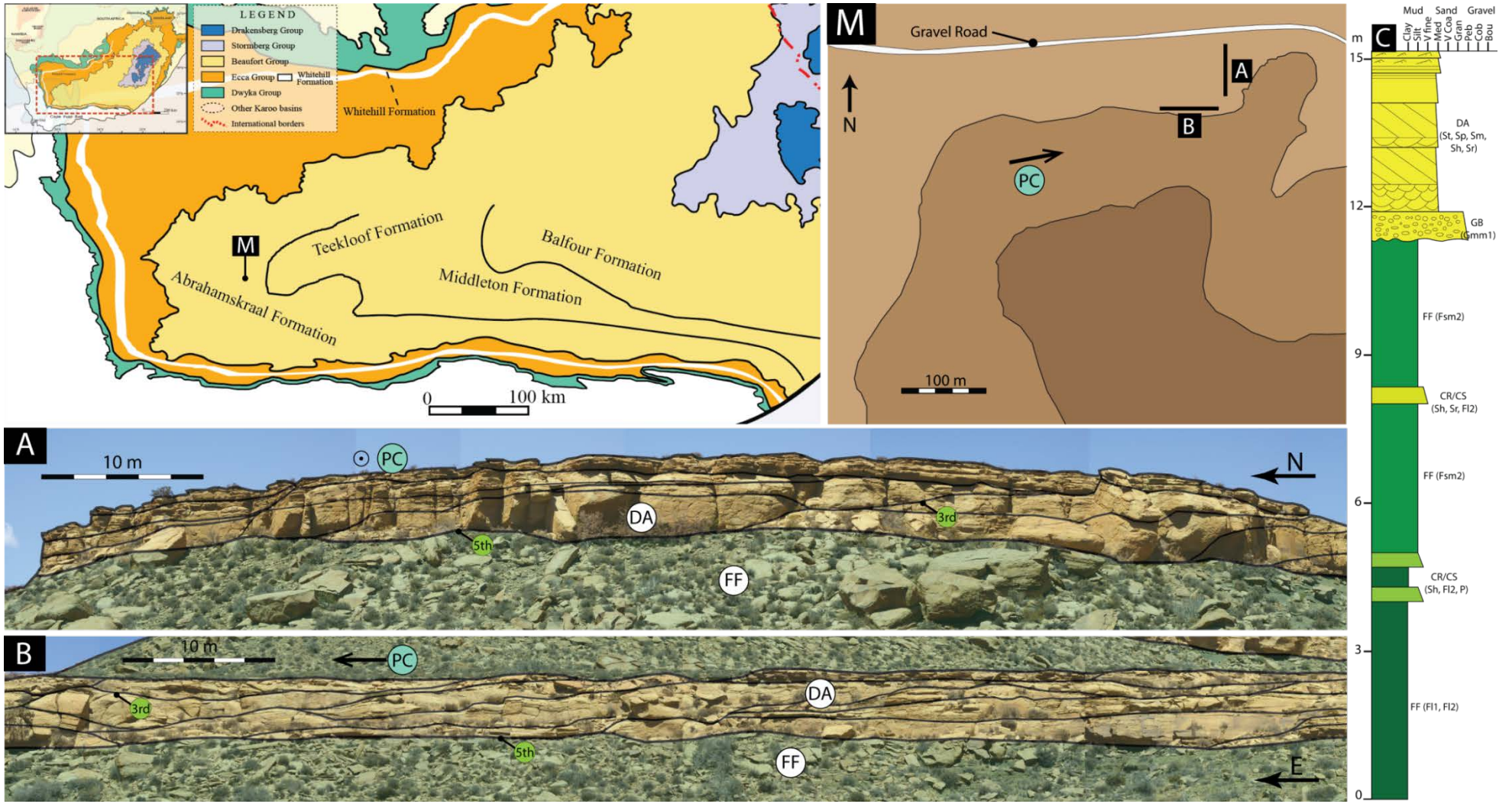

Figure 15: Illustration of an Abrahamskraal Formation channel belt exposure (Su-Abr1 site) used for facies quantification. False colour image in A and B (yellow = channel elements, green = floodplain elements). Downward accretion bars (DAs) are the main internal architectural element of the formation. A and B show two perpendicular sections (in M) of the same channel belt, and it is possible to see the vertical stacking nature (A) and the down-current shape (elongated ribbons, B) and boundaries of the DAs. Note that palaeocurrent (PC) in the area is to the NEE. The channel belt rests on a 5th-order erosive bounding surface (1.5 m relief); DAs are separated by 3rd order concave-up boundaries. C -Sedimentary log produced in the field, and includes facies and architectural elements details that are not captured in the facies maps A and B (e.g. GB, CR and CS elements). Proportions derived from C, are incorporated into the facies quantification analysis.

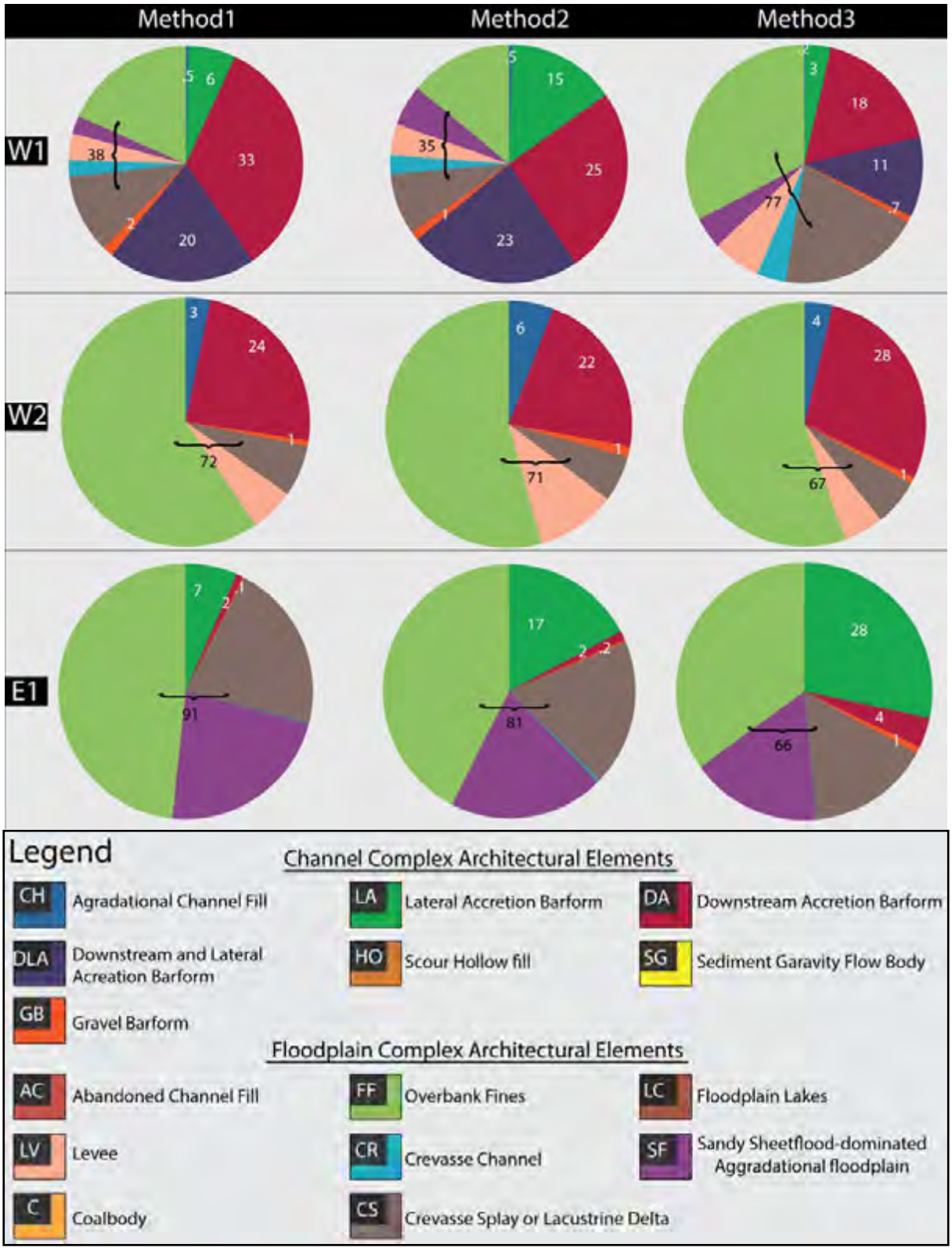

Figure 16: Quantitative facies analysis results for the Abrahamskraal Formation following the methodology in Figure 9. Results were compiled from various outcrop facies maps reconstructions (e.g. Figure 15). Proportions vary for each method; advantages and disadvantages of each one are discussed in the methodology section. DA architectural element is the most abundant of the channel complex elements in the western facies. Significant proportions of lateral accretion (LA) and hybrid downward-lateral accretion (DLA) elements are also found.

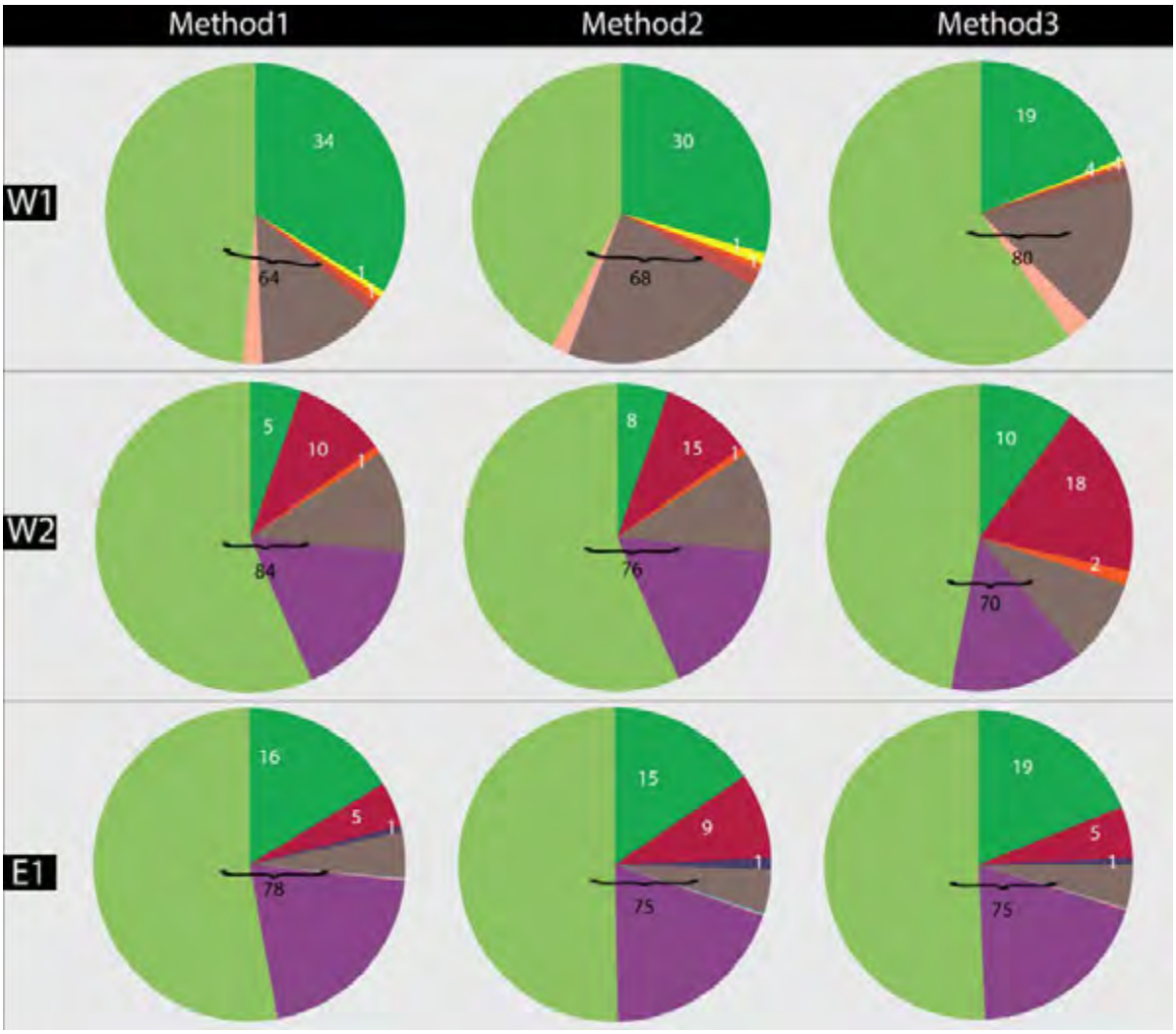

Figure 17: Quantitative facies analysis results for the Teekloof Formation following the methodology in Figure 9. The results from the three averaging methods are very similar. The dominant architecture element is the lateral accretion bars (LA). DA elements also found in the formation. See legend in Figure 16.

4.3.2. DIMENSIONS AND CLASSIFICATION OF THE SANDBODIES (EXTERNAL ARCHITECTURE)

In this section, single storey sandbodies and channel belt elements are classified according their measured dimensions with respect to width and thickness (W/T), geomorphic setting and internal architecture (Gibling, 2006; Methodology Ch. 3.2, Figures 8, 10 and 34). Measured width and thickness values are summarized in Table 5.

Width and thickness values reported in the literature vary from absolute (stated or implied in diagrams) to a value range, where the minimum and/or maximum values for either or both, W and T are given (Gibling, 2006). For this work, only absolute values are provided and only for those single channel stories, channel belts and channel complexes that could be directly measured in field, even though, on visual assessment, the channel complex elements in certain units appear to be continuous for kilometres in the study area. However, their actual lateral continuity could not be

validated with close up studies due to the inaccessibly of the outcrops. This cautious approach ensures that uncertainties that arise from estimating inaccessible outcrops are avoided.

Width (W) versus thickness (T) of the single storey sandbodies and channel belt elements

In the lower Teekloof Formation, the maximum width values of ~773 m in the west, and 230 m in the east are greater than the width values in the upper Abrahamskraal Formation (Table 5). Similarly, the mean widths in the lower Teekloof Formation (~130 m in the west and ~91 m in east) are greater than in the upper Abrahamskraal Formation (Table 5). Thicknesses trends seem to be more variable, with the Teekloof Formation being thicker in the east with a maximum of 30 m, a mean of 5.8 m versus a maximum 5.6 m and a mean of 3.8 m for the upper Abrahamskraal Formation. In contrast, the western study area shows the opposite trend (Table 5). All in all, the maximum and mean values indicate that the single storey sandbodies and channel belt elements are wider in the west and thicker in the east for the upper Abrahamskraal and lower Teekloof formations.

Table 5: Summary of the width and thickness values of the sandbodies in the upper Abrahamskraal and lower Teekloof formations in the western and eastern study areas. Note that no qualitative distinction has been made between the single storey sandbodies and channel belt elements.

Formations		Width (m)			Thickness (m)			W/T	Number
		Max	Min	Mean	Max	Min	Mean		
Eastern Facies	Teekloof Fm	230.0	18.1	91.2	30.0	1.2	5.8	7-40	20
	Abrahamskraal Fm	124.7	6.9	41.1	5.6	1.3	3.8	2-30	5
Western Facies	Teekloof Fm	772.7	7.0	130.7	3.2	0.2	1.6	10-200	8
	Abrahamskraal Fm	219.6	11.7	83.6	5.6	0.7	3.1	10-40	14

W/T ranges were obtained from Figure 19

Width vs. thickness plots were performed in a log-log space, because the sandbodies dimensions range over more than 5 order of magnitudes (Gibling, 2006). All measurements from both study areas are presented in Figure 18, and plots of the individual formations are in Figure 19. Lines of equal W/T ratio (e.g. W/T = 10) are included in the graphs as well as population envelopes of different river styles. Based on Gibling (2006), these river style envelopes can be used comparatively as a first proxy for the identification of the fluvial style in which the sandstone bodies were generated.

A positive correlation between width and thickness values is observed (Figures 18 and 19). Most measurements plot between the W/T = 10 and W/T = 100 lines, indicating that the majority of

sandstone bodies in both study areas are narrow sheets, and occasionally broad ribbons. Furthermore, most measurements plot in a region were many river style envelopes overlap, and therefore inferences connecting width and thickness values to a river style is very difficult without systematically quantifying a much larger number of sandbodies in the two formations. Some data points plot outside all river style envelopes (below T = 1, Figures 18 and 19) which is due to the fact that Gibling(2006) only considered sandbodies thickness values above 1m when compiling the database.

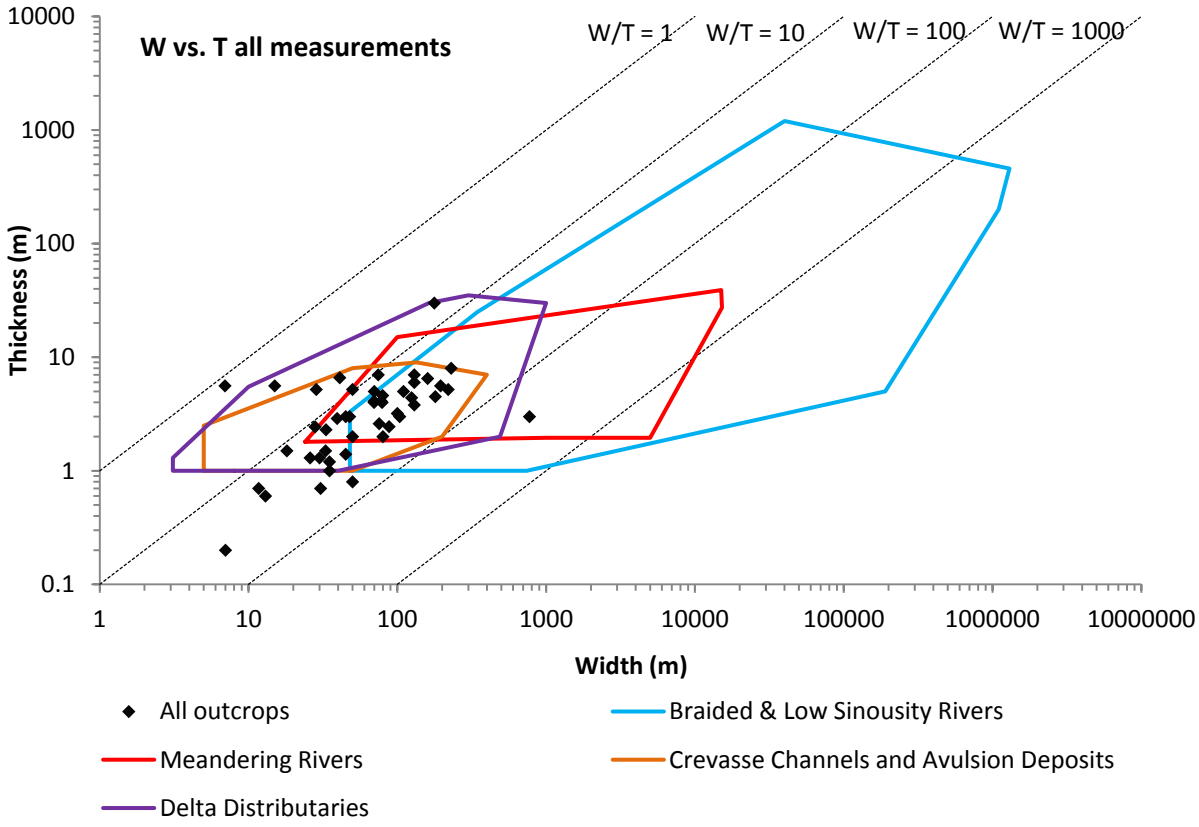

Figure 18: Width (W) vs. thickness (T) plot for all sandstone body measurements in both study areas. Note the positive correlation between W and T. Most measurements plot between the "W/T = 10" and "W/T = 100" lines indicating that sandstone bodies (single storey elements and channel belts) tend to be narrow sheets and broad ribbons. Envelope polygons corresponding to different river styles are taken from Gibling(2006).

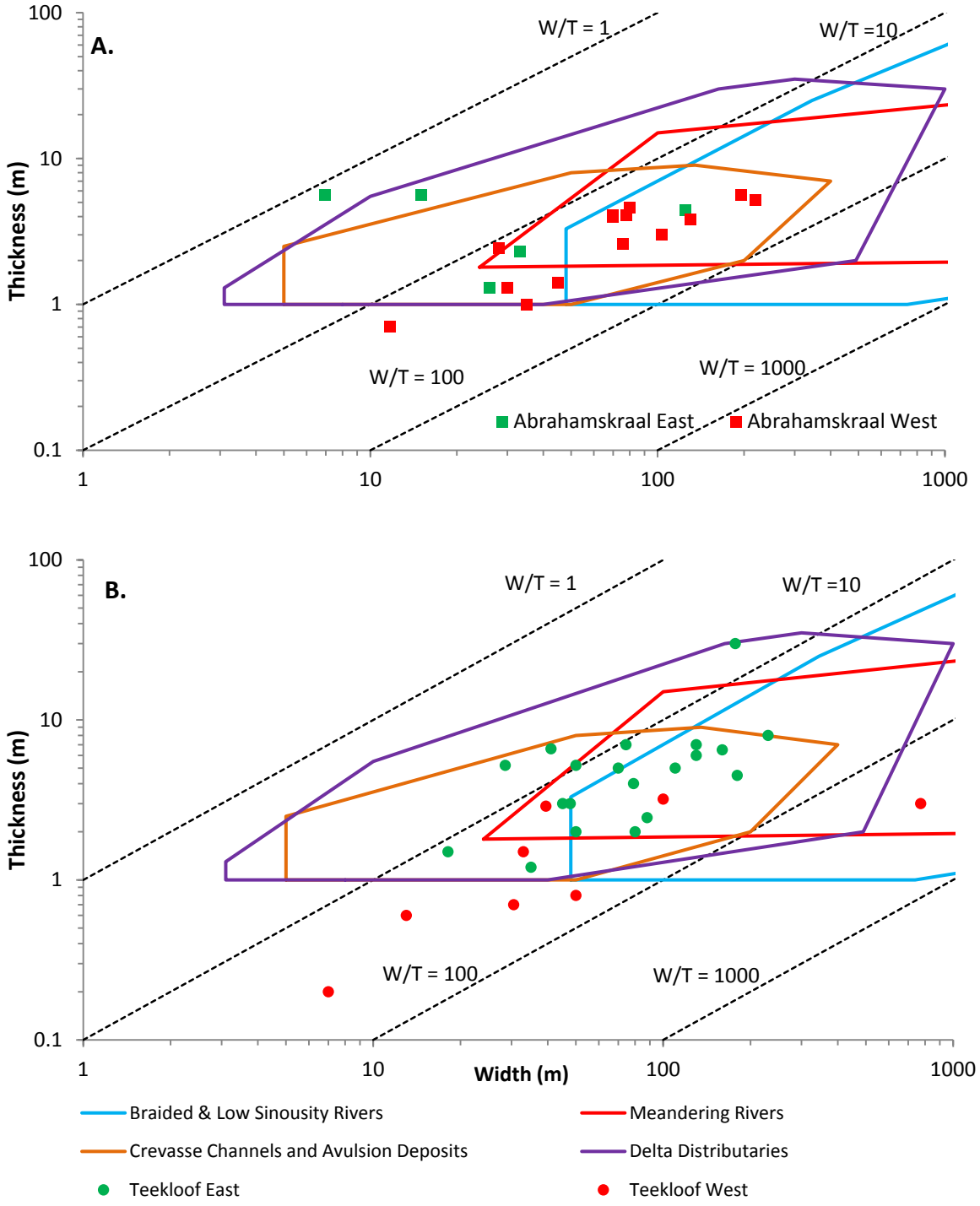

Figure 19: Width (W) vs. Thickness (T) plots for the Abrahamskraal (A) and the Teekloof (B) formations. Envelope polygons corresponding to different river styles are taken from Gibling(2006).

Sandbody Classification

The sandstone bodies are classified according to the scheme presented in Figure 8 and 35, and the results are summarised in Table 6. The results in Table 6 indicate that most channel sandstones in the upper Abrahamskraal Formation, apart from the crevasses/floodplain channels, can be classified as deposits of braided or low sinuosity rivers, especially in the western study area. The sandstones of the lower Teekloof Formation on the other hand can be mainly classified as products of meandering rivers in the west, and as mixture of braided and meandering rivers in the east.

Table 6: Number of sandstone bodies and their classification for the Abrahamskraal and the Teekloof (B) formations. Classification scheme and flow chart can be found in Figures 8 and 35 respectively (Gibling, 2006).

River Styles	Abrahamskraal Fm		Teekloof Fm	
	West	East	West	East
Braided/Low Sinuosity	8	1	0	3
Meandering	1	2	4	2
Crevasses/Floodplain Channels	8	3	4	14
Valley fills	0	0	1	1

Summary of the Channel Complexes Architectures in the study areas

A summary of the different combinations of external and internal architectures has been compiled, and representations are shown in the Architecture Plates (Figures 20, 21, 22 and 23). Hierarchy and terminology are presented in Figure 7 and Table 4.

In both formations and study areas, the most common motif identified is the laterally continuous (for 10s of Km) sandstone horizons (e.g., Figure 21H). These have been identified to be low amalgamation channel-belt complexes, made of individual channel belt sheets and ribbons. Occasionally, high amalgamation (valley-shaped) vertically stacked channel complexes are also found (Figure 23A). Horizons with multiple laterally continuous channel-belt complexes are found in close proximity (10-20 m vertical separation), and this allowed the identification of channel complex sets (CCS; e.g., Figures20A and 21H). A total of seven channel complex sets have been established in both study areas (4 in the west and 3 in the east). Furthermore, seven Architecture Types (AT) composing the different channel-belt complexes (therefore the complex sets as well) have also been described. Each Architecture Type is a mixture of external and internal architectural elements, making up a single channel belt, and on occasions, a channel-belt complex.

Upper Abrahamskraal Formation

Four channel complex sets have been identified in the upper Abrahamskraal Formation; three (CCS1, CCS2 and CCS3) in the west (e.g. Figure 20A), and one CCS5 in the east. All the complex sets

comprise typical laterally extensive channel-belt complex sheet deposits. Four Architecture Types were identified (AT1, AT2, AT3 and AT4) in the upper Abrahamskraal Formation.

AT1 are channel belts sheets/ribbons made entirely of downstream accretion bars (DAs). These are generally, flat-topped, occasionally with top scour structures and have a wavy erosional base with 1-2 m relief. In particular, AT1 is found in high abundance in the CCS1, CCS2 and CS5 complex sets. Field examples of AT1 can be found in Figures 11A, 15B and 20A.

AT2 are flat-topped channel belt sheets, dominated by a mixture of DA and DLA elements. Locally, LA elements are also present. They are found in CS2 and CS3 complex sets (Figure 20B, Figure 22C).

AT3 are concave-up channel belt ribbons and sheets, dominated by lateral accretion bars (LA). Downstream accretion bars are found in a few occasions. Floodplain complex elements are found filling up the concave-up shape. This architecture type was mainly encountered in CS3 (Figure 20C).

AT4 is a channel shaped ribbon, dominated by downstream accretion bars. It is characterized by a central concave-up scour structure, aggradationally filled by DAs, often with attached wings (i.e., levees) and floodplain elements forming a flat top (Figure 21A). AT4 is encountered throughout the study areas.

Lower Teekloof Formation

Three channel complex sets have been identified in the lower Teekloof Formation: CS4 in the west, and CS6 and CS7 in the east. The common architecture in the lower Teekloof Formation is laterally extensive channel-belt complexes. However, vertically stacked (high amalgamation) channel complexes were encountered both in the western and eastern facies areas (Figure 23A). The Architecture Types encountered in the lower Teekloof Formation are AT1, AT2, AT4, AT5, AT6 and AT7.

AT1 was encountered in the eastern Teekloof Formation facies, as part of CC7. AT2 was encountered in the western (CCS4) and eastern facies areas (CCS6, Figure 22C). AT4 was encountered in different parts of the succession.

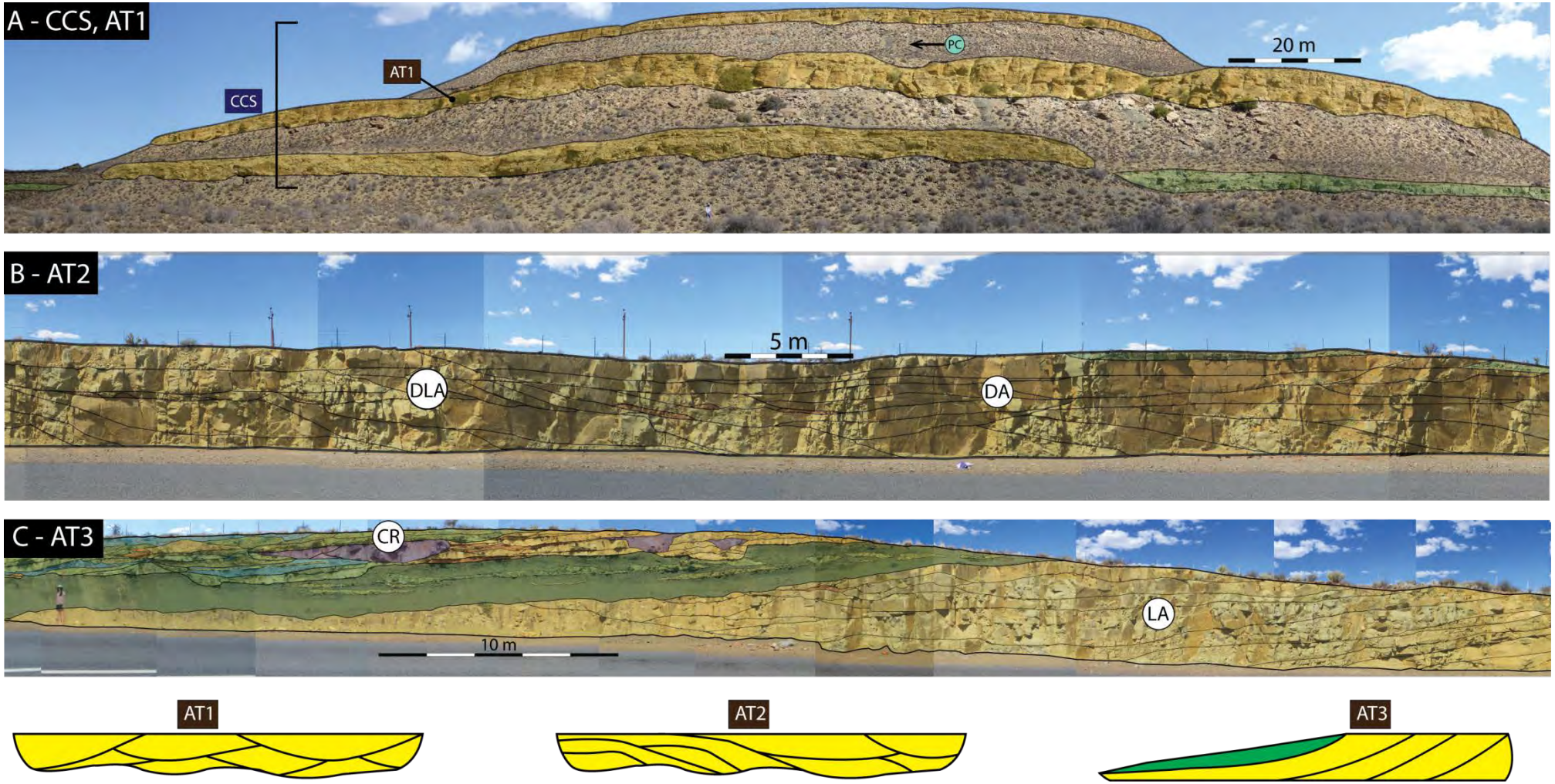

Figure 20: Architecture Plate 1, showing different Architecture Types encountered in both formations. **A** shows the common laterally extensive channel belt architecture. The Channel belts can be traced for Kms in the field (i.e. low amalgamation channel-belt complexes). Channel complex sets are the grouping of closely spaced and genetically related channel complexes. **A** also shows the Architecture Type 1, which are channel belts entirely composed of DA elements (for detailed internal architecture see Figures 11A and 15A). **B** - Architecture Type 2, which are similar to AT1, but they shows a combination of DLA and DA elements, and occasionally LA elements. **C** - Architecture Type 3, which are channel belt sheets/ribbons with a characteristic concave-up top surface. AT3 are dominated by LAs, and Das are also encountered. Note false colour and boundaries were introduced in the images. **A -** Su-Abr3 site**, B -** A2site**, C** - A5 site.

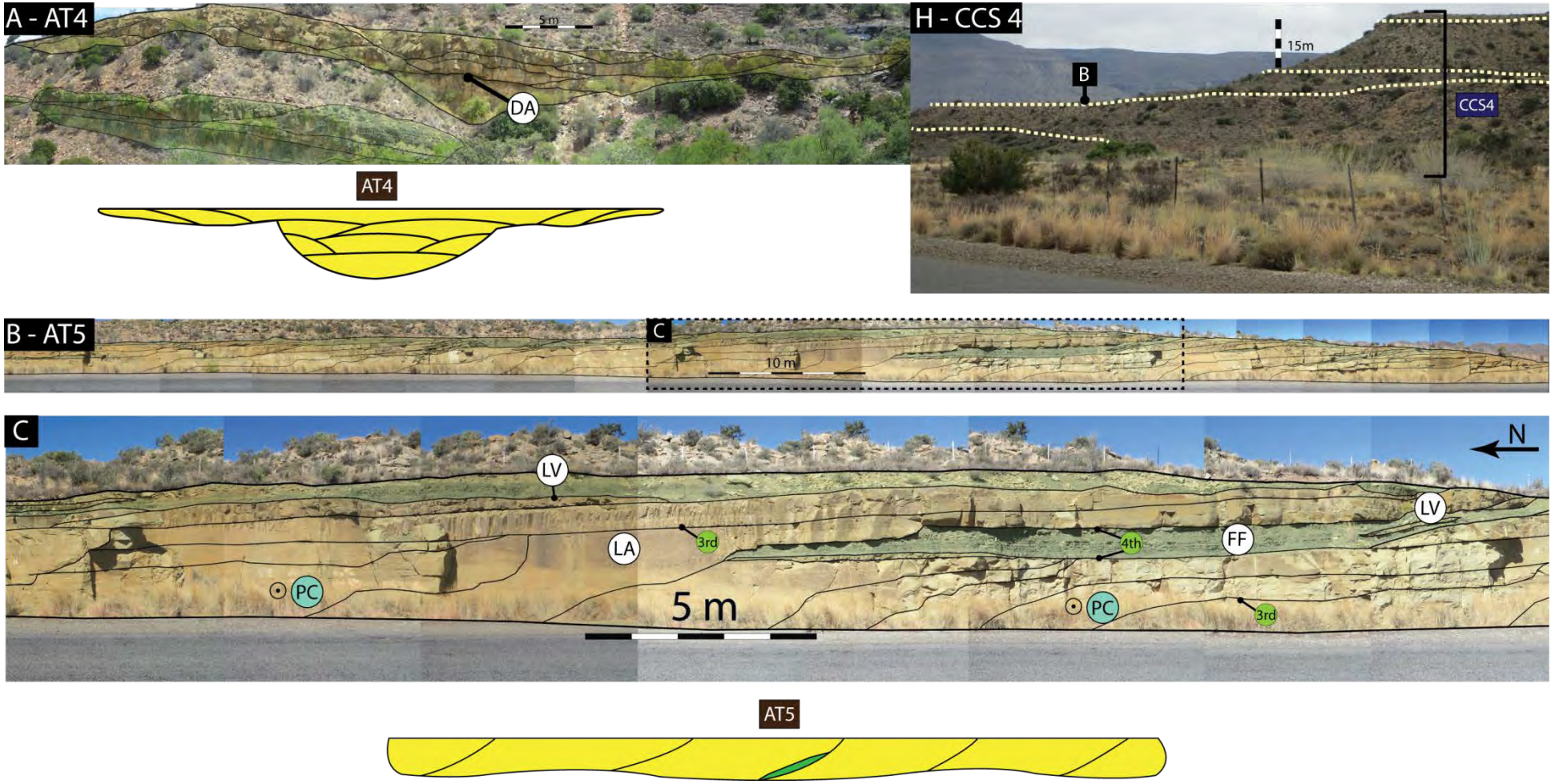

Figure 21: Architecture Plate 2, illustrating the Architecture Types 4 and 5. **A** - Architecture Type 4, are channel shaped ribbons, dominated by DA elements, they encountered in both formations. **H** - Shows Channel Complex Set 4, an arenaceous interval in the lower Teekloof Formation, composed 5 laterally continuous channel-belt complexes. **B, C -** shows the Architectural Type 5, which are channel belt sheet deposits entirely composed of lateral accretion bars (Las) that are often separated by thin laminated fines. Note that false colour and surface boundaries were introduced in the images. A- OC1 site B, C - P6 site.

AT5 are flat-topped channel belt sheets made entirely of lateral accretion bars. It has a wavy erosional base (1-2 m relief), and floodplain elements often occupy LA's surface boundaries, and upper portions of the belt. AT5 is the most abundant architecture in the west (CCS4), and is also encountered in the east (CCS6) (Figure 21).

AT6 are vertically stacked valley-shaped channel-belt complex ribbons, dominated by downstream accretion bars. Lateral accretions are dominant in the upper portion of the complex. These complexes are very thick, up to 50 m, and 100-150 m wide. They are encountered in the western (CCS4) and eastern (CCS6) facies of the Teekloof Formation (Figure 23A).

AT7 is a channel-belt complex made of multiple sheet and ribbon deposits, displaying degrees of lateral juxtaposition, as well as vertical aggradation. The channel deposits are dominated by lateral accretion bars, and downstream bars are also present. Some of the elements are closely related to floodplain deposits, due to their aggradational characteristics (Figure 23C).

Table 7: Summary of the description and distribution of the defined Architecture Types (AT) in the lower Beaufort Group in the study areas.

Architecture Types (AT)	Descriptions	Illustration	Abrahamskraal Formation		Teekloof Formation	
			West	East	West	East
AT1	Channel belt sheet/ribbon entirely made of DA elements. Found in high abundance in CCS1, CCS2 and CS5 complex sets. (Figures 11A, 15B and 20A).	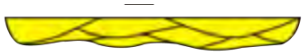	√	√		√
AT2	Similar to AT1, but dominated by a mixture of DA and DLA elements. Found in CS2 and CS3 complex sets (e.g. Figure 20B).		√	√		√
AT3	Concave-up channel belt ribbon/sheet, dominated LAs. Mainly encountered in CS3 complex set (Figure 20C).	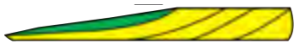	√		√	
AT4	Channel-shaped belt ribbon dominated by DA elements. Encountered throughout both study sections (Figure 21A).		√	√	√	√
AT5	Channel belt sheet entirely made of LA elements. The most abundant architecture type in CCS4 complex set (West) and it is also common in the east (CCS6; Figure 21).				√	√
AT6	Succession dominated, valley shaped channel-belt complex ribbon, dominated by DA elements. Found in CCS4 and CCS6, western and eastern facies (Figure 23A).				√	√
AT7	Channel-belt complex made of multiple sheets and ribbons, with multilateral and vertical juxtaposition properties. Encountered throughout the studied sections (Figure 23C).		√	√	√	√

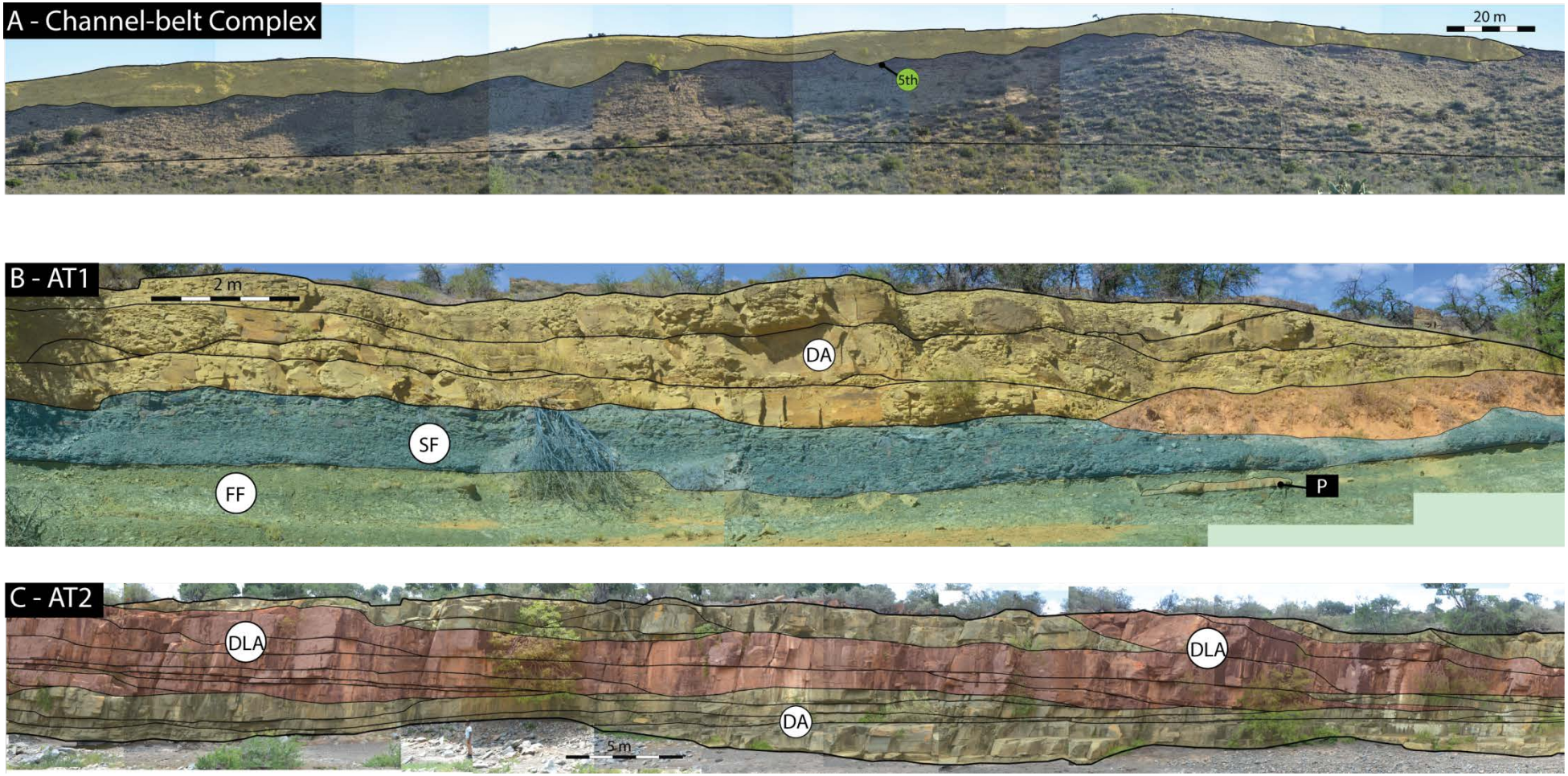

Figure 22: Architecture Plate 3, showing architecture types of the upper Abrahamskraal (**A** and **B**) and lower Teekloof formations (**C**) in the eastern facies area. **A** - a multilateral channel-belt complex in the upper Abrahamskraal Formation with a flat top and erosional base. Internally, it is made of vertically accreted DA elements (**B**), and LA elements. **B** - Example of the AT1 architecture type in the eastern facies area. **C -** AT2 facies in the eastern facies area. Note false colour and boundaries were introduced in the images A - OC8 Site, B - KM3 site, C - KM4 site.

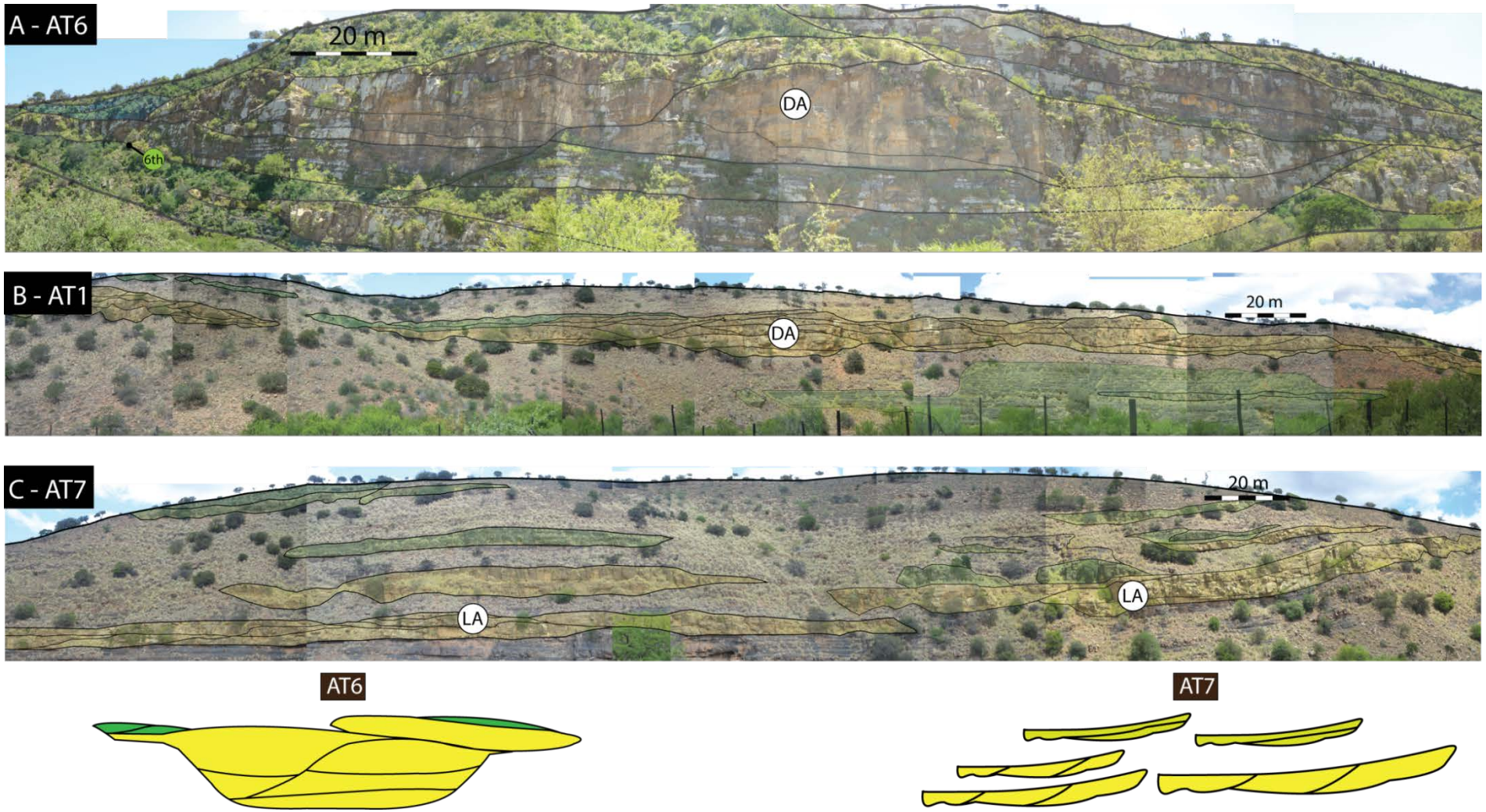

Figure 23: Architecture Plate 4, showing the architecture types in the lower Teekloof Formation, eastern facies area. **A -** Show a high amalgamation, vertically stacked channel-belt complex ribbon. It is a very thick (~50m) succession-dominated unit, indicating a high aggradation and/or reoccupation rates. This unit defines the AT6 architecture type, and is present both in the western and eastern facies of the Teekloof Formation. **B**–AT1 architecture type with a flat-top, and irregular, erosional base channel-belt sheet, dominated by DA elements. **C** - AT7 architecture type, which is a complex defined by multiple LA dominated, channel-belt sheets and ribbons displaying multilateral and vertical juxtaposition properties. Note that false colour and boundaries were introduced in the images**. A -** KM7 site; **B -** OC3 site; **C** - OC2 site.

4.4. Paleo-current Analysis

In the study area, the most common and relatively reliable palaeocurrent direction indicators are trough and planar cross-bedded sandstones. Sole markings (e.g., gutter casts), parting lineations and lateral accretion beds are additional features used to obtain palaeocurrent readings. The results of the palaeocurrent analysis are summarized in Table 8 and Figure 24. Numbers denote the three individual locations within the western (W) and eastern (E) facies areas where measurements were collected. At each individual location, a conscious effort was made to gather measurements from both the Abrahamskraal and overlying Teekloof formations in order to assess potential spatiotemporal changes in the Palaeocurrent patterns.

Mean paleo-current directions at the two locations (W1 and W2) in the western facies area indicate palaeocurrents from roughly the southwest to the northeast for both the Abrahamskraal and Teekloof formations. The only exception is Teekloof Formation at location W1 where the flow direction is roughly from W to E. Significant differences are found in the vector magnitudes (25.1; 4.3) and consistency ratios (0.81; 0.54) at W1 location, respectively. The discrepancies in vector magnitude (and direction) at W1could be influenced by the differences in dataset sizes (i.e., palaeocurrent indicators for the Teekloof Formation proved difficult to find in the field at this site). At W2 location, the more robust datasets provided results that can be more confidently interpreted: the main flow direction for both units is from SW to NE; the consistency ratios and vector magnitudes are relatively high suggesting strong, unidirectional currents. In the eastern facies area (E1), the results indicate palaeocurrents from the south to the north; however the limited number of measurements lowers the confidence in the results.

All in all, the data show that at the sampling locations W1, W2, E1 (Table 8), the regional palaeocurrent patterns remained the same through time, however changed though space, because currents were sourced from SW in the Western facies area and from S in the Eastern Facies area (see Figure 24).

	Western Facies						Eastern Facies		
	W1			W2			E1		
Teekloof Formation	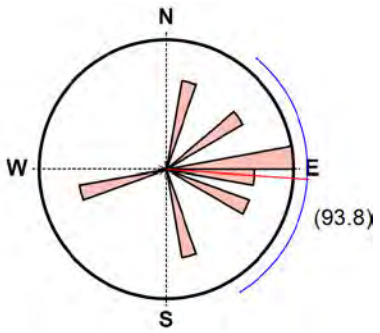			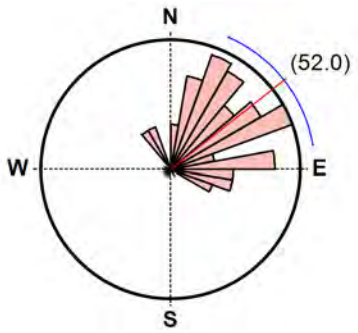			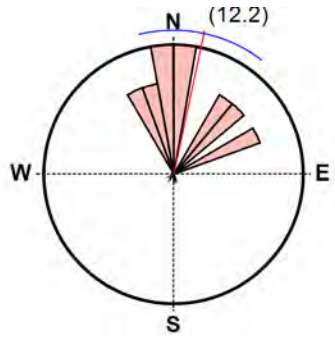		
	n - 8	MD - 93.78°	SD - ± 54.82°	n - 54	MD - 51.9°	SD - ± 29.23°	n - 9	MD - 12.15°	SD - ± 26.24°
	VM - 4.34	CR - 0.54		VM - 46.9	CR - 0.87		VM - 8.06	CR - 0.90	
Abrahamskraal Formation	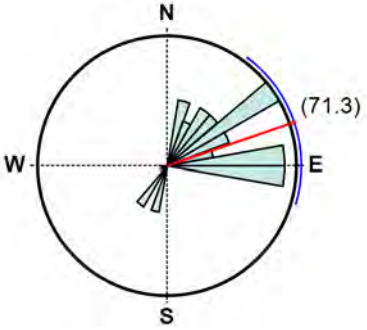			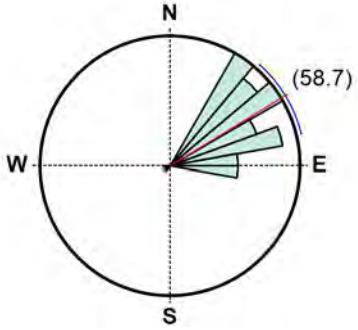			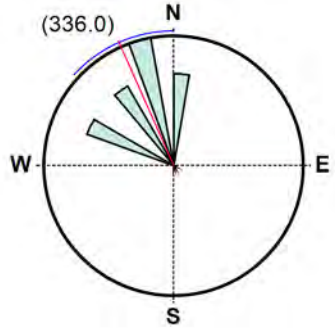		
	n - 31	MD - 71.26°	SD - ±35.37°	n - 18	MD - 58.7°	SD - ± 18.01°	n - 5	MD - 336.05°	SD - ± 23.98°
	VM -25.09	CR - 0.81		VM - 17.1	CR - 0.95		VM - 4.56	CR - 0.91	

Table 8: Summary of the rose diagrams of the palaeocurrent measurements obtained from the Abrahamskraal and Teekloof formations in the Western (W) and Eastern Facies (E) areas at 3 locations. N - Number of Readings; MD - Mean Direction; VM - Vector Magnitude; CR - Consistency Ratio; SD - Standard Deviation.

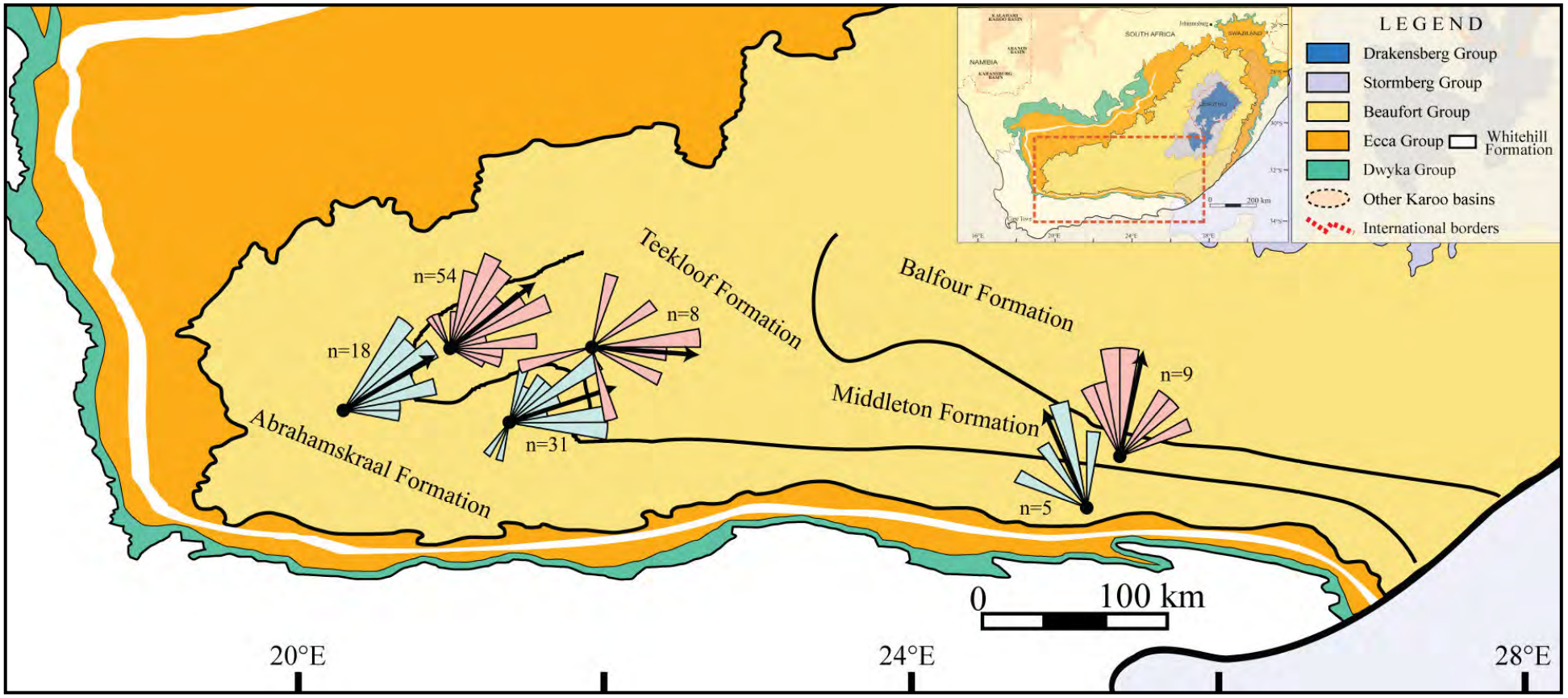

Figure 24: Palaeocurrent rose diagrams obtained from the Abrahamskraal and Teekloof formations in the western (W) and eastern (E) facies areas plotted on the simplified map of the lower Beaufort Group in the southern part of the main Karoo Basin (see Table 8 for details). Results indicate source areas in the SW and S for the western and eastern facies, respectively, but no or negligible change in the direction of the main palaeo-slopes though time.

4.5. Petrographic studies

Modal analyses of the sandstones were performed by counting 300 grains per slides (Table 9). The results were plotted on Quartz-Feldspar-Lithic fragment ternary diagrams (Figure 25) which indicate that all sandstone samples are feldsphatic greywackes both in the Abrahamskraal and Teekloof formations. The samples are dominated by quartz, mainly polycrystalline quartz (Qp -Table 9), however sand and silt size plagioclase feldspar, micas and different lithic fragments such as chert, carbonate and opaque minerals (presumably oxides) are also present. The degree of preservation of feldspar is good, occasional etching and alterations to clay are present. The sandstones are generally fine-grained, with sub-rounded and low to medium sphericity grains that form a homogenous, occasionally laminated fabric. The sandstones are generally sub-mature with an >15% of clayey matrix (up to 30%). The samples show low porosity and occasionally, carbonate cement is present.

The distribution of the samples in the ternary diagrams (Figure 25) shows no spatiotemporal changes in the composition, because the samples generally plot in the same area, with the exception of a few Teekloof Formation samples that appear to be richer in feldspar, especially in the eastern facies area.

Table 9: Mineral modal analysis of sandstone samples derived from identifying 300 sediment grains per slide. Results are shown in percentages. Qm - Monocrystalline Quartz; Qp - Polycrystalline Quartz; Fp - Plagioclase Feldspar; Fk - Alkali Feldspar; Lv - Volcanic Lithic; Lm - Metamorphic Lithic; Lp Plutonic Lithic- ; Ls - Sedimentary Lithic; Accs - Accessory Minerals (mica, pyroxenes and amphiboles); Un - Unidentified Minerals; SD - Standard Deviation.

		Samples	Qm	Qp	Fp	Fk	Lv	Lm	Lp	Ls	Accs	Un
Teekloof Formation	E. Facies	KM6B	11.3	45.7	18.0	0.3	0.0	0.7	2.7	12.7	8.7	0.0
		KM8	4.0	45.7	25.3	0.3	0.0	0.0	0.7	13.0	10.3	0.7
		KM6A	22.3	35.0	24.0	0.3	0.0	0.0	1.7	9.3	7.3	0.0
		KM10	22.3	35.0	24.0	0.3	0.0	0.0	1.7	9.3	7.3	0.0
	W. Facies	Su-Tee1	23.0	41.0	16.3	0.0	0.0	0.0	1.7	14.0	4.0	0.0
		PA10	7.0	66.7	9.3	0.3	0.0	0.0	1.3	12.0	2.7	0.7
		PA11	15.0	44.3	23.3	0.0	0.0	0.0	1.3	11.3	4.7	0.0
		P8	24.0	45.3	14.7	0.0	0.0	0.3	3.0	7.7	5.0	0.0
		P7	10.3	52.7	8.7	0.7	0.0	1.0	0.3	16.3	9.7	0.3
		P6	16.0	50.7	13.0	1.0	0.0	0.0	0.3	14.0	5.0	0.0
		P3	8.7	52.0	17.7	3.0	0.0	3.3	7.0	1.3	7.0	0.0
	Av.		14.9	46.7	17.7	0.6	0.0	0.5	2.0	11.0	6.5	0.2
	SD		7.2	8.9	5.9	0.9	0.0	1.0	1.9	4.1	2.4	0.3
Abrahamskraal Formation	E Facies	KM31	7.7	60.0	10.3	0.3	0.0	0.3	0.3	12.7	8.3	0.0
		KM12	28.0	31.7	25.7	0.0	0.0	0.0	0.0	11.0	3.7	0.0
		KM5A	30.7	45.0	11.0	0.0	0.0	0.0	1.3	5.3	6.7	0.0
	W. Facies	Su-Abr 5	17.0	52.0	13.0	0.0	0.0	0.0	4.3	12.7	1.0	0.0
		PA1	17.3	59.0	11.0	0.0	0.0	0.3	0.3	3.3	8.7	0.0
		PA2	8.3	61.0	14.3	1.3	0.0	0.0	0.0	9.7	5.3	0.0

	A0	12.7	61.7	3.7	0.0	0.0	0.0	1.0	16.7	4.3	0.0
	A2	7.0	58.3	13.3	0.7	0.0	0.3	0.3	15.0	4.7	0.3
	A-9	10.0	46.0	14.0	0.0	0.0	0.7	1.3	20.7	7.3	0.0
	A8	22.3	43.0	13.7	0.0	0.0	1.0	1.7	11.0	7.3	0.0
	A5	18.3	55.3	8.0	0.0	0.0	0.0	0.3	11.3	6.7	0.0
	A4	15.7	55.0	18.7	0.0	0.0	0.0	3.0	4.3	3.3	0.0
Av.		16.3	52.3	13.1	0.2	0.0	0.2	1.2	11.1	5.6	0.0
SD		7.8	9.2	5.4	0.4	0.0	0.3	1.3	5.1	2.3	0.1

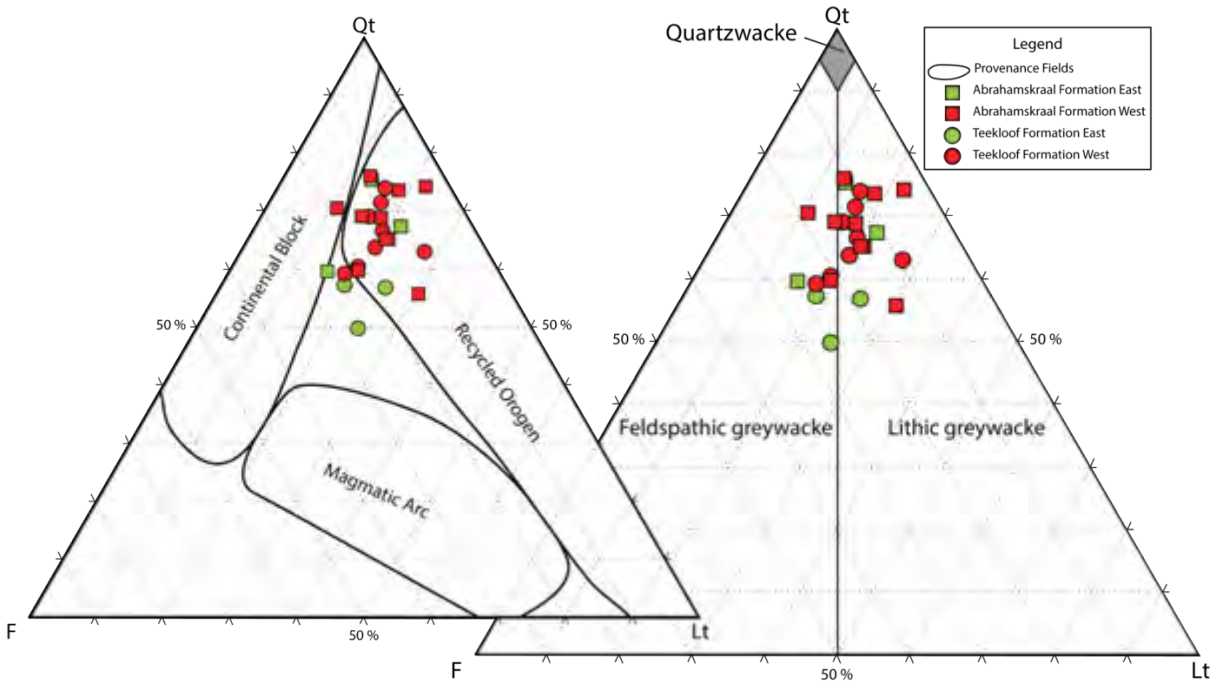

Figure 25: Quartz-Feldspar-Lithic (QFL) ternary diagram showing the composition and provenance of the sediments. (Right triangle) Majority of the samples classify as lithic greywackes, and are dominated by quartz. Teekloof Formation samples appear to be richer in feldspars (av. ~18%) compared to the Abrahamskraal Formation, which is richer in quartz (av. ~52%). (Left triangle) Interpretative provenance fields indicating that the source of sediments remained an orogenic setting from where sediments were recycled throughout the deposition of these formations (Ingersoll et al., 1984; Dickinson, 1985).

4.6. Geochemistry

4.6.1. X-Ray Diffraction (XRD)

Bulk Rock XRD

The results for the quantitative X-Ray diffraction (QXRD) are displayed in Table 10, and the phases identified are: Muscovite-Mica, Orthoclase-Feldspar, Quartz, Chlorite, Kaolinite-Nacrite and Oligoclase-Feldspar. The bulk rock XRD spectra also displayed peaks in the range attributed to clay

minerals (2θ < 12°; Figure 28). Due to the lack of resolution in the procedure, identification and quantification of clays were not possible.

The results do not show significant differences in mineral percentages for the two formations. Major constituents for both formations are quartz (~42% av.), oligoclase (plagioclase series; ~35% av.) and muscovite (~12% av.). QXRD results show to be in good agreement with petrographic descriptions (Table 9and Figure 25). Discrepancies between the methods are only found in the high mica and plagioclase percentages shown in the QXRD results. This can be attributed to the fact that minerals in the matrix are also included in the QXRD results, but not accounted for by petrography due to the resolution limitation of the petrographic microscope in identifying small grains.

An XRD spectrum used in quantification of mineral phases is presented in Figure 26. The full data set of XRD scans can be found in appendices Figure 38. Measurements in the XRD machine and the quantification of phases (as detailed in the methodology Ch. 3.5.1, Page 33) were performed by an external consultant, at the Centre for Mineral Research (CMR), in the Chemical Engineering Department (University of Cape Town).

Table 10: Quantitative X-Ray Diffraction (QXRD) results for bulk rock sample analysis of samples from the Abrahamskraal and Teekloof formations. Muscovite-Mica, Oligoclase-Plagioclase Feldspar and Quartz are the most common mineral phases.

		Samples	Muscovite - Mica	Feldspar-Orthoclase	Quartz	Chlorite	Kaolinite-Nacrite	Feldspar - Oligoclase
Teekloof Formation	E. Facies	KM10	10.4	4.00	37.5	4.10	3.20	40.9
		KM6x	10.3	5.30	42.8	2.40	2.90	36.3
	W. Facies	SUTEE 6	13.2	4.60	37.6	2.50	2.20	40.0
		P6	11.7	5.00	43.2	2.50	2.30	35.3
		PA6	11.6	10.1	45.3	1.20	2.90	28.9
	Mean		12.2	6.6	42.0	2.1	2.5	34.7
Abrahamskraal Formation	E. Facies	KM3	15.7	3.50	37.2	3.00	5.30	35.3
		KM5A	22.0	3.20	29.8	3.80	3.10	38.1
	W. Facies	SU ABR4	10.0	3.40	50.4	1.00	2.90	32.3
		A0	13.9	3.80	45.1	2.40	2.50	32.3
		A2	12.9	3.30	44.0	1.80	1.70	36.4
		A-4	8.10	2.00	42.7	2.10	1.80	43.3
		A-8	10.2	2.10	43.0	2.70	2.80	39.2
		PA1	11.9	6.00	46.1	1.30	1.80	32.9
	Mean		12.9	3.7	42.2	2.3	2.7	36.2

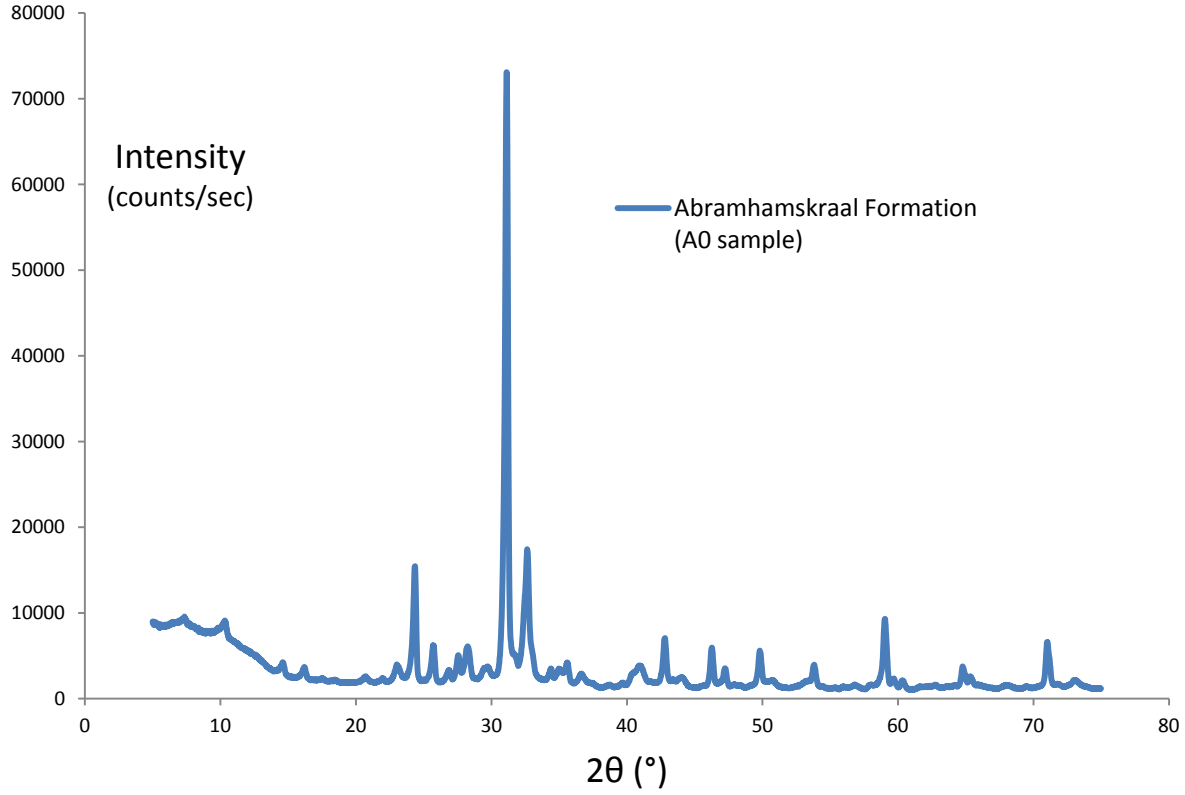

Figure 26: of a bulk XRD scan obtained for sample A0 from the lower Abrahamskraal Formation.

Clay Fraction XRD

Examples of the clay fraction XRD spectra obtained are presented in Figure 27.

The strong reflection peaks of quartz can be easily identified in all the XRD scans, typically at 2θ ~21° and 26.5°. The presence of quartz, even after clay fraction separation, shows that quartz is abundant in all grain size fractions in the samples. .

The clay phases that were frequently identified in all the XRD analysis are kaolinite, vermiculite, montmorilonite and illite. Other recurring and less frequently encountered phases are: saponite (smectite group), lepidolite (mica group) and chlorite. Other frequently identified non-clay minerals are: quartz, Ca-albite and muscovite.

The results only allow for a semi-quantitative analysis, and show no particular spatiotemporal trend with respect to the presence of specific clay minerals. Further quantification of the clay phases would provide more clarity for the interpretation, and it should be the focus of future research.

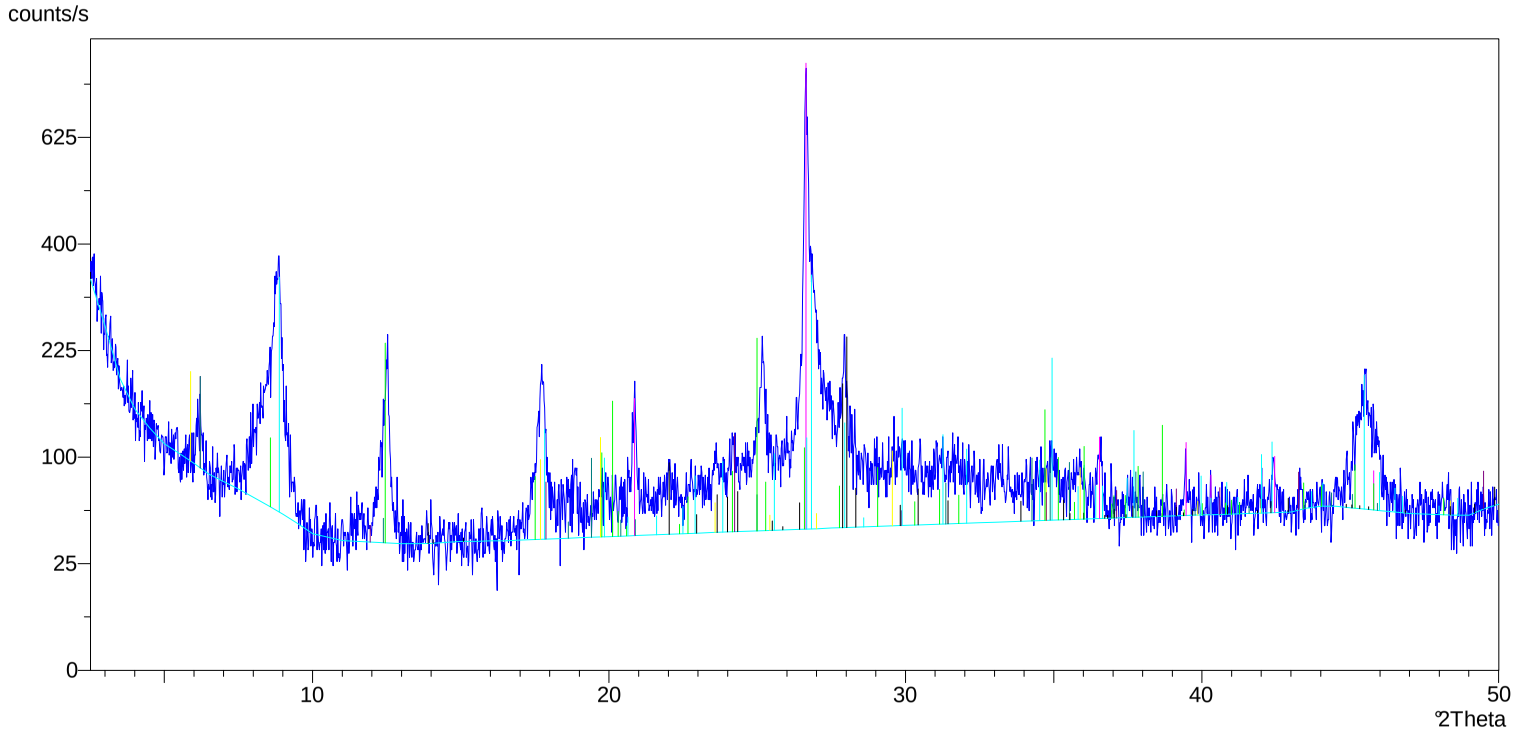

46-1045	Quartz, syn	D	SiO2
13-0135	Montmorillonite-15A	E	Ca0.2(Al,Mg)2Si4O10(OH)2!4H2O
13-0086	Saponite-15A	S	Mg3(Si,Al)4O10(OH)2!4H2O
16-0613	Vermiculite-2M	3	Mgx(Mg,Fe)3(Si,Al)4O10(OH)2!4H
24-0495	Illite-2M2	A	K0.7Al2.1(Si,Al)4O10(OH)2
06-0263	Muscovite-2M1	B	KAl2(Si3Al)O10(OH,F)2
41-1480	Albite, calcian, ordered	0	(Na,Ca)Al(Si,Al)3O8
29-1488	Kaolinite-1Md	A	Al2Si2O5(OH)4

Figure 27: Clay fraction XRD spectrum with all the interpreted peaks identification for the Abrahamskraal Formation western facies (A5N Location). Phases were identified primarily by the matching their 2θ and intensity of the two strongest peaks.

4.5.2. X-RAY FLUORESCENCE (XRF)

XRF data is presented in Table 10 and Table 12 (Ch. 6.3, Pg. 96). The different data trends are shown in Figures 28, 29 and30.

In terms of the major oxides, as expected, SiO_2 is the most abundant oxide ($70.73 \pm 3.970\ Wt\%$ ave.). SiO_2/Al_2O_3 ratio can be used as index of sedimentary maturation, reflecting the effects of transport and recycling in the rocks. High SiO_2/Al_2O_3 would indicate the prevalence of quartz minerals, over lithic fragments and feldspars, thus it would indicate a higher maturity (Roser et al., 2010). SiO_2/Al_2O_3 averages are 5.46 ± 0.46, and 5.65 ± 0.16 for the Teekloof and Abrahamskraal formations, respectively. The values are very close to each other, and they reflect some sediment maturation. The rest of the ratios ($\mathrm{Fe/Al;\ K/Al;\ Al/Ti}$) also show small deviations from their respective means, which are again very similar for both formations. Consistent variations in all the ratios are highlighted by the dotted lines in Figure 28, and they seem to coincide with the start and the end of the arenaceous interval (the Moodenaars Member of the Abrahamskraal Formation).

The Chemical Index of Alteration (CIA) is one of the main weathering proxies used in this work (Figure 28 and Figure 30).Standard and molar CIA were both calculated, with minimum values being found at SuAbr1 site (CIA_{mo} = 0.76; CIA_{st} = 43.3) and the maximum at A5N site (CIA_{mo} = 1.58; CIA_{st} = 61.3) (Table 11), and, the averages for both formations is 1.23 ± 0.19 for CIAmo and 54.8 ± 4.2 for CIA_{st}. Although the absolute values of both CIA-methods are different, the relative proportions are the same. This can be observed in Figure 28 where both CIA_{mo} and CIA_{st} have exactly the same stratigraphic trend. Therefore stratigraphic interpretations can be based on one of the methods only; and, the results are in the field of what is attributed to feldspar composition. When CIA_{mo} is plotted against $K_2O/N_2O$and Al_2O_3, it can be used as an aridity indicator (Goldberg and Humayun, 2010). The results suggest that dry environmental conditions prevail during the deposition of both formations (Figure 29).

ICV values vary from 0.81 (A2 site) and 1.58 (Su-Abr1 site) with an overall average of 0.97 ± 0.15. ICV stratigraphic trend (Figure 28) is in essence a mirror image of CIA trends, and further supports the interpretation of the dry environment at the time of deposition.

Table 11: XRF data from selected samples from the Abrahamskraal and Teekloof formations collected from both the western and eastern facies areas.

		Sample	SiO_2	Al_2O_3	CaO	Na_2O	K_2O	CN	CIA_{st}	CIA_{mo}	ICV
Teekloof Formation	E. Facies	KM10	66.8	13.5	3.5	3.9	0.8	7.4	49.9	0.99	1.22
		KM8	67.5	14.2	1.4	5.1	0.8	6.5	54.6	1.21	1.05
		KM6x	70.8	12.3	2.1	3.8	1.6	5.9	51.2	1.05	1.02
	W. Facies	PA6	69.3	11.8	3.7	2.7	2.3	6.4	46.2	0.85	1.13
		P8	72.3	12.9	0.7	4.2	1.4	4.9	57.1	1.33	0.92
		P6	71.5	12.9	0.8	3.7	1.6	4.5	58.2	1.39	0.88
		SU-TEE6	70.0	13.6	0.9	4.0	1.9	4.9	57.3	1.34	0.93
		SU TEE-1	73.0	12.0	1.2	3.9	1.2	5.1	54.8	1.21	0.99
	Av.		70.2	12.9	1.79	3.90	1.44	5.69	53.7	1.17	1.02
	SD		2.21	0.83	1.21	0.67	0.53	1.00	4.21	0.19	0.11
Abrahamskraal Formation	E. Facies	KM5A	65.8	16.4	1.8	3.6	2.9	5.5	56.8	1.31	0.88
		KM3	67.1	14.6	2.0	3.4	1.7	5.4	57.0	1.32	0.90
		KM2A	62.6	15.3	5.5	1.1	4.0	6.6	48.5	0.94	1.07
	W. Facies	PA3	74.0	11.9	0.7	3.7	1.4	4.3	57.6	1.36	0.89
		PA1	71.7	12.0	1.9	3.2	1.8	5.1	52.9	1.13	0.92
		A5	72.8	12.0	1.0	3.3	1.7	4.2	57.2	1.33	1.01
		A4	74.5	12.2	0.7	3.5	1.9	4.2	57.4	1.35	0.84
		A2	73.0	12.8	0.6	3.7	1.7	4.4	58.2	1.39	0.81
		A1	71.1	13.2	0.9	3.8	1.8	4.8	56.9	1.32	0.91
		A0	70.8	13.1	1.7	3.2	2.2	4.9	55.2	1.23	0.90
		A4N	73.2	12.3	0.8	4.6	1.1	5.4	54.7	1.21	0.91
		A5N	69.8	14.0	0.9	2.5	2.8	3.4	61.3	1.58	0.90
		A6N	75.0	11.5	0.7	4.0	1.0	4.7	56.4	1.29	0.92
		A8N	72.3	12.6	1.0	4.0	1.5	4.9	55.9	1.27	0.85
		SU-ABR4	77.5	10.9	0.5	3.4	1.4	3.9	57.4	1.35	0.82
		SU ABr-1	68.4	10.5	4.1	3.2	1.0	7.3	43.3	0.76	1.49
	Av.		71.215	12.830	1.540	3.396	1.879	4.936	56.151	1.260	0.940
	SD		3.779	1.573	1.393	0.766	0.787	0.979	4.250	0.189	0.161

CN= CaO + Na_2O; CIA_{St} - Standard Chemical Index of Alteration; CIA_{mo} - Molar Chemical Index of Alteration; ICV - Index of Compositional Variation; b.d. - Below detection limits of the machine; SD - Standard Deviation.

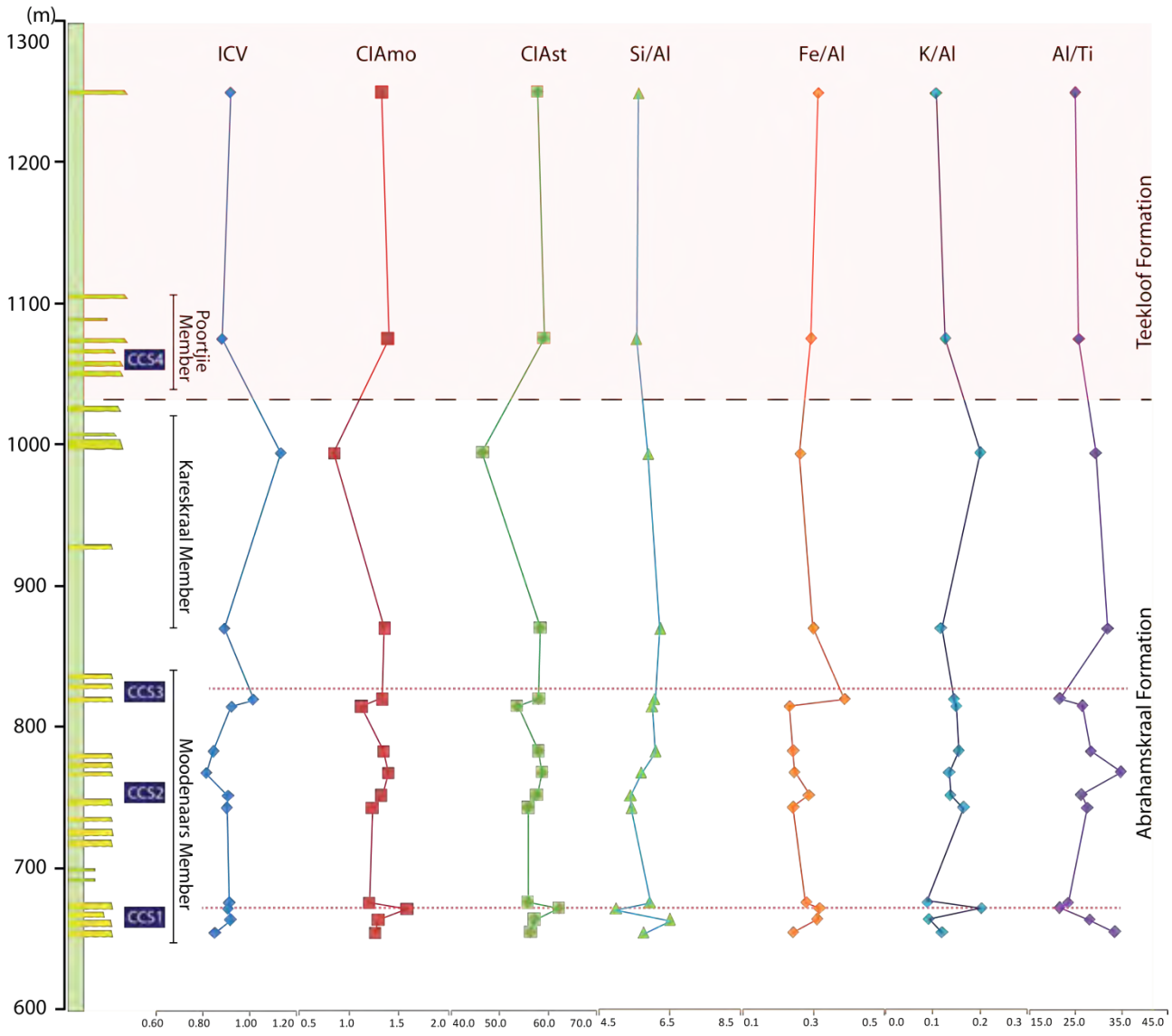

Figure 28: Stratigraphic distribution of the geochemical data across the boundary between the Abrahamskraal and Teekloof formations in the western study area (W1).

A-CN-K ternary diagram is a graphic representation of the chemical index of alteration (CIA), and is shown in Figure 30. The samples from both formations plot in the same general area, which indicates weak chemical weathering, and plot almost parallel to the A-CN tie line. A very weak trend towards the CN is also observed, because the majority of the samples from upper Abrahamskraal Formations are slightly richer in Al_2O_3 than those from the lower Teekloof Formation.

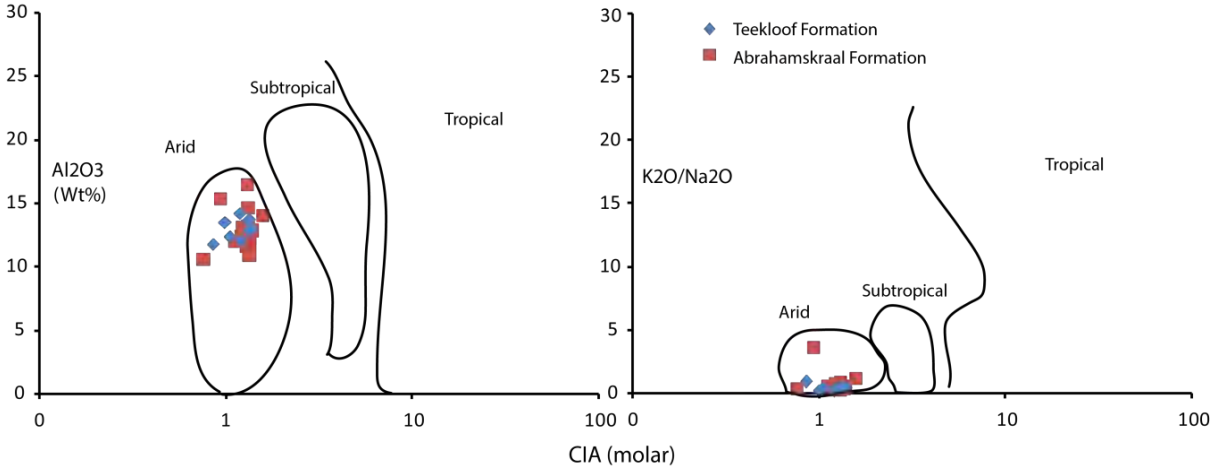

Figure 29: CIA_{mo} vs.K_2O/Na_2O and CIA_{mo} vs.Al_2O_3 values based on the XRF data derived from the Abrahamskraal and Teekloof formations can be used as aridity indicators. The CIA results are around 1 for both formations, indicating prevalence for physical rather than chemical weathering. The formations also have similar values for the oxides. Plot adapted from Goldberg and Humayun (2010).

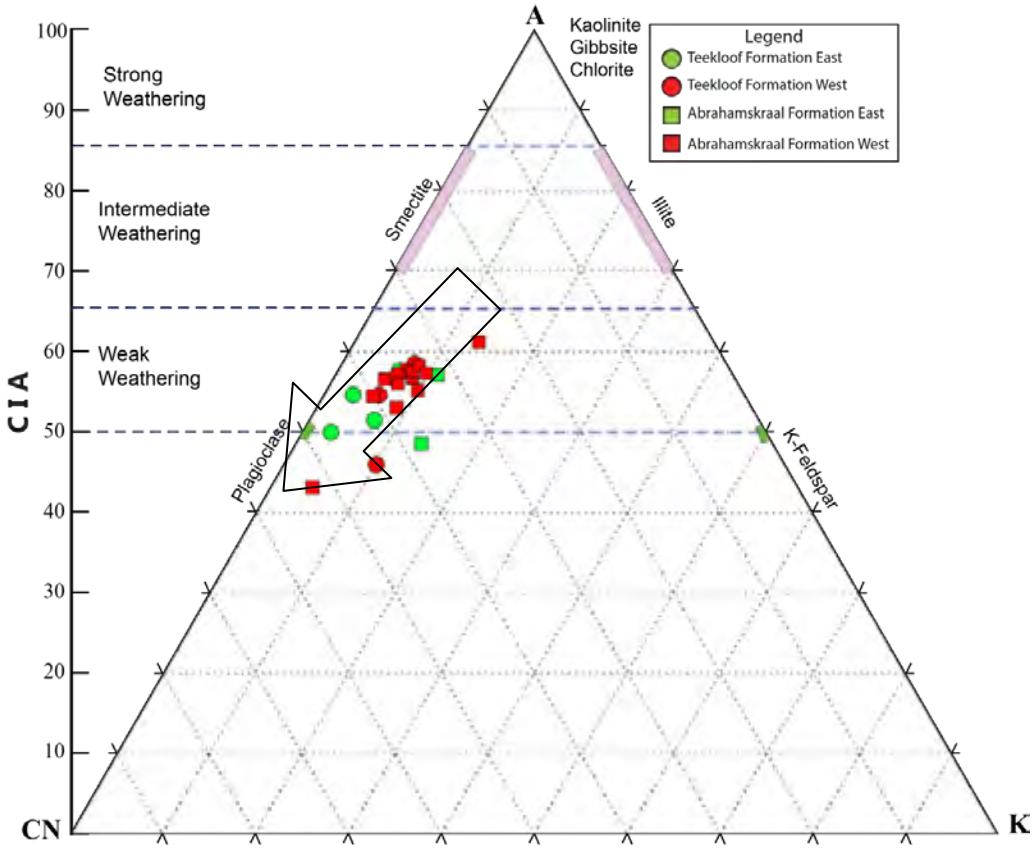

Figure 30: Al_2O_3- (CaO+Na_2O)-K_2O (A-CN-K) ternary diagram for the analysis of the weathering index (CIA) and trends in the sediment source in the Abrahamskraal and Teekloof formations. Chemical weathering affecting the formations was not significant, giving the tendency for the preservation of plagioclase. A very weak stratigraphic trend (marked by the arrow) towards the CN corner (i.e., enrichment in feldspar in the Teekloof Formation) is somewhat noticeable. The ranges and interpretations of CIA_{st} are: kaolinite 90-100, illite 75-85, muscovite 75, feldspar 50, granites 45-55, and basalts 30-45(Nesbitt and Young, 1984; Fedo et al., 1995).

5. Interpretation of the Depositional Environments

5.1. Facies Analysis

5.1.1. GRAVEL FACIES

Gravel elements (GB; Gmm1, Gmm2 and Gch) indicate traction processes in high energy environments (e.g. flash floods) (Miall, 1985). Gravel facies are found throughout the lower Beaufort Group at the base of channel deposits, forming upward fining sequences (UFS; e.g. Figure 11), which indicate a gradual decrease in energy flow and are typical of fluvial systems (Allen, 1983; Miall, 1985).

The different gravel facies are a function of the characteristics of the channel flow and the sediments available. The structureless Gmm1 facies is the most predominant facies in the GB elements of the lower Beaufort Group. This suggests that plastic debris flow and short lived high energy currents were fairly common palaeo-flow events in these fluvial systems (Miall, 1985). Gch facies are the exception, since they indicate the existence of prolonged high energy traction currents capable of creating bedding and imbrications (Miall, 1985). Most gravel facies, in particular the intra-formational Gmm2 facies, are rich in angular mudstone clasts, which due to their shape and rheology, are presumed to be locally sourced (short travel distance) and resulted from ripping-up of nearby unconsolidated floodplain deposits (Stear, 1985).

In the western study area, gravel facies are more common in the upper Abrahamskraal Formation than in the lower Teekloof Formation (Figures 16 and 17), suggesting that the Abrahamskraal Formation formed under higher energy conditions, and/or possibly a higher frequency of flash floods events. In the eastern facies area, similar proportions of the gravel facies elements are found in the two formations. Quantitative results show that the eastern facies area is richer in gravel architectural elements than the western study area (Figure 16 and 17). In conclusion, energy levels of the eastern facies area seem to be not only greater than the western facies, but also more sustained through time, or alternatively, it was rejuvenated during the deposition of the section equivalent to the lower Teekloof Formation.

5.1.2. SANDSTONE FACIES

The interpretation of each sandstone facies is presented in Table 1. Channel complex elements in the lower Beaufort Group are volumetrically dominated by sandstone facies and upward fining sequences. A typical UFS starts with gravels (Gmm1) and/or coarse grained cross-bedded sandstones

(St, Sl), followed by Sp, Sh, Sm and lastly Sr facies element at the top of the sequence. The upward fining sequence indicates either an overall gradual decrease in channel flow energy (Miall, 1985), or, a lateral migration of the active channel profile causing a localized flow energy decrease with time. These two have natural progressions in fluvial systems, in which aggradation (leading to slope reduction) and lateral migration are common autogenic phenomena (Allen, 1983; Miall, 1985).

Channel storey elements in the western facies area, usually start with medium, occasionally coarse-grained sandstones, and grade into fine-grained sandstones that dominate the elements. In the eastern facies area, medium-grained sandstones are more common throughout the channel deposits, indicating an overall higher energy flow conditions for both formation.

Sandstone facies are also found within floodplain depositional elements and were interpreted as crevasse elements (CS and CR), levees (LV) and sandy floodplain sheet-floods (SF). These facies develop in the form of floodplain splays or even short-lived small channels, and usually result from the overload of the flow capacity in the main channel (Allen, 1983; Miall, 1985; Stear, 1985; Gulliford et al., 2014).

5.1.3. MUDSTONE FACIES

Mudstone facies develop in the low energy floodplain or abandoned channel areas of fluvial systems. Laminated mudstones (Fl1, Fl2) are very common facies in the lower Beaufort Group, and indicate the slow settling of mud-size particles from suspension. Massive mudstones (commonly Fsm2) are common in all facies areas, and may be interpreted as a result of a quick deposition (mass movement), or bioturbation disrupting any primary sedimentary structures (Rubidge et al., 2000).

The interbedding of green grey (Fsm2) and purple-red (Fl1) fines is a characteristic feature in the lower Beaufort Group. The colour variation is understood to be a result of variations in the water table height (shortly after deposition) driving the oxidation of iron. Grey-green colouration indicates reducing (anoxic), subaqueous conditions during high water table conditions. In contrast, purple-red coloration originates during low water table conditions, resulting in subaerial, oxidizing exposure, according to Wilson et al.(2014) who presented a conceptual model for the colour variation in the lower Beaufort Group. It is important to note that colouration may also be a result of diagenetic processes. Nevertheless, if variations in mudstone colour can then be associated with climatic conditions, the abundance of purple-red mudstones in the Teekloof Formation may indicate low water table, prolonged subaerial conditions and higher aridity (Wilson et al., 2014). Furthermore, in fluvial sequence stratigraphy, regional water table is considered a landward extension of relative sea level (Gulliford et al., 2014; Wilson et al., 2014), and drops in water table could signify a drop in relative sea level which in turn would cause incision of channels and local erosion of previously deposited strata (Catuneanu, 2006). Palaeosols and desiccation mudcracks facies are common in the

lower Beaufort and are considered as further indicators of prolonged and repeated wetting and drying events that occur in subaerial and semi-arid conditions (Retallack, 2005). In addition, they indicate soil formation processes and a decrease clastic sedimentation rates (Retallack, 2005).

5.1.4. FACIES ASSOCIATIONS

Architectural elements (AEs) are first level of facies associations considered, and represent the building blocks of the different channel and floodplain elements. A total of 13AEs are defined in this study (Table 3). The most abundant AEs in the lower Beaufort Group are downstream and lateral accretion barforms (DA and LA, respectively). Their abundance indicates the predominance of rivers with mobile channels. In the upper Abrahamskraal Formation and in the eastern lower Teekloof Formation, the high proportion of DA elements suggests braided river styles. In the western lower Teekloof Formation, the dominance LA element indicates the lateral migration of point bars, which are common in meandering rivers. Sandy-sheetflood elements (SF) are particularly common in the eastern facies of both formations (Figure 14). In contrast to the normal aggradational mudstone-dominated floodplains, the eastern facies are dominated by coarser sediments, which may indicate overall higher energy fluvial processes in the east.

Lateral grain size variation (LGV) is a common feature in floodplain related sandstones. These sandy (occasionally silty) ribbon beds grade into finer floodplain mudstones, and are interpreted as crevasse splay deposits (Miall, 1996), or alternatively, levee elements (Johnson and Vuuren, 1997). The lateral grain size variation occurs perpendicular to the main channel axis, since the splays originating these elements lose energy along the low gradients of the floodplain.

Multiple upward fining sequences (UFS) also display a repeated sequence of facies elements and are often found in multi-storey amalgamated channel belts (e.g., AT6 architecture type, Figure 23A). These may have formed from multiple reoccupation events of different-aged palaeo-channels that shared the same course along the palaeo-slope. Furthermore, as a consequence of the down-scouring action, a truncated sequence of facies and architectural elements would be generated (Stear, 1980; Gibling, 2006; Wilson et al., 2014). However, by using observations of the 1981 Laingsburg flood event, Stear(1985) proposes that multi-storey amalgamated channel belts could be a result of single large flood event with multiple flooding/erosion pulses, which are common in semi-arid climates.

The common combinations of external and internal architectures were grouped to form Architecture Types (AT). Seven Architecture Types have been established, and their descriptions and illustrations can be found in the Architecture Plates (Figures 20, 21, 22 and 23) and in Table 7. Multilateral, channel-belt complexes with erosional bases are the most common external architecture feature throughout the lower Beaufort Group in the southern main Karoo Basin. The laterally extensive

sandstone sheets that can be traced for tens of kilometres, and locally comprise architecture types: AT1, AT2, AT3 and AT5. The abundance of these km-wide multilateral channel-belt complexes suggests fluvial systems with high migration rates as well as high avulsion periodicity, in addition to, low channel aggradation and low amalgamation rates (Gibling, 2006; Gulliford et al., 2014; Wilson et al., 2014; Flood and Hampson, 2015). These conditions usually occur in alluvial environments with low gradient and low sedimentation rates, which was previously suggested for the lower Beaufort Group (Cole and Wipplinger, 2001; McCarthy and Rubidge, 2005; Gulliford et al., 2014; Wilson et al., 2014).

Table 12: Relative stratigraphic distribution of the established channel-belt complex sets and their architecture types in the Abrahamskraal and Teekloof formations.

		Western Facies			Eastern Facies		
		Channel Complex Sets (CCS)	Architecture Types (AT)		Channel Complex Sets (CCS)	Architecture Types (AT)	
Teekloof Formation				AT7	CS7	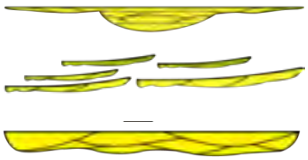	AT4 AT7 AT1
	Poortjie M.	CCS4	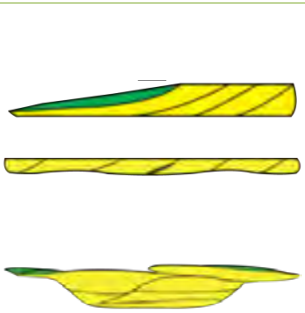	AT3 AT5 AT6	CS6	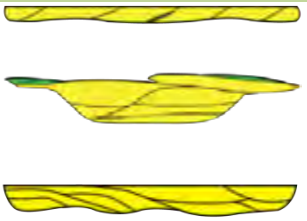	AT5 AT6 AT2
Abrahamskraal Formation	Kareskraal M.			AT2 AT4 AT3			
	Moordenaars M.	CCS3		AT3 AT2	CC5	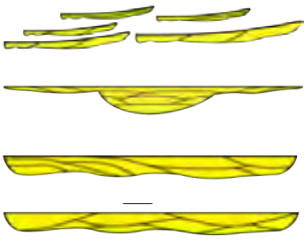	AT7 AT4 AT2 AT1
		CCS2	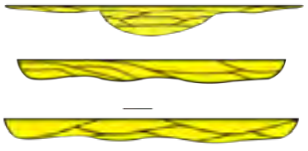	AT4 AT2 AT1			
		CCS1	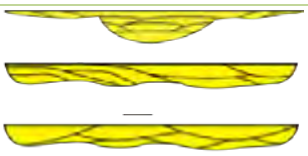	AT4 AT2 AT1			

Thick (up to 50 m), valley-shaped, vertically stacked channel-belt complexes (architecture type AT6, Figure 23C) have been locally identified in the lower Teekloof Formation in both study areas. This architecture type has also been reported by (Gulliford et al., 2014; Wilson et al., 2014) and is thought to originate in setting with high amalgamation and aggradation rates. This architecture can be explained by high energy fluvial systems with frequent channel reoccupation rates and strong scouring power. Alternatively, AT6 could represent a valley incision formed by base level drop that was subsequently filled by aggradational processes (Wilson et al., 2014). The localized dominance of architecture type AT6 represents a departure from what is otherwise considered the common architecture type (i.e., multilateral channel complex sheets). In addition to being localised and constrained to the lower Teekloof Formation, its presence strongly indicates a local anomaly in the sedimentation rates and/or accommodation space creation rates (Catuneanu, 2006; Zecchin and Catuneanu, 2013).

In addition to the architecture types, seven channel-belt complex sets (CCS) were also established by grouping the different channel-belt complexes that shared a close spatial relationship (vertically separated by 10-20 m, e.g. Figure 20A and 21H). Their relative stratigraphic positions and their observed architecture types are summarised in Table 12.

5.2. Petrographic analysis

The composition of detrital sediments depends on provenance, transportation, depositional environment and diagenesis (Ingersoll et al., 1984). Although each of these factors can have a significant impact of the final sediment composition, petrographic analyses in this study were aimed at understanding and identifying the provenance (source rock types) and the evaluating the depositional environment. Petrographic results are summarized in Table 9 and Figure 25.

The sandstones of both the upper Abrahamskraal and lower Teekloof formations were found to be mostly immature to sub-mature lithic greywackes (Figure 25). The low maturity of the rocks indicates short travel distances from the source to the depositional site. The high abundance of undulatory polycrystalline quartz, a mechanically weak mineral that eventually breaks into smaller monocrystalline quartz grains, also suggests low maturity and short transport distances of the sediments (Basu, 1985).

Undulatory polycrystalline quartz grains as well as the metamorphic lithic fragments suggest a metamorphic source (Basu, 1985), because undulations in quartz is a property that develops through deformation (i.e., metamorphic pressure). A metamorphic source is also indicted by the QFL ternary diagram (Figure 25), because most samples plot in the recycled orogenic province defined by

Dickinson (1985). In addition, unaltered felsic plutonic rocks are also thought to be among the sources, and this is indicated by the presence of monocrystalline quartz grains and abundance of plutonic lithic fragments (Basu, 1985). The absence of any metamorphic fabric or mineral assemblages suggests shallow burial conditions, and therefore undulations in quartz are thought to reflect the source rocks, and are not a product of burial diagenesis.

Plagioclase feldspars are common in the rock samples. Some appear well-preserved, while a good portion shows variable degrees of alteration in the form of etched boundaries, mica inclusions and overgrowth, particularly in the cleavages. The breakdown of feldspars is probably associated with physical weathering. This is suggested by CIA and A-CN-K ternary diagrams (Figure 28 and 30), which indicate bulk rock composition trending to feldspars.

Grain size can be indicative of the energy levels of the palaeo-flow. The sandstones in the western study area are consistently fine-grained, therefore indicating similar energy levels that can be presumed to have been low to moderate. In the eastern study area, medium-grained sandstones are more common, indicating higher energy levels compared to the to the western facies area.

5.3. Provenance History and Reconstruction/Evolution Model

Evaluation of the spatiotemporal variations of the observed facies, palaeocurrents and mineralogical composition are key in understanding and reconstructing the palaeo-environment of the lower Beaufort Group in the southern main Karoo Basin.

Palaeocurrent results (Figure 24) show two distinct sediment transport directions from the SW and S in the western and eastern facies areas, respectively. However, mineral modal distribution (Figure 25) and geochemical results are very similar for both formations throughout the region, and therefore indicate an orogenic source under similar climatic conditions for both the western and eastern facies areas. The results also suggest that the two geographically different sources were petrologically similar if not identical (i.e., laterally extensive orogenic belt) throughout the deposition of the Abrahamskraal and lower Teekloof formations. The data presented in this work is not statistically strong enough to further distinguish the sources.

In both facies areas, no significant changes in palaeocurrents, rock composition and geochemistry were observed across the stratigraphic boundary of the upper Abrahamskraal and lower Teekloof formations. These trends indicate the stability in the petrological composition of the source area, prevailing climate and the sediment transport direction through time. Therefore, it can be concluded that the observed spatiotemporal architectural differences observed across the formations are probably not linked to changes in climate or the composition and position of the provenance area, but are likely linked to specific geomorphic changes due to autogenic or tectonic (allogenic) controls.

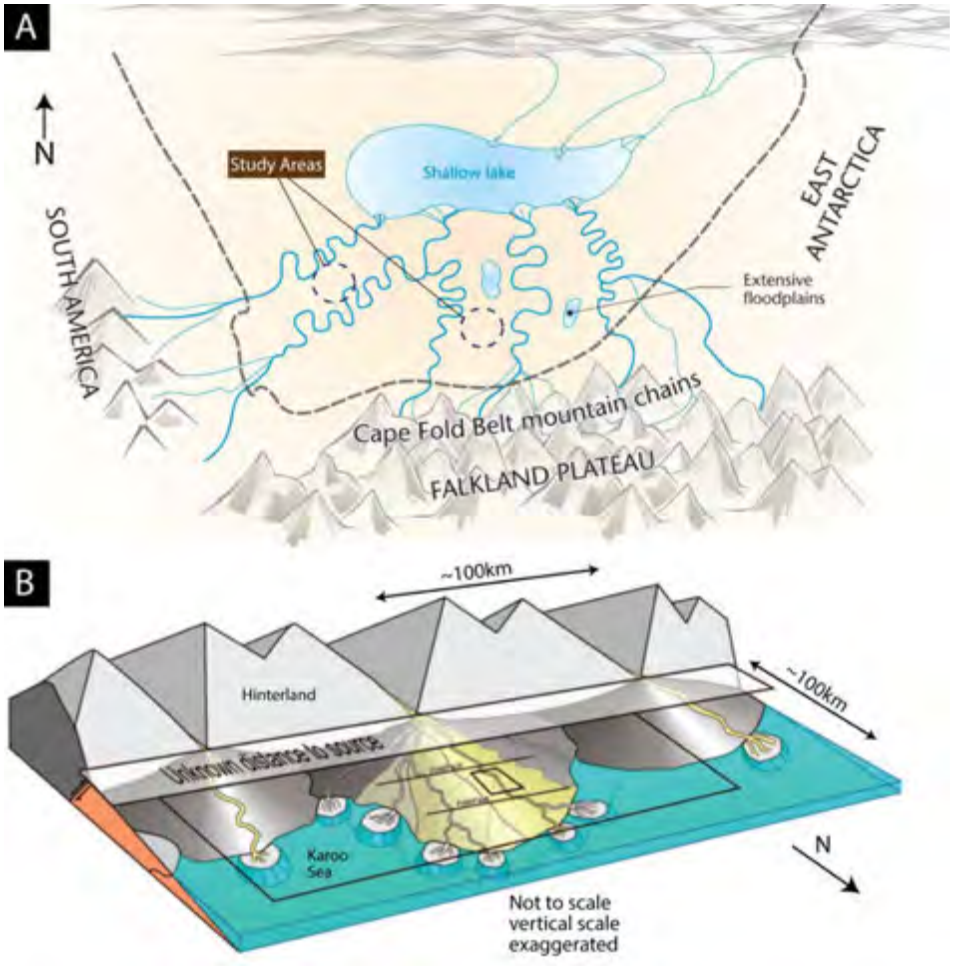

Figure 31: Regional depositional setting and provenance areas for the lower Beaufort Group. **A**- Illustrates the two different transportation directions for the southern main Karoo Basin. Mineralogical and geochemical data suggest similar composition for the two sources. **B** shows the interpreted overall alluvial system, which is thought to have been a mega fan-shaped distributive fluvial system (DFS; Gulliford et al., 2014; Wilson et al., 2014). Figures adapted after McCarthy and Rubidge (2005); Wilson et al. (2014).

In both study areas, the Abrahamskraal Formation contains facies indicative of higher energy levels than the Teekloof Formation. This could be attributed a change in the gradient of the regional palaeo-slope, with the Abrahamskraal Formation representing the initial steeper slopes resulting in architectural facies typical of braided rivers. Subsequently, the palaeo-slope then became shallower during the deposition of the Teekloof Formation, generating the meandering fluvial styles identified, particularly in the western facies area. In the east, the lower Middleton Formation deposits resemble that of braided rivers, and therefore the changes in palaeo-slopes through time were different in the two parts of the basin.

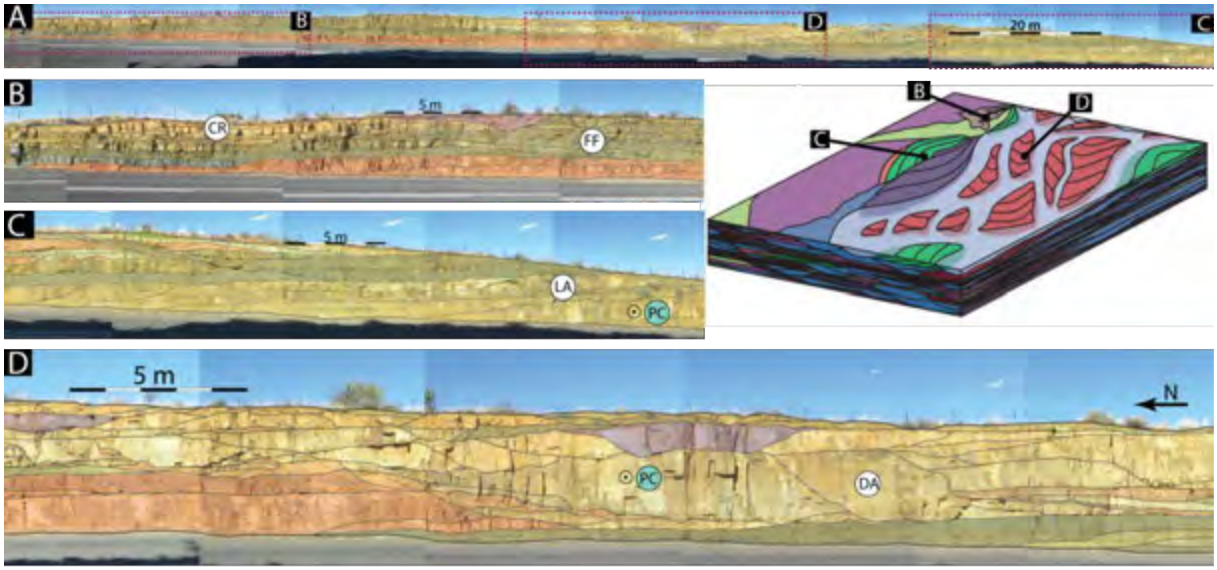

Figure 32: Model for a braided fluvial style, the fluvial style interpretation for the upper Abrahamskraal Formation and the eastern Teekloof Formation. Note that false colour and surface boundaries have been added to the images. Cartoon adapted from (Colombera et al., 2013).

An overall palaeo-environmental reconstruction is shown in Figure 31. It illustrates a large-scale alluvial system fed from the two provenance areas that were in the SW and S. River style reconstructions with field data examples are shown in Figures 32 and 33. It is proposed that the western and eastern upper Abrahamskraal Formation, as well as the eastern lower Middleton Formation, at least in certain areas, were most likely deposited by braided rivers. The western lower Teekloof Formation was most likely deposited by a meandering river. Climate and tectonic considerations are discussed in the next chapter.

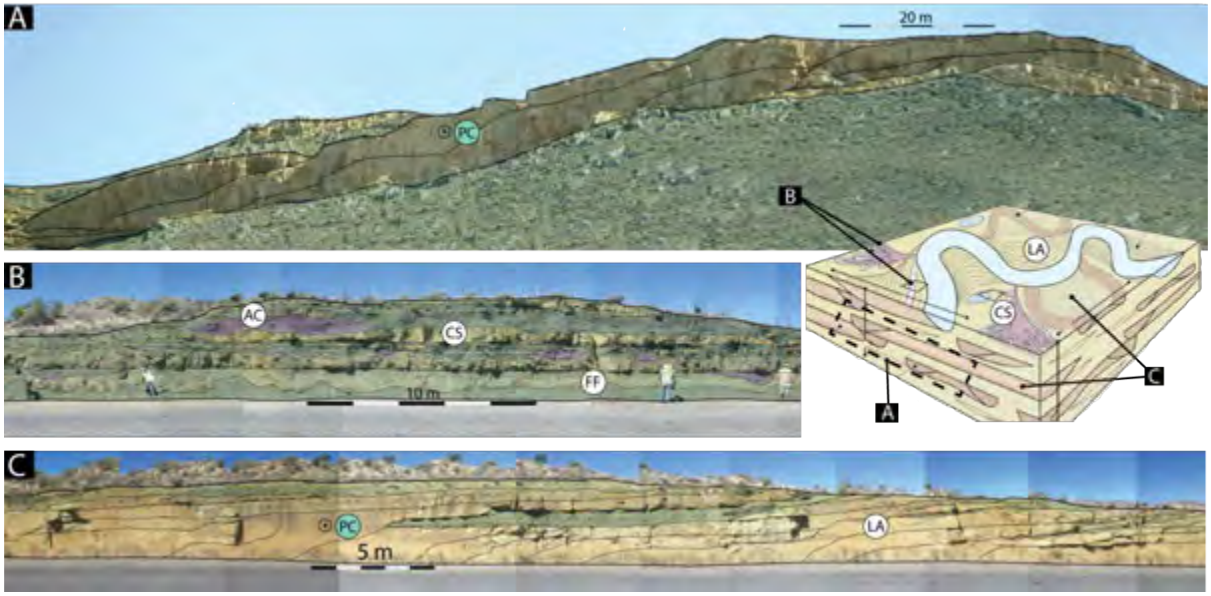

Figure 33: Model for a meandering fluvial system, the fluvial style interpretation for the western lower Teekloof Formation. Note that false colour and surface boundaries have been added to the images.

5.4. Discussion

External and internal architecture of the deposits show a distinctive evolution of fluvial style across the boundary of the upper Abrahamskraal and lower Teekloof formations. This includes an overall decreasing sandstone:mudstone ratio, a change from the common multilateral extensive channel complex sheets to the thick, amalgamated channel complex architecture (at the base of the Teekloof Formation), a change in internal architecture (thus river style) from DA-dominated to LA-dominated (mainly west facies areas). These major architectural trends are attributed here to changes in palaeo-slope gradient as well as changes in aggradation and/or channel reoccupation rates. However, the following questions remain: How and why were these regional slopes changing? How do the different architecture trends fit in the larger picture of the southern Karoo Basin evolution? What were the processes controlling the architecture trends? Why do the changes in architecture trends coincide with the mass extinction event reported by Day et al. (2015) who investigated the same stratigraphic interval?

While the data presented in this work may not have the robustness to fully address all of these questions, some considerations and conclusions can be drawn from the information available. The stratigraphic trends will be discussed in the light of autogenic (e.g., compensational stacking, avulsion, channel adjustment, etc.) and allogenic controls (climate, tectonics and eustacy).

5.4.1. AUTOGENIC CONTROL

To analyse large scale stratigraphic trends in the light autogenic controlling factors, an interplay of parameters need to be considered. The favoured alluvial model for the lower Beaufort Group is a progradational or aggradational mega fan-shaped distributive fluvial system (DFS, Figure 31B) (Gulliford et al., 2014; Wilson et al., 2014). This fan-shaped system is composed of multiple lobes separated by geomorphological ridges, with a variety of river styles on the proximal and distal facies. The key characteristics of this model are an upward increasing trends in grain size, channel deposit thickness and clustering (Gulliford et al., 2014). Although these trends have been reported in the lower Beaufort Group (Paiva, 2013, p. 57; Gulliford et al., 2014; Wilson et al., 2014), most of the data in this work does not seem to fit this model, where opposite trends are observed, in particular in the western facies.

It is noteworthy that the data presented in this work does not discard the DFS model (e.g., the occurrence of AT6 architecture type, reported in both facies areas at the base of the Teekloof formations; the thicker unit encountered in the eastern lower Teekloof Formation- Table 5). More specifically, the sandstone : mudstone ratio decrease mainly observed in the western facies can explained as possible a retreat of the DFS or a lateral shift in the axis of a lobe on the DFS (Gulliford et al., 2014).

5.4.2. ALLOGENIC CONTROLS

The deposits of the lower Beaufort Group are conformable with the underlying marine Waterford Formation in the Ecca Group, therefore the influence of eustatic controls may be present in the lowermost Abrahamskraal Formation, where base-level controlled architecture (i.e., incision valleys) are reported by Bordy and Prevec (2009) and Wilson et al. (2014). However, the influence of eustacy on the stratigraphic trends in the upper Abrahamskraal Formation is considered very limited and probably non-existent, because by this time the southern main Karoo Basin was likely fully continental (Catuneanu et al., 1998).

Palaeoclimate conditions can be difficult to interpret and evaluate, because climate is a complex and integrated system of many variables. Nevertheless, it is possible to evaluate some of the variables, and therefore create a limited realization of the palaeoclimate.

To date, the lower Beaufort Group is thought to have been deposited in a semi-arid climate with limited chemical weathering and low sedimentation rates (e.g., Stear, 1985; Cole and Wipplinger, 2001). This is supported by the geochemical and sedimentary facies data presented in this work (e.g., CIA, ICV values, desiccation cracks, calcareous palaeosols, mudstone colouration). Furthermore, the increase in average temperatures, probably as a result of large atmospheric release of greenhouse gasses (CO_2 and CH_4) from the extrusion of the Siberian Traps, has also been shown across the Permian and Permo-Triassic boundary based on oxygen and carbon isotopes values from Karoo vertebrate fossils (Rey et al., 2015). This contrasts the work of Catuneanu and Elango (2001) who strongly argued for the lack of climatic influence as a control in the deposition of Balfour Formation (Figure 3), the youngest unit in the lower Beaufort Group, and explained the stratigraphic trends with flexural tectonics only.

All in all, details of the climatic events during the Permian of the main Karoo Basin are still in consideration. In this study, geochemical and petrographic results revealed similar dry climatic signal for the two formations. The data from this work however lacks the robustness and resolution to provide strong evidence for the role of climate on the large scale stratigraphic trends. It then proposed that the trends observed could be primarily driven by tectonics and explained by using the approach of alluvial sequence stratigraphy (Wright and Marriott, 1993; Catuneanu, 2006; Zecchin and Catuneanu, 2013). This school of thought analyses stratigraphic trends in terms of rates of accommodation creation (i.e. subsidence) and rates of sedimentation, which in a climatically stable setting, are variables controlled mainly by tectonics.

Laterally extensive channel complexes are common in both formations. This architecture indicates that a shallow palaeo-slope, a low amalgamation setting and low sedimentation rates were common in both formations. Low sedimentation rates are also supported by the geochemical and

sedimentological data (i.e. palaeosol and desiccation cracks). Considering the foreland basin model (Catuneanu et al., 1998), it is possible that sedimentation rates remained constant and that subsidence rates changed. The fact that higher and more constant energy levels are found in the eastern facies areas may suggest differential subsidence rates in the basin.

6. Conclusions

The upper Abrahamskraal and lower Teekloof formations are dominated by floodplain complex elements, mainly made up of an alternating sequence of laminated purple-red mudstones (Fl1) and massive olive green-grey siltstone facies (Fsm2). Channel complex elements are subordinate to the floodplain deposits, and are characterized by cross-bedded (Sl, St, Sp) fine-grained, light brown sandstones. Gravel elements are more abundant in the upper Abrahamskraal Formation, indicating that fluvial higher energy levels were present in the formation. Summary of the lithofacies can be found in the Facies Plates (Figures11, 12, 13, 14) and in Table 1.

Across the boundary of the formations, the main stratigraphic trends observed are:

- An upward decrease in the sandstone: mudstone ratio. Channel complex elements are more abundant in the upper Abrahamskraal Formation. The exception being the base of Teekloof Formation, where the thickest sandstone channel complex in the sequence (Figure 23A), is an anomaly in the sandstone: mudstone ratio.

- A consistent external architecture of the channel complexes in all formations. Flat-topped, low amalgamation, laterally continuous (10s of Kms) channel complex sheets are the most common external architecture. Furthermore, internal architecture mapping (Figures 16 and 17) shows that the western facies progress from being DA-dominated (~25% at W1) in the upper Abrahamskraal Formation, to LA-dominated (~30% at W1) in the lower Teekloof Formation. Based on the external and internal architectures, seven architecture types were established (Figures 20, 21 and 23; Tables 7 and 12).

- A consistent palaeocurrent direction for all formations at each facies area (Figure 24). Western facies area has a transport direction to NE, whereas the eastern facies area has a transport direction to N. Furthermore, modal analysis (Figure 25) revealed a recycled orogenic provenance of similar composition for both the southern and south-western sources. Moreover, geochemical plots (Figures 28, 29 and 30) also show consistent values for the formations and indicate a dry climate with the prevalence of physical weathering.

All in all, the results point to stable sediment sources, persistent palaeocurrents, and possibly a constant palaeo-climate, and therefore the observed stratigraphic trends most likely resulted from tectonic action.

7. References

Allen, J.R.L., 1983. Studies in fluviatile sedimentation: Bars, bar-complexes and sandstone sheets (low-sinuosity braided streams) in the brownstones (L. devonian), welsh borders. Sediment. Geol. 33, 237–293.

Bahlburg, H., Dobrzinski, N., 2011. Chapter 6 A review of the Chemical Index of Alteration (CIA) and its application to the study of Neoproterozoic glacial deposits and climate transitions. Geol. Soc. London, Mem. 36, 81–92.

Basu, A., 1985. Reading provenance from detrital quartz. SEPM Short Course 148, 231–247.

Bordy, E., Hancox, P., Rubidge, B., 2005. The contact of the Molteno and Elliot formations through the main Karoo Basin, South Africa: a second-order sequence boundary. South African J. Geol. 108, 351–364.

Bordy, E.M., 2000. Sedimentology of the Karoo Supergroup in the Tuli Basin (Limpompo River Area, South Africa). Unpublished PhD thesis, Rhodes University.

Bordy, E.M., Catuneanu, O., 2001. Sedimentology of the upper Karoo fluvial strata in the Tuli Basin, South Africa. J. African Earth Sci. 33, 605–629.

Bordy, E.M., Prevec, R., 2009. Sedimentology, palaeontology and palaeo-environments of the Middle (?) to Upper Permian Emakwezini Formation (Karoo Supergroup, South Africa). South African J. Geol. 111, 429–458.

Bridge, J.S., 1997. Thickness of sets of cross strata and planar strata as a function of formative bed-wave geometry and migration, and aggradation rate. Geology 25, 971–974.

Bridge, J.S., Mackey, S.D., 1993. A revised alluvial stratigraphy model. Alluv. Sediment.

Cadle, A.B., Cairncross, B., Christie, A.D.M., Roberts, D.L., 1993. The Karoo Basin of South Africa: type basin for the coal-bearing deposits of southern Africa. Int. J. Coal Geol. 23, 117–157.

Catuneanu, O., 2006. Principles of Sequence Stratigraphy, First. ed. Elsevier, Amsterdam, Netherlands.

Catuneanu, O., Elango, H.N., 2001. Tectonic control on fluvial styles: the Balfour Formation of the Karoo Basin, South Africa. Sediment. Geol. 140, 291–313.

Catuneanu, O., Hancox, P.J., Rubidge, B.S., 1998. Reciprocal flexural behaviour and contrasting stratigraphies: a new basin development model for the Karoo retroarc foreland system, South Africa. Basin Res. 10, 417–439.

Catuneanu, O., Wopfner, H., Eriksson, P.G., Cairncross, B., Rubidge, B.S., Smith, R.M.H., Hancox, P.J., 2005. The Karoo basins of south-central Africa. J. African Earth Sci. 43, 211–253.

Coelho, A., 2007. TOPAS-Academic. Coelho Software, Brisbane, Australia.

Cole, D.I., 1992. Evolution and development of the Karoo Basin. Invers. tectonics Cape Fold Belt, Karoo Cretac. basins South. Africa 87–99.

Cole, D.I., Wipplinger, P.E., 2001. Sedimentology and molybdenum potential of the Beaufort Group in the main Karoo basin, South Africa, Memoir - geological survey. Department of Mineral and Energy Affairs, South Africa.

Collinson, J., 1996. Alluvial sediments. Sediment. Environ. Process. facies Stratigr. 3, 37–82.

Colombera, L., Mountney, N.P., McCaffrey, W.D., 2013. A quantitative approach to fluvial facies models: Methods and example results. Sedimentology 60, 1526–1558.

Cox, R., Lowe, D., Cullers, R., 1995. The influence of sediment recycling and basement composition on evolution of mudrock chemistry in the southwestern United States. Geochim. Cosmochim. Acta 59, 2919–2940.

Cox, R., Lowe, D.R., 1995. A Conceptual Review of Regional-Scale Controls on the Composition of Clastic Sediment and the Co-Evolution of Continental Blocks and their Sedimentary Cover. J. Sediment. Res. 65, 1–12.

Day, M.O., Ramezani, J., Bowring, S.A., Sadler, P.M., Erwin, D.H., Abdala, F., Rubidge, B.S., 2015. When and how did the terrestrial mid-Permian mass extinction occur? Evidence from the tetrapod record of the Karoo Basin, South Africa. Proc. Biol. Sci. 282.

Day, M.O., Rubidge, B.S., 2014. A brief lithostratigraphic review of the Abrahamskraal and Koonap formations of the Beaufort Group, South Africa: Towards a basin-wide stratigraphic scheme for the Middle Permian Karoo. J. African Earth Sci. 100, 227–242.

De Wit, M.J., 2011. The great shale debate in the Karoo. S. Afr. J. Sci. 107, 02–10.

Dickinson, W., 1985. Interpreting provenance relations from detrital modes of sandstones. Proven. arenites 333–361.

Dickinson, W.R., 1970. Interpreting Detrital Modes of Graywacke and Arkose. J. Sediment. Res. 40, 695–707.

Duke, W., Arnott, R., Cheel, R., 1991. Shelf sandstones and hummocky cross-stratification: new insights on a stormy debate. Geology 19, 625–628.

Duncan, R.A., Hooper, P.R., Rehacek, J., Marsh, J.S., Duncan, A.R., 1997. The timing and duration of the Karoo igneous event, southern Gondwana. J. Geophys. Res. 102, 127–138.

Fedo, C.M., Wayne Nesbitt, H., Young, G.M., 1995. Unraveling the effects of potassium metasomatism in sedimentary rocks and paleosols, with implications for paleoweathering conditions and provenance. Geology 23, 921–924.

Flood, Y., Hampson, G., 2015. Quantitative Analysis of the Dimensions and Distribution of Channelized Fluvial Sandbodies Within A Large Outcrop Dataset: Upper Cretaceous Blackhawk Formation. J. Sediment. Res. 85, 315–336.

Gibling, M.R., 2006. Width and Thickness of Fluvial Channel Bodies and Valley Fills in the Geological Record: A Literature Compilation and Classification. J. Sediment. Res. 76, 731–770.

Goldberg, K., Humayun, M., 2010. The applicability of the Chemical Index of Alteration as a paleoclimatic indicator: An example from the Permian of the Paraná Basin, Brazil. Palaeogeogr. Palaeoclimatol. Palaeoecol. 293, 175–183.

Gulliford, A.R., Flint, S.S., Hodgson, D.M., 2014. Testing Applicability of Models Of Distributive Fluvial Systems Or Trunk Rivers In Ephemeral Systems: Reconstructing 3-D Fluvial Architecture In the Beaufort Group, South Africa. J. Sediment. Res. 84, 1147–1169.

Hancox, P.., Rubidge, B.., 2001. Breakthroughs in the biodiversity, biogeography, biostratigraphy, and basin analysis of the Beaufort group. J. African Earth Sci. 33, 563–577.

Hillier, S., 2003. Quantitative analysis of clay and other minerals in sandstones by X-ray powder diffraction (XRPD). Int. Assoc. Sedimentol. Spec. Publ. 34, 213–251.

Ingersoll, R. V., Bullard, T.F., Ford, R.L., Grimm, J.P., Pickle, J.D., Sares, S.W., 1984. The Effect of Grain Size on Detrital Modes: A Test of the Gazzi-Dickinson Point-Counting Method. SEPM J. Sediment. Res. Vol. 54, 103–116.

Johnson, M., Vuuren, C. Van, 1997. The foreland Karoo Basin, South Africa, in: African Basins. Sedimentary Basins of the World. Amsterdam, Netherlands, pp. 269–317.

Johnson, M.., Van Vuuren, C.., Hegenberger, W.., Key, R., Show, U., 1996. Stratigraphy of the Karoo Supergroup in southern Africa: an overview. J. African Earth Sci. 23, 3–15.

Johnson, M.R., Vuuren, C.J. Van, Visser, J.N.J., Cole, D.I., Wickens, H.D., Christie, A.D.M., Roberts, D.L., Brandl, G., 2006. Sedimentary rocks of the Karoo Supergroup, in: Johnson M.R., et Al., Eds.,.

Geological Society of South Africa and Council for Geoscience, South Africa, pp. 461–499.

Keyser, A.W., Smith, R.M.H., 1978. Vertebrate biozonation of the Beaufort Group with special reference to the Western Karoo Basin. Geological Survey, Department of Mineral and Energy Affairs, Republic of South Africa.

Leclair, S.F., 2002. Preservation of cross-strata due to the migration of subaqueous dunes: an experimental investigation. Sedimentology 49, 1157–1180.

Lindeque, A., De Wit, M.J., Ryberg, T., Weber, M., Chevallier, L., 2012. Deep crustal profile across the Southern Karoo basin and beattie magnetic anomaly, South Africa: An integrated interpretation with tectonic implications. South African J. Geol. 114, 265–292.

Loubser, M., Verryn, S., 2008. Combining XRF and XRD analyses and sample preparation to solve mineralogical problems. South African J. Geol. 111, 229–238.

McCarthy, T., Rubidge, B., 2005. Story of Earth and Life: a southern African perspective on a 4.6-billion-year journey. Struik, Cape Town, South Africa.

Miall, A., 2013. Principles of Sedimentary Basin Analysis. Springer Science & Business Media, Toronto, Canada.

Miall, A., 1996. The geology of fluvial deposits. Springer Berlin Heidelberg, Berlin, Germany.

Miall, A.D., 1988. Architectural elements and bounding surfaces in fluvial deposits: anatomy of the Kayenta formation (lower jurassic), Southwest Colorado. Sediment. Geol. 55, 233–262.

Miall, A.D., 1987. Recent Developments in the Study of Fluvial Facies Models. Soc. Econ. Paleontol. Mineral.

Miall, A.D., 1985. Architectural-Element Analysis: A New Method of Facies Analysis Applied to Fluvial Deposits. Earth-Science Rev. 22, 261–308.

Moore, D., Reynolds, R., 1989. X-ray Diffraction and the Identification and Analysis of Clay Minerals, Second. ed. Oxford university press, New York.

Nesbitt, H., Young, G., 1982. Early Proterozoic climates and plate motions inferred from major element chemistry of lutites. Nature 299, 715–717.

Nesbitt, H.., Young, G.., 1984. Prediction of some weathering trends of plutonic and volcanic rocks based on thermodynamic and kinetic considerations. Geochim. Cosmochim. Acta 48, 1523–1534.

Paiva, F., 2013. Sedimentological and Structural Characterization of the Lower Beaufort Group in the SW main Karoo Basin, South Africa. Unpublished Honours thesis, University of Cape Town.

Payenberg, T., Willis, B., Bracken, B., 2011. Revisiting the subsurface classification of fluvial sandbodies. AAPG Annu. Conf. Exhib.

Reading, H., 2009. Sedimentary environments: processes, facies and stratigraphy, Third. ed. Blackwell Publishing Ltd., Oxford, UK.

Reading, H., 2001. Clastic facies models, a personal perspective. Bull. Geol. Soc. Denmark 48, 101–115.

Reineck, H.-E., Wunderlich, F., 1968. Classification and origin of flaser and lenticular bedding. Sedimentology 11, 99–104.

Retallack, G., 2005. Pedogenic carbonate proxies for amount and seasonality of precipitation in paleosols. Geology 33, 333–336.

Rey, K., Amiot, R., Fourel, F., Rigaudier, T., Abdala, F., Day, M.O., Fernandez, V., Fluteau, F., France-Lanord, C., Rubidge, B.S., Smith, R.M., Viglietti, P.A., Zipfel, B., Lécuyer, C., 2015. Global climate perturbations during the Permo-Triassic mass extinctions recorded by continental tetrapods from South Africa. Gondwana Res. 13.

Roser, B.P., Cooper, R.A., Nathan, S., Tulloch, A.J., 2010. Reconnaissance sandstone geochemistry,

provenance, and tectonic setting of the lower Paleozoic terranes of the West Coast and Nelson, New Zealand. New Zeal. J. Geol. Geophys. 39, 1–16.

Rubidge, B., Hancox, P., Catuneanu, O., 2000. Sequence analysis of the Ecca—Beaufort contact in the southern Karoo of South Africa. South African J. Geol. 103, 81–96.

Rubidge, B.S., 2005. 27th Du Toit Memorial Lecture: Re-uniting lost continents - Fossil reptiles from the ancient Karoo and their wanderlust. South African J. Geol. 108, 135–172.

Rubidge, B.S., Erwin, D.H., Ramezani, J., Bowring, S.A., de Klerk, W.J., 2013. High-precision temporal calibration of Late Permian vertebrate biostratigraphy: U-Pb zircon constraints from the Karoo Supergroup, South Africa. Geology 41, 363–366.

Singer, A., 1984. The paleoclimatic interpretation of clay minerals in sediments — a review. Earth-Science Rev. 21, 251–293.

Stear, W., 1985. Comparison of the bedform distribution and dynamics of modern and ancient sandy ephemeral flood deposits in the southwestern Karoo region, South Africa. Sediment. Geol. 45, 209–230.

Stear, W.M., 1980. Channel sandstone and bar morphology of the Beaufort group uranium district near Beaufort West. Trans. Geol. Soc. South Africa 83, 391–398.

Tankard, A., Welsink, H., Aukes, P., Newton, R., Stettler, E., 2012. Geodynamic interpretation of the Cape and Karoo basins, South Africa, in: Regional Geology and Tectonics: Phanerozoic Passive Margins, Cratonic Basins and Global Tectonic Maps. Elsevier, Amsterdam, Netherlands, pp. 869–945.

Tankard, A., Welsink, H., Aukes, P., Newton, R., Stettler, E., 2009. Tectonic evolution of the Cape and Karoo basins of South Africa. Mar. Pet. Geol. 26, 1379–1412.

Turner, B., 1999. Tectonostratigraphical development of the Upper Karooforeland basin: Orogenic unloading versus thermally-induced Gondwana rifting. J. African Earth Sci. 28, 215–238.

Veevers, J.J., Cole, D.I., Cowan, E.J., 1994. Permian-Triassic Pangean Basins and Foldbelts Along the Panthalassan Margin of Gondwanaland, Geological Society of America Memoirs, Geological Society of America Memoirs. Geological Society of America, Boulder, Colorado.

Visser, J., 1986. Lateral lithofacies relationships in the glacigene Dwyka Formation in the western and central parts of the Karoo Basin. Trans. Geol. Soc. South Africa 86, 373–383.

Visser, J.N.J., 1990. The age of the late Palaeozoic glacigene deposits in southern Africa. South African J. Geol. 93, 366–375.

Walker, R., 1984. Facies models, Second. ed. Geological Association of Canada, Canada.

Wilson, A., Flint, S., Payenberg, T., 2014. Architectural Styles and Sedimentology of the Fluvial Lower Beaufort Group, Karoo Basin, South Africa. J. Sediment. Res. 84, 326–348.

Wizevich, M., 1992. Photomosaics of outcrops: useful photographic techniques, in: Concepts in Sedimentology and Paleontology. SEPM Society for Sedimentary Geology, Tulsa, Ok.

Wright, V., Marriott, S., 1993. The sequence stratigraphy of fluvial depositional systems: the role of floodplain sediment storage. Sediment. Geol. 86, 203–210.

Zecchin, M., Catuneanu, O., 2013. High-resolution sequence stratigraphy of clastic shelves I: units and bounding surfaces. Mar. Pet. Geol. 39, 1–25.

8. Appendices

8.1. Methodology

8.1.1. FLUVIAL SANDSTONE BODIES CLASSIFICATION

KEY DIAGRAM FOR CLASSIFYING FLUVIAL BODIES

- Can basal erosion surface and correlative surfaces in extra-channel deposits be traced widely?
- Are dimensions an order of magnitude greater than other channel forms in the system?
- Is scale of erosional relief on basal surface several times the depth of scour in component channel fills?

YES to one or more: ***VALLEY FILLS***

- Is hiatus at valley base longer than about one geological period?
- Was valley cut into strongly lithified material?

YES to one or both: **VALLEY FILLS ON BEDROCK UNCONFORMITIES**

NO: **VALLEY FILLS WITHIN ALLUVIAL AND MARINE STRATA**

- Is valley fill associated with subglacial or proglacial deposits (in bedrock / sediments)?

YES: **VALLEY FILLS IN SUBGLACIAL AND PROGLACIAL SETTINGS**

NO to all of them: ***CHANNEL BODIES***

- Does body show evidence of channel mobility (e.g. multilateral; lateral accretion sets), and have relatively high W/T?

YES: ***MOBILE CHANNEL BELT DEPOSITS***

- Are lateral accretion sets prominent?

YES: **MEANDERING RIVER DEPOSITS**

NO: **BRAIDED AND LOW-SINUOSITY RIVER DEPOSITS**

NO:

FIXED CHANNELS AND POORLY CHANNELISED SYSTEMS

- Are channel bodies part of a distributary system?

YES or probably: choose between:

Channel bodies form part of inland systems near an upland source area, probably associated with large mobile belt deposits:
CHANNELS ON MEGAFANS

Channel bodies are associated with wetlands, tidal deposits, and other evidence of a coastal setting:
DELTA DISTRIBUTARIES

Channel body suite passes proximally into coarser grained alluvial fan deposits:
DISTAL ALLUVIAL FANS / APRONS

Small channel bodies associated with channel margins, levees deposits, and/or avulsion successions:
CREVASSE CHANNELS AND AVULSION DEPOSITS

NO: choose between:

Channel bodies most commonly form part of inland systems, without clear evidence for a distributary origin:
FIXED RIVER SYSTEMS

Small channel bodies or gully fills with fluvial components, intimately associated with floodplain deposits:
FLOODPLAIN CHANNELS

Channel bodies associated with eolian deposits:
CHANNELS IN EOLIAN SETTINGS

Figure 34: Classification diagram for fluvial channel deposits. Adapted from Gibling (2006).

8.1.2. PREPARATION OF SAMPLES FOR QXRD

Crush the Sample - Jaw crasher, size 2-5 mm chips. A portion can be used for clay fraction separation, be aware of separation bias. A splitter is recommended.

Grind the sample - Disk and cylinder. A portion can be used for XRF. Splitter recommended. Ball and pillow crushing procedure on a different section.

Splitting - Splitting of each sample is necessary in order to achieve a 3.5 g representative fraction of the sample. Rotary splitter used.

Loading into Microniser - Micronising was done with corandum bids on a sealed cylinder container ca 6 cm diameter, and samples dissolved in 6-8 ml of ethanol. Micronising is necessary to further decrease and homogenize grain sizes. Ethanol is used to create a paste, for homogeneity and to decrease friction effects.

Figure 35: Sample preparation for QXRD

Microniser and unloading - Micronising performed with machine XXX, during 10 minutes. Sample removed of cylinder with repeated washings of ethanol. Samples are placed on metallic trays that are put fume cupboard to dry. N.B. Samples should never be put in an oven, as they are in a flammable solution of ethanol

Collecting Samples - After drying for 1 or 2 days, samples are removed with a brush and put into sample vials. Samples are now ready for XRD

Figure 36: Sample preparations for QXRD 2

8.1.3. CLAY FRACTION SEPARATION

Crush the Sample - Used Jaw crasher, size 2-5 mm chips. Be aware of separation bias. A splitter is recommended. Further fining of the sample can be bad for clay separation, as one would be reducing the size all other minerals, which would then complicates separation of clay.

Wet Separation - Clay portion is separated by repeated washings of the cuttings into a container. Use 2 sieves, (1) > 64 µm and (2) >32 µm is this way it is possible to collect different sized clasts. Sand size particles collected in the 1st sieve, coarse silt particles are collected in the 2nd sieve. Fine silt and clays will be collected in a container below the two sieves.

Figure 37: Clay fraction separation

8.2. Supporting Data/results

Bulk rock XRD Spectra

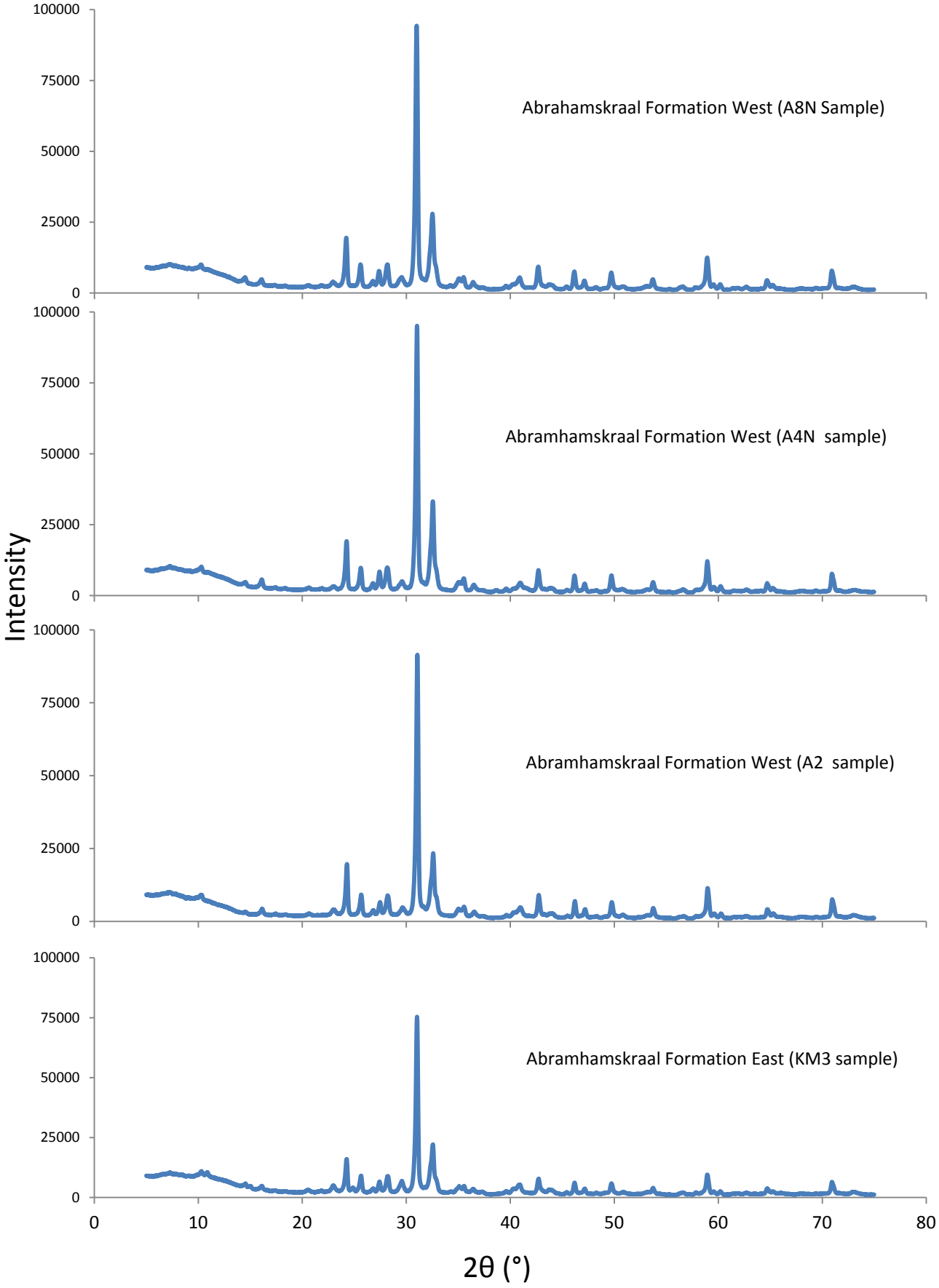

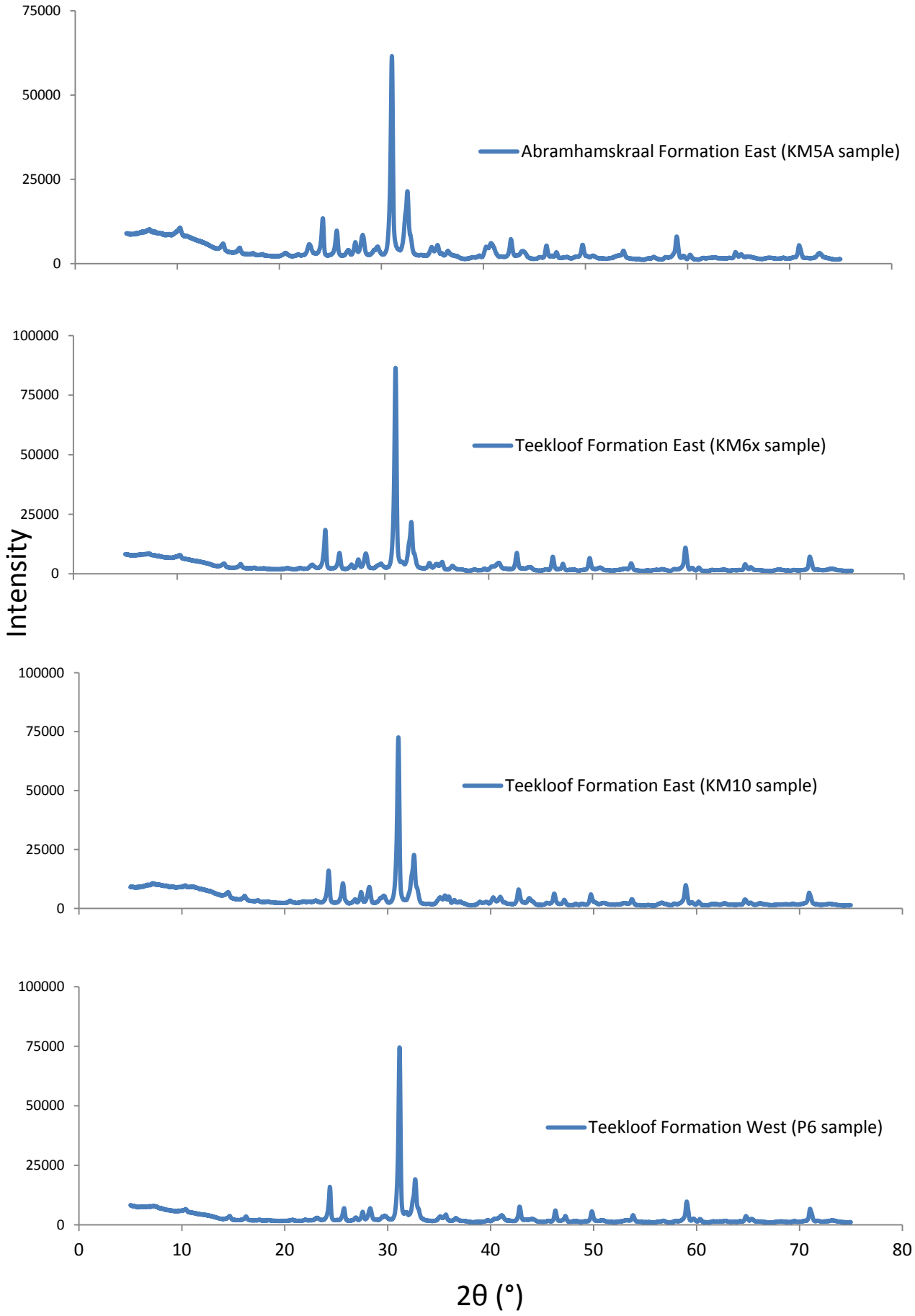
75000
50000
25000
0
Abramhamskraal Formation East (KM5A sample)
100000
75000
50000
25000
0
Teekloof Formation East (KM6x sample)
Intensity
100000
75000
50000
25000
0
Teekloof Formation East (KM10 sample)
100000
75000
50000
25000
0
Teekloof Formation West (P6 sample)
0
10
20
30
40
50
60
70
80
2θ (°)

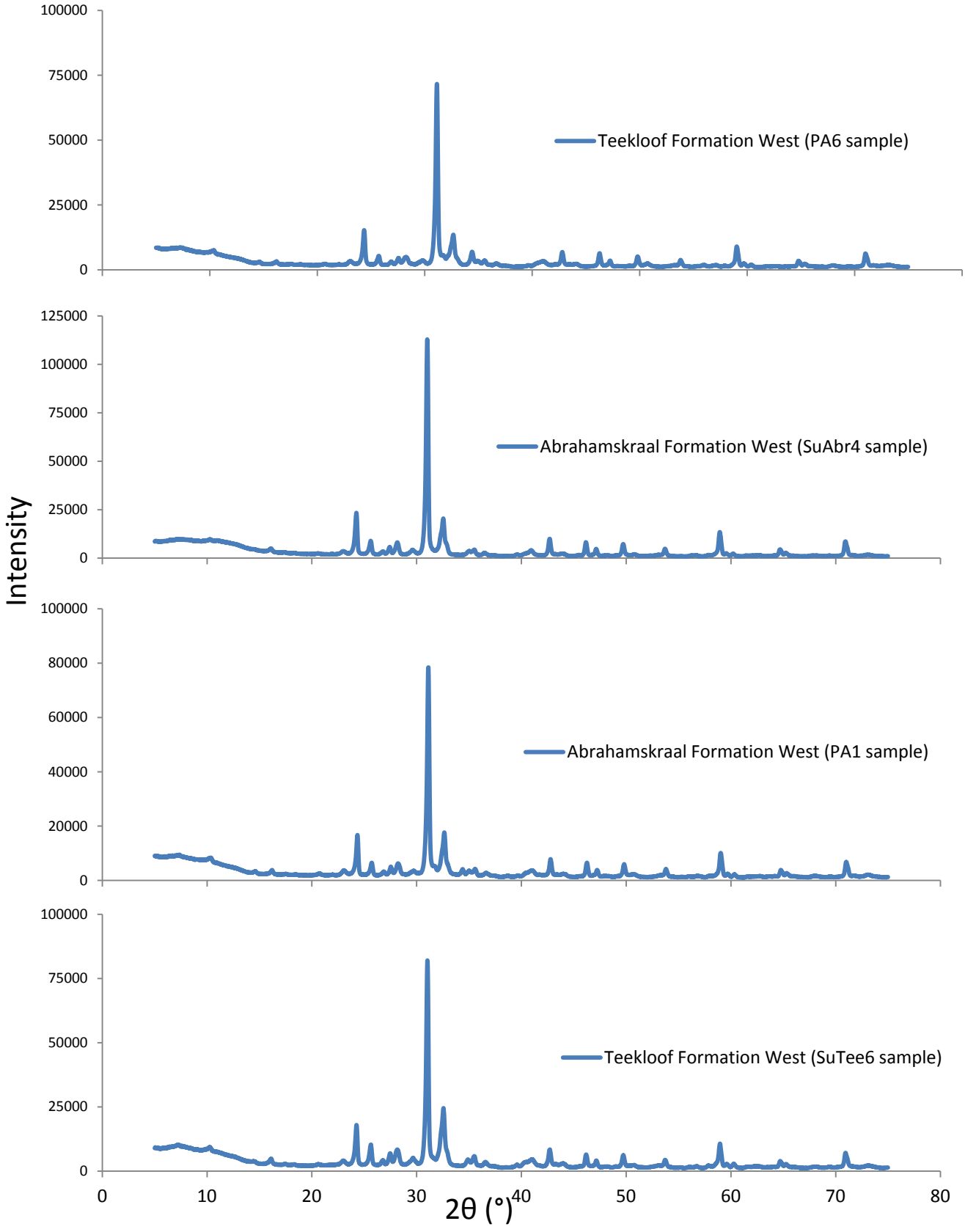

Figure 38 Bulk Rock XRD spectra

Petrographic Analysis - Point counting

Table 13: Modal analysis of samples' thin sections. 300 counts of course grained minerals. Qm - Monocrystalline Quartz; Qp - Polycrystalline Quartz; Fp - Plagioclase Feldspar; Fk - Alkali Feldspar; Lv - Volcanic Lithic; Lm - Metamorphic Lithic; Lp Plutonic Lithic- ; Ls - Sedimentary Lithic; Accs - Accessory Minerals (Mica, Pyroxenes Amphiboles); Un - Unidentified Minerals.

		Samples	Qm	Qp	Fp	Fk	Lv	Lm	Lp	Ls	Accs	Un
Teekloof Formation	E. Facies	KM6B	34	137	54	1	0	2	8	38	26	0
		KM8	12	137	76	1	0	0	2	39	31	2
		KM6A	67	105	72	1	0	0	5	28	22	0
		KM10	67	105	72	1	0	0	5	28	22	0
	W. Facies	Su-Tee1	69	123	49	0	0	0	5	42	12	0
		PA10	21	200	28	1	0	0	4	36	8	2
		PA11	45	133	70	0	0	0	4	34	14	0
		P8	72	136	44	0	0	1	9	23	15	0
		P7	31	158	26	2	0	3	1	49	29	1
		P6	48	152	39	3	0	0	1	42	15	0
		P3	26	156	53	9	0	10	21	4	21	0
Abrahamskraal Formation	E Facies	KM31	23	180	31	1	0	1	1	38	25	0
		KM12	84	95	77	0	0	0	0	33	11	0
		KM5A	92	135	33	0	0	0	4	16	20	0
	W. Facies	Su-Abr 5	51	156	39	0	0	0	13	38	3	0
		PA1	52	177	33	0	0	1	1	10	26	0
		PA2	25	183	43	4	0	0	0	29	16	0
		A0	38	185	11	0	0	0	3	50	13	0
		A2	21	175	40	2	0	1	1	45	14	1
		A-9	30	138	42	0	0	2	4	62	22	0
		A8	67	129	41	0	0	3	5	33	22	0
		A5	55	166	24	0	0	0	1	34	20	0
		A4	47	165	56	0	0	0	9	13	10	0

Geochemistry - XRF results

Table 14: XRF Results

		Samples	SiO2	TiO2	Al2O3	Fe2O3	MnO	MgO	CaO	Na2O	K2O	P2O5	SO3	Cr2O3	NiO	H2O-	LOI	Sum	CIA	CIA(molar)
Teekloof Formation	W. Facies	SU-TEE6	70.0	0.5	13.6	4.1	0.1	1.3	0.9	4.0	1.9	0.2	0.0	0.0	0.0	0.4	2.1	99.0	57.304	1.342
		SU-TEE1	73.00	0.48	12.03	4.11	0.07	0.95	1.20	3.92	1.19	0.13	b.d.	0.01	0.01	0.00	2.29	99.38	54.804	1.213
		PA6	69.3	0.4	11.8	3.1	0.1	1.0	3.7	2.7	2.3	0.1	0.0	0.0	0.0	0.7	4.3	99.5	46.161	0.857
		P8	72.33	0.52	12.88	4.05	0.06	0.89	0.72	4.18	1.39	0.12	b.d.	b.d.	0.01	0.14	1.88	99.17	57.094	1.331
		P6	71.5	0.5	12.9	3.8	0.0	0.9	0.8	3.7	1.6	0.2	0.0	0.0	0.0	1.4	2.1	99.5	58.162	1.390
	E. Facies	KM10	66.8	0.9	13.5	5.9	0.1	1.4	3.5	3.9	0.8	0.2	0.0	0.0	0.0	0.3	1.9	99.0	49.889	0.996
		KM8	67.48	0.71	14.19	5.17	0.08	1.72	1.41	5.10	0.77	0.15	b.d.	0.01	0.01	0.07	2.86	99.73	54.649	1.205
		KM6x	70.8	0.5	12.3	3.6	0.1	1.1	2.1	3.8	1.6	0.1	0.1	0.0	0.0	0.3	2.8	99.1	51.234	1.051
Abrahamskraal Formation	W. Facies	SU-ABR4	77.5	0.4	10.9	2.6	0.0	0.6	0.5	3.4	1.4	0.1	0.0	0.0	0.0	0.4	1.5	99.2	57.384	1.347
		SU-ABR1	68.36	1.23	10.52	5.01	0.11	1.04	4.10	3.19	1.02	0.19	0.01	0.01	0.01	0.24	4.12	99.16	43.259	0.762
		PA3	74.03	0.37	11.89	3.57	0.05	0.87	0.67	3.65	1.40	0.11	0.03	b.d.	0.01	0.21	2.33	99.19	57.631	1.360
		PA1	71.7	0.5	12.0	2.8	0.1	0.8	1.9	3.2	1.8	0.1	0.1	0.0	0.0	1.5	2.7	99.1	52.945	1.125
		A5	72.77	0.56	12.01	4.67	0.06	0.91	0.97	3.26	1.74	0.15	0.01	0.01	0.01	0.09	2.04	99.25	57.163	1.334
		A4	74.46	0.43	12.22	2.98	0.04	0.76	0.68	3.51	1.89	0.10	0.02	b.d.	0.01	0.09	2.10	99.30	57.414	1.348
		A2	73.0	0.4	12.8	3.1	0.0	0.8	0.6	3.7	1.7	0.1	0.0	0.0	0.0	1.1	1.8	99.3	58.244	1.395
		A1	71.12	0.50	13.19	3.80	0.05	1.04	0.95	3.84	1.79	0.12	0.03	b.d.	0.0078	0.11	2.45	99.00	56.905	1.320
		A0	70.8	0.5	13.1	3.2	0.1	1.1	1.7	3.2	2.2	0.1	0.1	0.0	0.0	0.5	2.6	99.0	55.234	1.234
		A4N	73.2	0.5	12.3	3.5	0.1	0.7	0.8	4.6	1.1	0.2	0.0	0.0	0.0	0.3	1.2	98.5	54.707	1.208
		A5N	69.77	0.65	14.00	4.47	0.05	1.22	0.88	2.54	2.84	0.15	b.d.	b.d.	0.01	0.13	2.94	99.66	61.256	1.581
		A6N	75.03	0.41	11.55	3.58	0.06	0.84	0.68	3.98	1.05	0.11	b.d.	b.d.	0.01	0.11	2.04	99.44	56.422	1.295
		A8N	72.3	0.4	12.6	3.1	0.0	0.8	1.0	4.0	1.5	0.1	0.0	0.0	0.0	1.4	1.9	99.0	55.862	1.266
	E. Facies	KM5A	65.8	0.6	16.4	4.0	0.1	1.4	1.8	3.6	2.9	0.2	0.0	0.0	0.0	0.3	2.4	99.5	56.793	1.314
		KM3	67.1	0.6	14.6	4.3	0.1	1.1	2.0	3.4	1.7	0.1	0.0	0.0	0.0	1.3	2.9	99.2	56.951	1.323
		KM2A	62.58	0.46	15.27	3.64	0.06	1.59	5.53	1.11	3.98	0.13	b.d.	b.d.	0.01	0.05	5.12	99.52	48.528	0.943

Visited sites Information

Table 15: List of the visited sites

Formation	Site	GPS	Altitude (m)
Teekloof Formation	P8	S32,199658; E21,626391	1249
	P7	S32,208928; E21,622029	1107
	P6	S32,224104; E21,625165	1075
	P5	S32,238293; E21,628787	1058
	P4	S32,261200; E21,632950	1052
	P3	S32,262079; E21,634888	1062
	P2	S32,264093; E21,638217	1073
	P1	S32,273335; E21,645674	1069
	PA11	S32° 14.888; E21° 00.952	1113
	PA10	S32,25075; E22,02247	1100
	PA9	S32,25189; E22,0285	1090
	PA8	S32,25459; E22,0368	1074
	PA7	S32,25468; E22,04409	1036
	PA6	S32,2448; E22,06109	994
	Su-Tee1	S32°19'02.4"; E21°15'22.2"	1472
	Su-Tee2	S32°18'53.5";E21°15'2.9"	1484
	Su-Tee3	S32°16'28.5";E21°15'46.1"	1395
	Su-Tee4	S32°16'17.8";E21°15'37.4"	1378
	Su-Tee5	S32°15'20.8";E21°22'45.7"	1407
	Su-Tee6	S32°15'15.1";E21°22'12.7"	1408
	Su-Tee7	S32°15'10.1"; E21°22'50.0"	1445
	Su-Tee8	S32°15'36.8"; E21°23'42.8"	1442
	Su-Tee9	S32°27'02.7"; E21°11'47.5"	1741
	Su-Tee10	S32°27'36.2"; E21°11'00.1"	1529
	Su-Tee11	S32°28'59.6"; E21°09'06.9"	1444
	KM8	S32°56'9.14"; E4°40'15.33"	450
	KM10	S32 59' 39.7; E25 18' 50.9	533
	KM6A	S32 57 42,9; E25 03 50	396
	KM6C	S32 57 51; S25 03 54.4	388
	KM4	S32°56'38.45"; E25°3'44.65"	445
Abrahamskraal Formation	PA5	S32,26834; E22,06494	986
	PA4	S32,27021; E22,07129	967
	PA3	S32,29582; E22,13455	870
	PA2	S32,30892; E22,17766	815
	PA1	S32,33549; E22,20666	785
	A9	S32° 17.888; E21° 39.469	1030
	A8	S32,31803; E21,66902	1005
	A7	S32,345274; E21,675316	928
	A6	S32,373463; E21,703040	837
	A5	S32,376277; E21, 703159	820
	A4	S32,391677; E21,720833	783
	A3	S32,402064; E21,725344	775
	A2	S32,414709; E21,733937	768
	A1	S32,424353; E21,741065	752
	A0	S32°26,881';E21° 46,380'	743
	A-1	S32° 27,295'; E21° 46,406'	731

	A-2	S32° 27,683’; E21° 46,461’	719
	A-3	S32° 30,211’; E21° 48,755’	670
	A-4	S32° 30,906’; E21° 49,147’	676
	A-5	S32° 31,301’; E21° 49,420’	672
	A-6	S32° 31,732’; E21° 49,698’	664
	A-7	S32° 31,907’; E21° 49,742’	661
	A-8	S32° 32,230’; E21° 49,699’	655
	A-9	S32° 32,561’; E21° 49,701’	655
	Su-Abr1	S32°24'02.5"; E20°55'51.1"	1420
	Su-Abr2	S32°24'22.0"; E20°57'08.0"	1405
	Su-Abr3	S32°24'22.0"; E20°57'08.0"	1362
	Su-Abr4	S32°24'31.1"; E21°00'24.3"	1388
	Su-Abr5	S32°25'29.1"; E21°01'44.0"	1387
	KM3	S 33° 4'37.91";E25° 0'59.32"	296
	KM12	S33 00' 21.2"; E 25 09' 48,9"	334
	KM13	S33 04.288' E25 00.521'	283
	KM2A	S 32°50'45.12";E24°24'56.03"	791
	KM5	32°57'28.18"S; 24°53'53.70"E	389
	KM6D	S32 58' 0.7''; E25 03' 48,2''	393
	KM11	S33 00' 15.6"; E25 14' 23.6"	392
	KM1	S32 50,58 E24 25,068	780